Bioprocess engineering

Published by Woodhead Publishing Limited, 2013

Related titles:

MATLAB® in bioscience and biotechnology
(ISBN 978-1-907568-04-6)
MATLAB® in bioscience and biotechnology presents an introductory Matlab course oriented towards various collaborative areas of biotechnology and bioscience. It concentrates on Matlab fundamentals and gives examples of its application to a wide range of current bioengineering problems in computational biology, molecular biology, bio-kinetics, biomedicine, bioinformatics, and biotechnology. In the last decade Matlab has been presented to students as the first computer program they learn. Consequently, many non-programmer students, engineers and scientists have come to regard it as user-friendly and highly convenient in solving their specific problems. Numerous books are available on programming in Matlab for engineers in general, irrespective of their specialization, or for those specializing in some specific area, but none have been designed especially for such a wide, interdisciplinary, and topical area as bioengineering. Thus, in this book, Matlab is presented with examples and applications to various school-level and advanced bioengineering problems – from growing populations of microorganisms and population dynamics, reaction kinetics and reagent concentrations, predator–prey models, mass-transfer and flow problems, to sequence analysis and sequence statistics.

An introduction to biotechnology: The science, technology and medical applications
(ISBN 978-1-907568-28-2)
An introduction to biotechnology is a biotechnology textbook aimed at undergraduates. It covers the basics of cell biology, biochemistry and molecular biology, and introduces laboratory techniques specific to the technologies addressed in the book; it addresses specific biotechnologies at both the theoretical and applications levels.
Biotechnology is a field that encompasses both basic science and engineering. There are currently few, if any, biotechnology textbooks that adequately address both areas. Engineering books are equation-heavy and are written in a manner that is very difficult for the non-engineer to understand. Numerous other attempts to present biotechnology are written in a flowery manner with little substance. The author holds one of the first PhDs granted in both biosciences and bioengineering. He is more than an author enamoured with the wow-factor associated with biotechnology; he is a practicing researcher in gene therapy, cell/tissue engineering, and other areas and has been involved with emerging technologies for over a decade. Having made the assertion that there is no acceptable text for teaching a course to introduce biotechnology to both scientists and engineers, the author committed himself to resolving the issue by writing his own.

Electroporation-based therapies for cancer: From basics to clinical applications
(ISBN 978-1-907568-15-2)
Electroporation-based therapies for cancer looks at electroporation-based therapies for cancer. Cancer kills about one American per minute, amounting to over 500,000 deaths in the US and millions, worldwide, each year. There is a critical need for safe, effective, and affordable alternative treatment modalities, especially for inoperable, recurring and chemo-resistant cancers, that do not respond well to current treatment regimen. Electrical-pulse-mediated, enhanced drug delivery technique, known as electroporation is one of the ways to effectively treat these patients. Towards this end, this book provides a comprehensive overview of electroporation-based clinical studies in the hospitals for various cancer treatments including melanomas, head and neck cancers, chest wall breast carcinomas and colorectal cancers and research studies in the lab using cell lines, primary cells, and animals. This technique is especially suitable for low and middle-income countries, where due to lack of infrastructure and resources, many cancers are diagnosed at late stages and this safe, effective, economical, out-patient-based and quick (it only takes a few minutes to treat a tumor) technique is a boon to these patients for palliative and other care with enhanced quality of life. From basics to clinical medical applications of electroporation are discussed by interdisciplinary authors including practicing oncological surgeons, medical professional, and academic and other researchers.

Details of these and other Woodhead Publishing books can be obtained by:

- visiting our web site at www.woodheadpublishing.com
- contacting Customer Services (e-mail: sales@woodheadpublishing.com; fax: +44(0) 1223 832819; tel: +44(0) 1223 499140; address: Woodhead Publishing Limited, 80 High Street, Sawston, Cambridge CB22 3HJ, UK)

If you would like to receive information on forthcoming titles, please send your address details to Customer Services, at the address above. Please confirm which subject areas you are interested in.

Published by Woodhead Publishing Limited, 2013

Bioprocess engineering

An introductory engineering and life science approach

KIM GAIL CLARKE

Oxford Cambridge Philadelphia New Delhi

Published by Woodhead Publishing Limited, 2013

Woodhead Publishing Limited, 80 High Street, Sawston,
Cambridge, CB22 3HJ, UK
www.woodheadpublishing.com
www.woodheadpublishingonline.com

Woodhead Publishing, 1518 Walnut Street, Suite 1100, Philadelphia, PA 19102-3406, USA

Woodhead Publishing India Private Limited, G-2, Vardaan House, 7/28 Ansari Road,
Daryaganj, New Delhi – 110002, India
www.woodheadpublishingindia.com

First published in 2013, Woodhead Publishing Limited

British Library Cataloguing-in-Publication Data
A catalogue record for this book is available from the British Library

Library of Congress Control Number: 2013944154

Woodhead Publishing ISBN: 978–1–78242–167–2 (print)
ISBN: 978–1–78242–168–9 (online)

Typeset by RefineCatch Limited, Bungay, Suffolk
Cover design by Cat M. Clarke
Printed in the UK and USA

To William (Bill) with love and gratitude

Published by Woodhead Publishing Limited, 2013

List of figures

2.1	The Phylogenetic Tree of Life	9
2.2	Intracellular structures of (a) prokaryotes and (b) eukaryotes	16
2.3	Classification according to carbon and energy requirements	19
3.1	The families of D-aldoses (a) and ketoses (b) from three to six carbon atoms	27
3.2	Conversion of D-glucose from straight chain to pyranose form	28
3.3	Sucrose	28
3.4	Starch	29
3.5	Cellulose	29
3.6	The parent purine (a) and pyrimidine (b) compounds	34
3.7	Adenosine mono-, di- and triphosphate	35
3.8	Nicotinamide adenine dinucleotide (a), flavin adenine dinucleotide (b) and co-enzyme A (c)	36
3.9	The nucleotides RNA (a) and DNA (b)	37
4.1	Protein synthesis	43
4.2	Regulation of enzyme synthesis	45
5.1	Energy release and sequestration	54
5.2	The electron transport chain or oxidative phosphorylation	56

Published by Woodhead Publishing Limited, 2013

5.3	Reduction of the active groups NAD (a), FAD (b) and CoQ (c)	56
5.4	Glycolysis	60
5.5	Tricarboxylic acid cycle	63
5.6	β-Oxidation of fats	69
6.1	CSTR schematic	89
6.2	CPFR schematic	90
7.1	Characteristic microbial growth phases	106
7.2	Exponential growth of a single bacterial cell	107
7.3	Batch growth curves determined from cell dry weight (—) and cell numbers (----)	110
7.4	The effect of substrate concentration on specific growth rate	113
7.5	A simple continuous culture system incorporating a CSTR	119
7.6	Predictions of cell and substrate concentrations in a continuous system at steady state with a single feed concentration	125
7.7	Predictions of cell and substrate concentrations in a continuous system at steady state with multiple feed concentrations	126
7.8	Selection of wild type during continuous culture of genetically modified organisms with reversion	129
8.1	Possible resistances to oxygen transfer according to the Two Film Theory model	150
8.2	Oxygen concentration profile during the dynamic method in a system with respiring cells	163
9.1	Geometrically similar vessels: $H_2/T_2 = H_1/T_1$; $H_2/D_2 = H_1/D_1$	175

Published by Woodhead Publishing Limited, 2013

10.1 Influence of sterilisation temperature on efficiency of sterilisation 192
10.2 Dependence of thermal death and degradation rates on temperature 198
10.3 Thermal destruction of contaminating microorganisms as a function of the extent of destruction and extent of axial dispersion 203
11.1 Recovery of microbial products: an overview 212

Published by Woodhead Publishing Limited, 2013

List of plates

2.1 Filamentous fungal colonies showing spreading hyphae. The dark areas on the first two plates are fungal spores 14

6.1 A laboratory membrane reactor housing a ceramic support for enzyme immobilisation. Substrate fed into shell side, product from lumen side as permeate 88

7.1 Aeration showing bubble intensity highest around impellers 103

7.2 Flask cultures in a shaker incubator on the lab bench 104

7.3 Instrumented laboratory stirred tank reactor 105

7.4 A laboratory scale bubble column reactor 118

8.1 High speed photography of bubble diameter and size distribution in a bubble column reactor (camera at front) 153

8.2 Edge detection on original image and contrast mapping of detected bubbles 154

Published by Woodhead Publishing Limited, 2013

Preface

Biotechnology is an expansive field incorporating expertise in both the life science and engineering disciplines. In biotechnology, the life scientist is concerned with developing the most favourable biocatalysts, while the engineer is directed towards process performance, defining conditions and strategies that will maximise the production potential of the biocatalyst. Increasingly, the synergistic effect of the contributions of engineering and life sciences is recognised as key to the translation of new bioproducts from the laboratory bench to commercial bioprocess.

Fundamental to the successful realisation of the bioprocess then, is a need for process engineers and life scientists competent to evaluate biological systems from a cross-disciplinary viewpoint. This book aims to generate core competencies through an understanding of the complementary biotechnology disciplines and their interdependence, and an appreciation of the challenges associated with the application of engineering principles in a life science context. Its ultimate goal is to maximise the potential of the engineering approach when addressing concepts as diverse as process manipulation for enhancement of bioproduct accumulation, reactor design and scale up for peak process performance and the development of downstream protocols for optimal purification of biomaterials.

This book is primarily, but not exclusively, intended as a textbook for postgraduate or senior undergraduate students

Published by Woodhead Publishing Limited, 2013

and covers material suitable for a comprehensive semester course in Bioprocess Engineering. Initial chapters focus on the microbiology, biochemistry and molecular biology that underpin biocatalyst potential for product accumulation. The following chapters develop kinetic and mass transfer principles that quantify optimum process performance. The text is wide in scope, relating to bioprocesses using bacterial, fungal and enzymic biocatalysts, batch, fed-batch and continuous strategies and free and immobilised configurations.

Finally, I would like to acknowledge and thank the many who have provided invaluable insights during my travels through the field of Bioprocess Engineering. The late Professor Geoffrey Hansford (University of Cape Town, South Africa), Dr John Wase (University of Birmingham, United Kingdom) and Dr Terrence Watson (Centre for Scientific and Industrial Research, South Africa) deserve special mention. And to my graduate students over the years, thank you all for your hard work and dedication in moving the boundaries of current knowledge.

Kim G. Clarke, January 2013

About the author

Professor Kim Clarke is an academic in the Department of Process Engineering, University of Stellenbosch, and a registered Professional Engineer. She holds a PhD and BSc (Chemical Engineering), both from the University of Cape Town, South Africa, and an MSc (Biological and Chemical Engineering) from the University of Birmingham, United Kingdom. She has developed and lectured university courses in bioprocess engineering for over 15 years and has twice been a recipient of the University of Stellenbosch Award for Excellence in Education (2007 and 2010). In addition, she heads a research group in bioprocess engineering where her research profile focuses on the application of chemical engineering principles in the development and optimisation of biological processes. Her research is specifically directed towards fundamental kinetic and mass transfer studies which quantify the principles governing process performance and define process strategies for optimisation of the production potential of the biocatalyst.

Published by Woodhead Publishing Limited, 2013

1

Historical development: from ethanol to biopharmeceuticals

DOI: 10.1533/9781782421689.1

Abstract: Biotechnology has a long history, but rapid advances have been seen in the past forty years. This chapter provides a brief overview of bioprocesses, from 6000BC to the present day.

Key words: history, biotechnology, bioprocess engineering, advances, *Penicillium, Eschericia coli*.

Biotechnology is a fast expanding field frequently mooted as the new environmentally sustainable route to providing commercially viable alternatives to conventional chemical technologies. Yet biotechnology is deeply rooted in the past when traditionally food preservation and wine making dominated, with the earliest bioprocess recorded around 6000BC.[1] For over 7000 years, microorganisms provided sustenance (bread, yoghurt, cheese, vinegar, potable alcohol) under self-sustaining[2] conditions before their existence was known. In the late seventeeth century, with the invention of the microscope,[3] 300× magnification became possible and microorganisms were viewed for the first time. For about a hundred years after their discovery, microorganisms were believed to have arisen spontaneously from non-living

Published by Woodhead Publishing Limited, 2013

matter (dubbed the theory of spontaneous generation) and the enormity of the discovery of an entire new life form was completely overlooked. The theory of spontaneous generation was finally disproved in the mid 1800s[4] when microorganisms were demonstrated to come from pre-existing life and finally recognised as the causative agents facilitating the bioprocess. This discovery signalled the start of commercial bioproduction.

During the late nineteenth century, bioprocesses themselves were beginning to be understood. Initially bioprocesses in the West and East developed differently. In the West, submerged culture bioprocesses were established, while solid state or surface culture was developed in the East. With the new understanding of bioprocesses, the emphases changed from exclusively food-related products to include industrial products. Submerged culture was typified by ethanol, acetate, lactate and glycerol while surface culture produced fungal enzymes. At this stage, however, bioprocesses were still limited to those that were self-sustaining with little need and no regard for environmental control or asepsis.

The engineering of large scale bioprocesses was developed largely during the first half of the twentieth century in response to the needs of the two World Wars for bioprocesses which required stringent aseptic conditions and environmental control on an industrial scale. The first of these bioprocesses, the production of the solvents acetone and butanol by *Clostridium acetobutylicum*, was developed in 1915[5] to supply acetone for cordite and aeroplane dope during World War 1. This was historically the first bioprocess that was not self-sustaining. The environmental conditions together with the rich nutrients were suitable for a variety of competing microorganisms. For the first time, process equipment had to be developed to operate under strict asepsis and the process

Published by Woodhead Publishing Limited, 2013

conditions had to be controlled to optimise the yield of solvents by *C. acetobutylicum*.

Later, during World War II, butanol became the preferred product from this fermentation when it was used in the manufacture of synthetic rubber. After the wars, butanol was exploited extensively as a solvent in the nitrocellulosic lacquers used in the expanding automobile industry until the advent of cheap oil supplies rendered the biological route to butanol uneconomical in the USA. The acetone–butanol bioprocess remained commercially viable in South Africa where the solvents were produced from molasses,[6] until it was superseded by coal to liquid fuel technology[7] in the mid 1980s. Ironically, interest in the acetone–butanol process has recently resurged in the move to replace fossil fuels with microbially produced butanol, or biobutanol, as it has now become known.

The major advance in bioprocess development which occurred during World War 2 was the large scale production and purification of penicillin,[8] using the *Penicillium* mould discovered nearly 20 years earlier.[9] This introduced a new level of control since *Penicillium* spp., unlike *Clostridium* spp., require oxygen to grow and the technology for large scale aerobic bioprocesses was yet to be developed. Necessity being the mother of invention, the design of equipment was developed for the supply of considerable quantities of air during large scale aseptic operation. Another pivotal breakthrough in the success of penicillin production, and one not often realised, was the development of the downstream purification of the penicillin. A novel extraction process was devised,[10] using amylacetate as the solvent, by making use of pH to alter the distribution of penicillin between the aqueous and solvent phases.[11] In this process, the contact time of the penicillin and amylacetate was minimised with the use of centrifugal extraction.

Published by Woodhead Publishing Limited, 2013

At this stage, scale up was constrained to multiplication of elements. Penicillin was produced in small milk bottles, increasing the number of bottles to thousands in an attempt to meet the demand for this product. However, rapid advances in bioprocess development over the next 40 years saw the technology progress to more sophisticated engineered processes such as large scale submerged production of antibiotics, vitamins, amino acids and enzymes.

From the late 1950s isolated enzymes were used as biocatalysts. Initially, only extracellular enzymes were exploited, such as amylases and proteases for the hydrolysis of starch and proteins respectively. The first intracellular enzyme to be used commercially was xylose isomerase. Xylose isomerase, which catalyses the isomerisation of glucose to fructose, was used in conjunction with amylase for the production of fructose from corn starch. The abundance of corn in the 1970s provided the stimulus for large scale manufacture of sweet syrups[12] using this process.

Prior to 1960, bioprocesses were almost exclusively batch operations. A major advance of the 1960s was the development and optimisation of large scale continuous bioprocesses. A notable example was the production of yeast from hydrocarbons as single cell protein in the 1960s, intended for human and animal consumption, which contributed significantly to the advancement of bioprocess scientific and engineering knowledge. Unfortunately, protein for human consumption never realised its potential, with excessive regulatory controls and/or the cost of raw material held responsible. Nevertheless, numerous continuous processes enjoy success to date in a wide variety of industries. In the early 1980s, continuous processing spread to the mineral industry via the BIOX®[13] process for tank bioleaching of base and noble metals from sulphite ore, a process now extensively used worldwide.

Published by Woodhead Publishing Limited, 2013

After recombinant DNA technology was developed in the late 1970s, a new era of biotechnology was heralded. By the 1980s, genetic manipulation had removed many of the boundaries previously constraining the range of commercially viable bioproducts and bioprocess engineering advanced in great strides. Most notable of these early recombinant bioproducts is insulin, commercially manufactured using genetically modified *Escherichia coli*. Insulin was the first of the recombinant biopharmaceuticals and precipitated the now expansive biopharmaceutical market based on recombinant DNA technology.

Today, the biological route is frequently preferred over the chemical route. Bioprocess conditions are moderate and biocatalysts very specific so that comparatively few by-products are produced; further, bioprocesses are environmentally benign. Bioprocess-derived products are ubiquitous in diverse industries, including food and beverage, health care (therapeutics and diagnostics), cosmetic, agricultural, biomining, fuels (ethanol and butanol), bioremediation, mineral processing and waste treatment. In the future, biotechnology promises to broaden its impact further through its contribution to new technologies, one example being power generation without noxious combustion gases, such as biological hydrogen production for use in fuel cells.[14]

There has never been a time when the Bioprocess Engineer has been more indispensable to realising the future promise of biotechnology.

1.1 Notes

1. Fermentation of sugar to ethanol by the Babylonians and Sumerians.

Published by Woodhead Publishing Limited, 2013

2. The ideal natural environment for the fermentation of interest and unfavourable for competing microorganisms.
3. Antonie van Leeuwenhoek (1632–1723).
4. Louis Pasteur (1822–1895).
5. Chaim Weizmann (1874–1952), later the first president of Israel.
6. National Chemical Products, Germiston, South Africa.
7. SASOL, South Africa, world leaders in coal to liquid technology.
8. Howard Florey (1898–1968), Ernst Chain (1906–1979), William Heatley (1920–1971). Florey and Chain were awarded a Nobel prize in 1945 jointly with Alexander Fleming for their work on penicillin.
9. Alexander Fleming (1881–1955).
10. Attributed to William Heatley.
11. Low pH, penicillin acid dissolves readily in the amylacetate; high pH, penicillin salt moves rapidly out of the organic and into the aqueous phase.
12. Fructose is 1.5 times sweeter than glucose.
13. The BIOX® process, pioneered in Barberton, South Africa, for gold recovery, is currently operational world wide with plants in Brazil, Australia, West Africa, China and Uzbekistan.
14. Fuel cells produce power without combustion with water as the sole by-product.

Published by Woodhead Publishing Limited, 2013

2

Microbiology

DOI: 10.1533/9781782421689.7

Abstract: Bioprocesses can be largely classified into three stages: preparation, production and purification. Preparation frequently involves nutrient media and equipment sterilisation, while bioreaction kinetics, oxygen transfer and operational strategy are key to the production stage, as are separation operations to product purification. Central to the successful bioprocess is, however, not only the optimisation of these three stages, but also a biocatalyst which is capable of utilising substrate efficiently and forming the desired product with few or no by-products. Without this, the bioprocess will be constrained, despite the best efforts to maximise the upstream production kinetics and downstream product recovery. So, as the successful bioprocess begins with an effective biocatalyst, so should the Bioprocess Engineer start with developing a knowledge in microbiology, biochemistry and molecular biology relevant to bioprocess design, operation and scale up and the significance of these subjects in defining optimum bioprocess performance.

To this end, the initial chapters focus on the microbiology, biochemistry and molecular biology that underpin biocatalyst potential for product accumulation. Chapter 2 begins with an introduction to microbes which includes their classification, morphology, internal structures, and nutrient and energy requirements.

Published by Woodhead Publishing Limited, 2013

Key words: taxonomy, morphology, cellular structure, prokaryotes, eukaryotes, nutrients.

2.1 Microorganisms: the core of cellular bioprocesses

2.1.1 Taxonomy

All living species are classified according to a hierachical system[1] which groups like organisms into levels (called ranks or taxa), the most basic of which is the species.[2] This level is followed by the more general genus, a group of closely related species which have the same major characteristics but differ in minor ways. Genera are grouped into families, families into orders, which in turn are grouped into classes, then into phyla and then into what used to be the highest order, the kingdoms. Initially, five kingdoms were defined:[3] monera (bacteria and later, archaea), protists[4], fungi, plants and animals. The development of the electron microscope in the 1950s, however, revealed only two radically different types of internal cell structure (Section 2.2): the relatively simple prokaryotes or prokaryotic cells, comprising the bacteria, and the more complex eukaryotes, or eukaryotic cells, comprising the protists, fungi, plants and aminals.

With the advances in molecular biology, genetic similarity rather than outward apearance or behaviour became the primary means of classification. Molecular biology for instance led to the identification of a large genetic difference between the prokaryotic bacteria and archaea, previously grouped in the monera kingdom. Archaea were discovered to exhibit genes and some metabolic pathways that were closer to the eukaryotes than to bacteria. To take this into account, the monera kingdom was divided into the bacteria (or

Published by Woodhead Publishing Limited, 2013

eubacteria) and the archaea (or archaebacteria) kingdoms and the five kingdom model revised into the currently accepted six kingdom model with archaebacteria, eubacteria, protists, fungi, plants and animals making up the six kingdoms.

Later, an additional rank above that of the kingdom was introduced: the domain. All life forms were classified into three primary taxonomic domains according to similarity of genetic characteristics: eubacteria and archaebacteria (the prokaryotic cells) and eukarya (the eukaryotic cells), where eukarya included the protists, fungi, plants and animals.[5] Genetic evidence suggests that each of these domains ascended separately from a common univeral ancestor at the beginning of life on earth. Today it is widely accepted that archaea are the most ancient form of life linked to our evolutionary roots.

The branching diagram or Phylogenetic Tree of Life[6] represents the three primary lines of descent, each of which is divided into several distinct branches (or cladograms[7]) (Figure 2.1). The branches identify the evolutionary relationships between different species as defined by physical

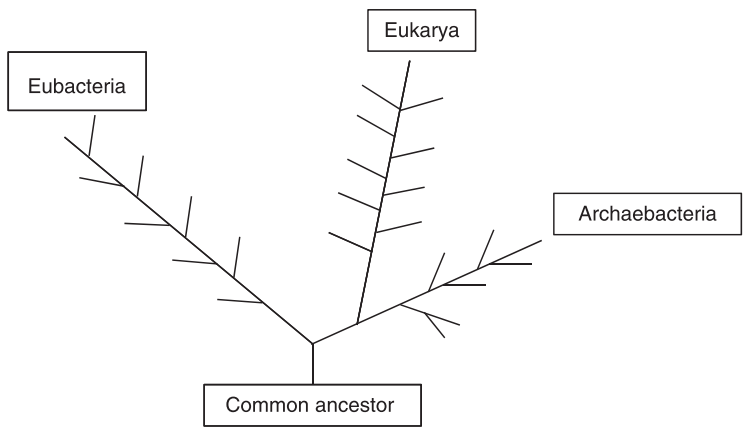

Figure 2.1 The Phylogenetic Tree of Life

Published by Woodhead Publishing Limited, 2013

and/or genetic similarities and differences, while the branch points (or nodes) represent points in evolution where the different ranks split from each other to form separate lineages or branches. This representation recognises the fundamental divide between the bacteria and the archaea, as well as the association between the archaea and eukarya.

All species are identified by their scientific name according to the Latin binomial system.[8] Binomial nomenclature is composed of both the generic and the specific names. The first letter of the genus is capitalised while all letters in the species are in lower case. Since they are both written in Latin, these names are always written in italics, or alternatively underlined, e.g. *Saccharomyces cerevisiae* (abbr. *S. cerevisiae*), a fungus which is arguably one of the most commercially significant microorganisms.

The most industrially important microorganisms are traditionally bacteria and fungi and the following chapters will for the most part concentrate on these microorganisms. However, mention should be made of the potential of archea for industrial bioprocesses. The ability of archaea to perform in adverse conditions[9] such as high temperatures (with advantageously high reaction rates) has generated increasing interest. Some archaea live optimally in environments considered the extreme limits of life. In fact, this has prompted many scientists to suggest that, should life exist on other planets, these life forms would be simlar to the extremophilic archaea. Existing examples of the use of archaea include *Sulfolobus*, acidothermophilic archaea which grow at an optimal temperature around 80°C and a pH below 3, used for bioleaching of Cu from sulphite ores, and *Methanopyrus,* a methanogen which can survive at a temperature of 120°C and has potential for both energy generation and CO_2[10] sequestration. Further, enzymes extracted from extremophilic archaea are particularly sought

Published by Woodhead Publishing Limited, 2013

after and scientists travel to extreme environments (e.g. Antarctica, Mammoth Hot Springs, USA) to collect and harness these thermophilic, halophilic and cryophilic treasures.

2.1.2 Microscopic morphology

2.1.2.1 Prokaryotes

Prokaryotes are unicellular microorganisms which replicate by binary fission only, resulting in daughter cells of identical morphology. Binary fission as the mechanism of replication is a fundamental assumption of Monod growth kinetics which predicts an exponential increase in cell concentration during non-limited growth in batch culture (Section 7.2.1). Monod growth kinetics is regarded as the basis for most biokinetic models and form the foundation of the majority of continuous and fed-batch bioprocess design equations (Sections 7.3 and 7.4).

The most common prokaryotic morphological types are spherical (cocci), rod-shaped (bacilli), curved (vibrios), spiral (spirilli), helical (spirochetes) and filamentous (actinomycetes). Bacterial sizes range in length from 1–2 μm for cocci to 1–10 μm for bacilli and up to 30 μm for the filamentous actinomycetes. The cells may exist singly or in pairs, chains or clusters. Cell size and goupings are important parameters when selecting appropriate solid/liquid separation operations during downstream processing (Section 11.2).

The prokaryotic bacteria are frequently able to sporulate where endospores, and later mature spores, develop under adverse environmental conditions. These non-vegetative forms are capable of germinating after exceedingly long periods (up to 20 years in soil) and are resistant to stress, especially high temperatures. In fact, short periods of high

Published by Woodhead Publishing Limited, 2013

temperatures can actually stimulate spores into vegetative growth. Some bacteria, e.g. *Bacillus stearothermophilus,* form spores which are particularly resistant to temperature. These and similar spores, if present, could compromise the effectiveness of media and equipment sterilisation prompting the use of *B. stearothermophilus* as the yardstick for the design of effective sterilisation procedures (Section 10.1).

Sporulation can also compromise process performance since dormant spores are incapable of forming product. For example, during batch production of butanol by *Clostridium acetobutylicum*, sporulation occurs at higher solvent concentrations, thus limiting butanol accumulation. Sporulation during continuous operation too has serious consequences. Since the sporulatng cell has ceased to divide, eventually the microorganism will be washed out of the system with zero product resulting (Section 7.3.1). Some organisms undergo cell elongation rather than sporulation during continuous culture (e.g. *C. acetobutylicum*), but since elongation is also a non-dividing morphology, the cells will similarly be lost to the system. In the case of elongating cells though, the cells may still form product. Hence, a strategy to retain the elongated cells in the continuous system, such as cell separation and recycle, or cell inmmobilisation, can be applied to render continuous operation feasible.

2.1.2.2 Eukaryotes

The most common eukaryotes in bioprocesses are the fungi. Fungi may be divided into two distinct morphological groups: filamentous and non-filamentous. The non-filamentous morphology is typified by yeasts, unicellular fungi with an oval shape 3–10 μm long, which usually reproduce by vegetative growth in the form of binary fission, budding or a combination of both. Some yeasts are dimorphic,

Published by Woodhead Publishing Limited, 2013

i.e. they can elongate to form strings of connected budding yeast cells (pseudohyphae) which can reach 30 μm in length. Cell growth by binary fission with budding is generally well approximated by Monod growth kinetics developed for binary fission (Section 7.2.1). However, to provide a clearer insight into the growth rate under these conditions, the degree of budding, or budding index, should also be quantified. On the other hand, the growth of dimorphic yeasts typically follow a linear rather than exponential model so the Monod growth kinetics developed for binary fission do not nessarily apply.

The filamentous fungi are characterised by multicellular branching filaments, or hyphae, which in most fungi are segmented by internal walls or septa. Filamentous fungi reproduce via elongation of the hyphae apical tips, or through germination of fungal spores (Plate 2.1). As with dimorphic yeasts, the growth mechanism is different from that of binary fission and cognisance should be taken of this difference when applying Monod growth kinetics.

Fungi (colloquially known as 'enzyme factories') are particularly important in enzyme production and their morphology plays a significant role in process optimisation. The hyphal conglomerate can form either a filamentous mass or microbial flocs (pellets) of 100 μm or more. Both morphologies can impact appreciably on the process performance. The filamentous mass tends to increase the culture viscosity, leading to heterogenous regimes and oxygen transfer limitation (Section 8.1) with concomitant reduced yields and productivities. The microbial flocs or pellets, on the contrary, tend not to alter the suspension properties, but they may lead to oxygen limitaion at the pellet core, resulting in hollow pellets and likewise a reduced capacity for product formation. The form the mycellia takes (filamentous or pellets) depends on the microorganism as well as the process

Published by Woodhead Publishing Limited, 2013

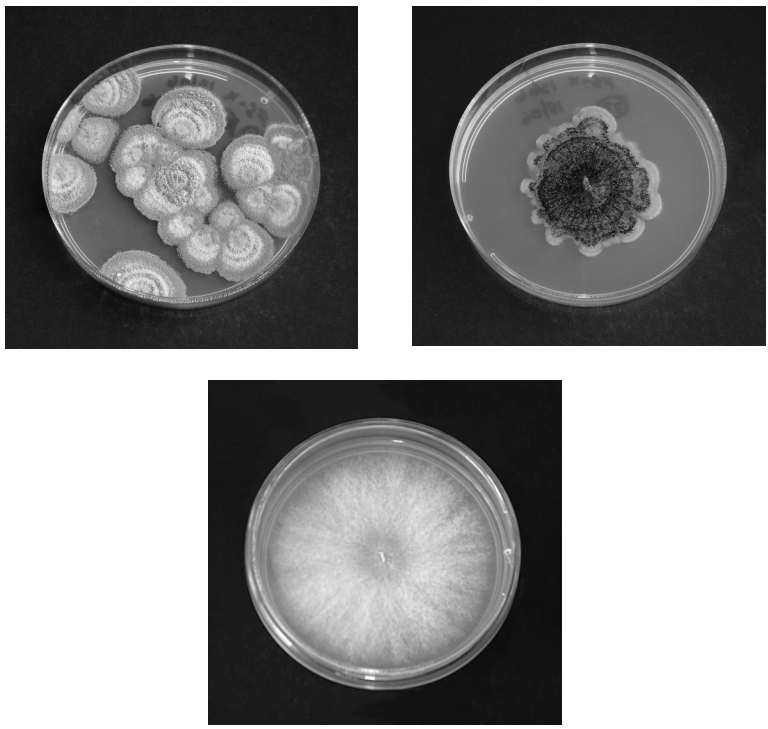

Plate 2.1 Filamentous fungal colonies showing spreading hyphae. The dark areas on the first two plates are fungal spores. Photo: J. van Rooyen

conditions (e.g. pH). For instance, *Penicilliun canescens* and *Aspergillus niger* exist as a filamentous mass and pellets respectively during production of glucose oxidase, an enzyme which serves as a diagnostic tool in blood glucose determination and as an additive to prevent rancidity in foods.

While filamentous morphology is known to have the potential to influence the production kinetics indirectly through its alteration of the fluid properties, it may also have a direct impact on product accumulation. When considering the walls of hyphae, the lateral walls have been shown to be

Published by Woodhead Publishing Limited, 2013

rigid with pores that are too small to allow excretion of large molecules such as enzymes. In contrast, the pores in the apical tips are considerably larger than those in the lateral walls, large enough for enzyme secretion. This suggests that the degree of enzyme secretion from the cells will be dependent on the proportion of apical tips (or branches) in the mycelium, and that modification of process conditions and strategy to maximise branching would enhance production of extracellular enzymes. Currently, this remains a hypothesis which has yet to be tested.

2.2 Cellular structure and sites of metabolic reactions

2.2.1 Prokaryotes

Prokaryotes are single cell organisms containing an amorphous cytoplasmic mass surrounded by a cell membrane and cell wall (Figure 2.2). The bacterial cell wall contains peptidoglycan (archaea contain pseudo peptidoglycan) which confers structural strength and protection against osmotic pressure. The cell membrane lines the cell wall with folds that permeate into the cytoplasm. It consists of a fluid phospholipid (Section 3.2) bilayer where the hydrophilic phosphate groups orientate towards the aqueous phases external and internal to the cell, thereby shielding the hydrophobic lipid ends. The membrane is impregnated with proteins, regulates transport of molecules in and out the cell, and is the site of respiratory (Section 5.1.2) and photosynthetic metabolic activity. Rupture of the cell membrane results in cell lysis; this forms the underlying mechanism of the biosurfactant group[11] of antimicrobials which rely on their surface active nature to disrupt the phospholipid bilayer.

Published by Woodhead Publishing Limited, 2013

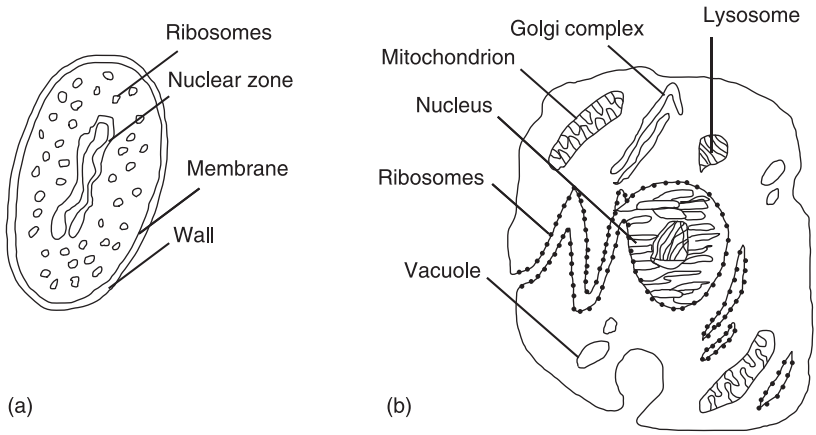

Figure 2.2 Intracellular structures of (a) prokaryotes and (b) eukaryotes

A double stranded DNA and ribosomes are housed in the cytoplasm. The DNA is reponsible for reproduction and transference of hereditary information (Section 4.1). Plasmids, or circular double-stranded DNA, can occur in bacteria. These plasmids are capable of replicating when transferred into a suitable host and are used in genetic manipulation (Section 4.3). There is no nuclear membrane (although the neoplasm is differentiated from the cytoplasm) or any other membrane-bound organelle. All cellular activity takes place within the cytoplasmic mass.

Some bacteria have a flagellum or flagella to confer mobility, while others produce extracellular capsules or slime layers. Bacterial slime layers usually result in increased complexity of downstream processing specifically with regard to cell separation (Section 11.2) and, in the case of an intracellular product, preparation of cell extracts (Section 11.3). Slime layers can also have significant effects on upstream processing where slime causes cells to adhere to surfaces. Attached cells may exhibit altered kinetics with

Published by Woodhead Publishing Limited, 2013

corresponding altered yields and productivities. On the other hand, attached cells in continuous processes could result in an increased system capacity for product formation through cell retention.

Bacteria are often differentiated into two large distinct groups, Gram positive or Gram negative (according to a diagnostic test),[12] depending on the constituents of their cell walls. Gram positive bateria have a relatively thick cell wall of more than 50% peptidoglycan while Gram negative bacteria have considerably less peptidoglycan (about 10%) and an additional outer lipopolysaccharide membrane. Gram positive bateria retain a crystal violet stain on decolourisation with acetone or alcohol whereas Gram negative bacteria lose the stain as the lipopolysaccharide membrane is removed by the solvent.

2.2.2 Eukaryotes

Eukaryotes are single or multicellular organisms with internal membrane bound organelles and compartmentalisation of cellular functions. While there is a wide variation between different eukaryotes, many share common features and components giving rise to the concept of a typical eukaryotic cell (Figure 2.2).

In fungal cells, a cell wall, the major component of which is a structural polymer, chitin, provides structural strength. The cytoplasmic membrane lining the cell wall is one of many membranes embedded in the cell. The cell nucleus is surrounded by a double membrane, the nuclear envelope, which extends to form the endoplasmic reticulum. The ribosomes, attached to the endoplasmic reticulum, are the site of protein synthesis. Membrane-enclosed organelles in the cytoplasm include the mitochondria, which house the respiratory and energy generation pathways for

Published by Woodhead Publishing Limited, 2013

the catabolism of carbohydrates (Sections 5.2.1 and 5.2.2) and fats (Section 5.2.3), the golgi complex which functions to transport compounds to other parts of the cell and to the cell surface, lysosomes, which contain hydrolytic enzymes which function in intracellular digestion, peroxisomes, which contain enzymes involved in removal of electrons and hydrogen, and vacuoles, which function to maintain internal hydrostatic pressure and to contain and export unwanted substances from the cell. Microorganisms, e.g. algae, which generate energy from light, contain chloroplasts which are the site of photosynthetic reactions.

Some filamentous fungi form a slimy extracellular polysaccharide especially towards the end of fermentation, possibly as a carbon store when nutrients such as nitrogen and/or phosphate are insuffient to allow full use of the available carbon. The slime tends to increase the pressure drop across the filter cake during downstream separation of the fungal mass (Section 11.2).[13] This is best avoided by harvesting before initiation of slime formation, as is done during production of penicillin by *Penicillium chrysogenum*.

2.3 Classification according to carbon and energy requirements

All microorganisms require carbon as a source for the synthesis of cellular constituents and an energy source for energy to drive the synthesis. Carbon sources for synthesis may be organic compounds (e.g. carbohydrates, fats) or inorganic compounds (e.g. CO_2). Energy sources may comprise organic compounds (as for carbon source), inorganic compounds (e.g. Fe, S, H_2) or light. Microorganisms have been classified according to their carbon requirements

Published by Woodhead Publishing Limited, 2013

for synthesis as heterotrophs (organic carbon) or autotrophs (inorganic carbon) (Figure 2.3). Heterotrophs and autotrophs have been further classified according to their energy source as chemo- (organic or inorganic compound) or photo- (light) heterotrophs or autotrophs.

By far the majority of industrial processes utilise chemo-heterotrophs. For this reason the cellular activity in the following chapters will concentrate on biochemical reactions which utilise organic compounds as both carbon and energy sources (Sections 5.1, 5.2 and 5.3). Nevertheless, some chemo-autotrophs, and to some extent some photo-autotrophs, have had major impacts in biotechnology and merit mention.

Currently, the most industrially important chemo-autotrophs are arguably *Acidithiobacillus ferrooxidans*, *Acidithiobacillus thiooxidans* and *Leptospirillum ferrooxidans*. These microorganisms are responsible for the bioleaching of noble (Au) and base (Fe, Cu, U) metals from ore which relies on the biological regeneration of the leach

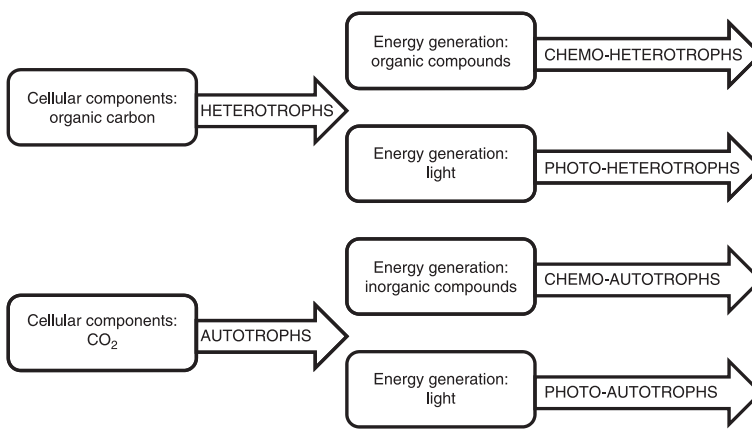

Figure 2.3 **Classification according to carbon and energy requirements**

Published by Woodhead Publishing Limited, 2013

solution by the oxidation of reduced Fe and/or S species in tanks or *in situ* in ore heaps. Heap bioleaching has facilitated recovery from low-grade ore for which tank bioleaching is not economically feasible. Use of the archaea *Sulfolobus* for bioeaching is more recent; these archaea similarly oxidise reduced Fe and S componds to obtain energy.

Another important group of chemo-autotrophs is the methanogenic archaea which utilise H_2 as their energy source. Methanogens are obligate anaerobes which produce CH_4 from CO_2 and H_2. For decades they have been mooted as a significant solution to the decreased availability of fossil fuel reserves. Their use has been widespread in the digestion of sewage sludge and other high COD[14] wastes. Large sources of microbial CH_4 generation have remained essentially untapped. Lake Kivu in central Africa is estimated to contain over 60 billion cubic metres of dissolved CH_4, thought to be produced by microbial reduction of volcanic CO_2. Projects are currently underway to safely harness the CH_4 for electricity generation in Rwanda in central Africa.

Photo-autotrophs which have enjoyed renewed interest include several species of algae used for biodiesel[15] production. These algae are adept at accumulating high internal concentrations of triglycerides, fatty acids esterified to glycerol (Section 3.2). Triglycerides are extracted from the algal cell and catalytically transesterified with methanol or ethanol to form methyl or ethyl fatty acid esters (biodiesel) and glycerol. Biodiesel has been mooted as potentially providing a secure alternative fuel from renewable resources. This process has the distinct advantage of being able to utilise used oils destined for disposal, and to produce glycerol as a by-product, which itself can serve as a substrate for biological conversion to a range of value added products.

Published by Woodhead Publishing Limited, 2013

2.4 Nutrient requirements

In addition to carbon, other nutrients are required for cell maintenance, growth, reproduction and product synthesis. A well balanced nutrient medium contains the elements carbon, nitrogen, phosphate and sulphur as well as traces of other elements with Mg, Mn, Fe and K being the most usual. Specific vitamins and/or amino acids also need to be added in some form if the microorganism is unable to synthesise these.

The most widely used carbon sources are the carbohydrates (simple and complex) and fats. Cellulose and hemicellulose have become more established as carbon sources through the push for ethanol and butanol production as fuels from renewable lignocellulosic sources.

Hydrocarbons also act as a carbon source during the biological remediation of hydrocarbon contaminated soil and water, a route which offers several advantages over physical and chemical treatment, not the least of which is an environmentally benign solution. Moreover, hydrocarbons themselves provide a carbon source with much promise. Alkanes, in large supply as by-products from gas to liquid technologies, can be converted to a broad range of value added products by a wide variety of microorganisms. Bioprocesses involving hydrocarbon substrates, however, introduce a number of process challenges, especially with respect to the supply of sufficient oxygen to the cells. The hydrocarbon molecule, unlike the carbohydrate molecule, typically contains no oxygen, thus the entire cellular requirement for oxygen has to be met by delivering oxygen to the cells via air sparging. The problem is exacerbated by an increased viscosity of the hydrocarbon-containing dispersion which augments fluid resistance, thus decreasing the rate of oxygen transfer (Section 8.1).

Published by Woodhead Publishing Limited, 2013

Microorganisms are able to use both inorganic and organic nitrogen sources, although one or the other is sometimes preferred by individual microorganisms. Inorganic nitrogen sources include NH_3, NH_4^+, NO_3^- and NO_2^-. Organic nitrogen sources such as yeast extract, peptone and whey not only contain nitrogen but also certain growth factors. A preference for an organic source may simply indicate a requirement for one or other amino acid or vitamin contained in the organic source. Amino acids and vitamins can be added separately to a nutrient medium containing inorganics only if required but this is expensive and so limited to small scale bioprocesses.

Nitrogen sources such as NO_3^- and NO_2^-, in addition to fulfilling their nutrient function, may be used by organisms which utilise anaerobic respiration to grow in the absence of oxygen (Section 5.1.2). *Bacillus subtilis*, a facultative microorganism[16] notable for the production of biosurfactants which exhibit antimicrobial activity, for instance will use a NH_4^+ nitrogen source as a nutrient in the presence of oxygen but will convert some to NO_3^- for use in anaerobic respiration in the absence of oxygen.

A number of minerals besides nitrogen are necessary to ensure proper functioning, the most important one being phosphate. This is frequently added in the form of the potassium salts, KH_2PO_4 and K_2HPO_4, their Na counterparts, or a mix of the two. Occasionally NH_4PO_4 is used which adds both nitrogen and phosphate. The choice of phosphate salt depends mainly on two aspects: the organism may respond poorly to high concentrations of the accompanying cation (e.g. there is a threshold maximum K concentration for *B. subtilis*) or the buffering capacity afforded by the salt(s) is insufficient. Other minerals are usually supplied in trace amounts, either as a defined trace element solution or as additives in tap water.

Published by Woodhead Publishing Limited, 2013

2.5 Notes

1. Taxonomy has its roots in the work of Carolus Linneaus (1707–1778) who grouped species according to their physical characteristics. After publication of *The Origin of the Species* by Charles Darwin in 1859, taxonomy changed to encompass all aspects of evolutionary knowledge.
2. A species is defined as a population of organisms that have a high degree of genetic similarity. In organisms which reproduce sexually, a species is generally accepted as a group of organisms that interbreed.
3. Proposed by Robert Whittaker (1920–1980) in 1969.
4. Unicellular organisms (e.g. algae, protozoa).
5. The three domain system was introduced by Carl Richard Woese (b. 1928) who defined archaea as a new taxonomic domain.
6. Elucidated and redrawn by Carl Woese to recognise the fundamental divide between the bacteria and the archaea.
7. A clade is a branch containing a common ancestor and all subsequent descendants.
8. Carolus Linneaus introduced the binomial method for the scientific naming of every species.
9. E.g. hot sulphur springs, hot deep sea hydrothermal vents and salt lakes.
10. Desired as a form of greenhouse gas reduction.
11. Biosurfactants comprise a hydrophobic lipid chain attached to a hydrophilic group, e.g. sugar (rhamnolipids) and protein (lipoproteins).
12. Developed by Hans Christian Gram (1850–1938).
13. Filamentous fungi are almost exclusively separated by filtration.
14. Chemical oxygen demand, a measure of pollution load.
15. A lipid-based fuel comprising long chain alkyl esters which can be used in diesel engines, either alone or blended with petrodiesel.
16. Able to adapt their metabolism to grow in either an aerobic or anaerobic environment.

Published by Woodhead Publishing Limited, 2013

3

Metabolic macromolecules

DOI: 10.1533/9781782421689.25

Abstract: The microorganism, biocatalyst to all cellular bioprocesses, grows to suit its own purposes: to survive and to prosper. To do this, the microorganism brings about biochemical change by metabolising nutrients to generate energy and/or precursors, and to synthesise cellular components. Biochemical changes take place in a series of intermediate steps, each catalysed by a specific enzyme, and are referred to as the metabolic pathways or the metabolism of the microorganism.

In the bioprocess, however, the needs of the microorganism to live and reproduce are replaced by the drive to enhance product formation. Process conditions are manipulated so that the microorganism is exploited to overproduce the desired product and maximising the production potential of the microorganism becomes the core focus.

Maximising production potential requires knowledge of engineering principles to predict and enhance process performance. However, to apply engineering principles appropriately in a biotechnology context requires an appreciation of the complexities and challenges associated with processes relying on living organisms, or biologically active molecules extracted from living organisms, as catalysts. It becomes expedient then for the Bioprocess Engineer to develop an understanding of the biochemical

Published by Woodhead Publishing Limited, 2013

reactions which make up the microbial metabolic pathways (Sections 5.1, 5.2 and 5.3).

Metabolic pathways involve a number of specific macromolecules and it is useful to first understand the structure and function of each before elucidating the pathways. In Chapter 3, the macromolecules in the cell cytoplasm are described and their purpose and functionality in the different metabolic pathways discussed.

Key words: carbohydrates, lipids, proteins, nucleotides, nucleic acids.

3.1 Carbohydrates

The most common organic compounds utilised as a carbon and energy source are the carbohydrates. Carbohydrates are mono- or polyhydroxyaldehydes or ketones with the generic formula $(CH_2O)_n$ (Figure 3.1). The monohydroxyaldehydes or ketones are simple carbohydrates known jointly as monosaccharides. Monohydroxyaldehydes, or aldoses, each contain an aldehyde group (HC = 0), e.g. glyceraldehyde, ribose, xylose and glucose. Monohydroxyketones, or ketoses, each contain a ketone group (C = O), e.g. dihydroxyacetone, fructose and sorbose. Aldoses and ketoses found in living organisms have three to seven carbon atoms and all exist as the D-stereoisomers, i.e. the hydroxyl group on the carbon furthest from the aldehyde or ketone group is configured towards the right.

Aldoses and ketoses are usually written in the pyranose[1] (or ring) form in metabolic pathways, e.g. D-glucose is converted to D-glucopyranose (Figure 3.2). In the pyranose form, the hydroxyl group on C_1 can exist in either the α-form (downwards) or the β-form (upwards).

Published by Woodhead Publishing Limited, 2013

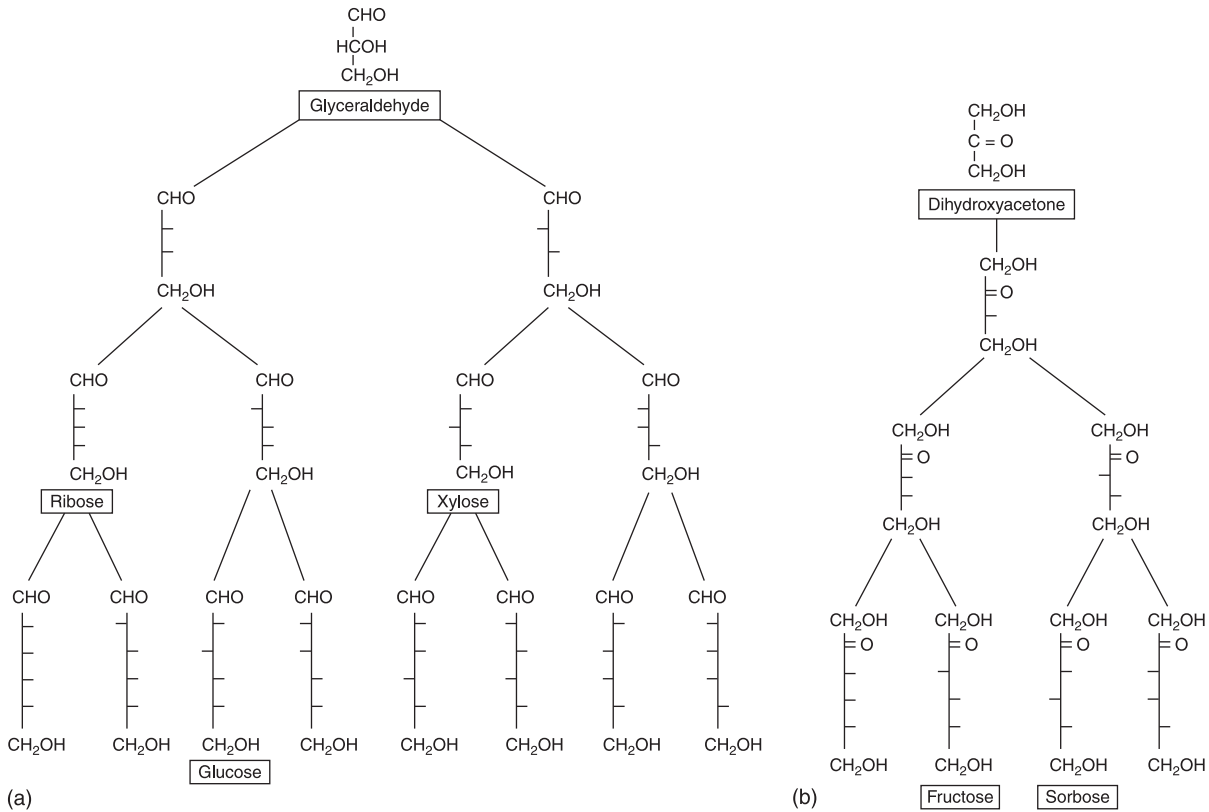

Figure 3.1 The families of D-aldoses (a) and ketoses (b) from three to six carbon atoms

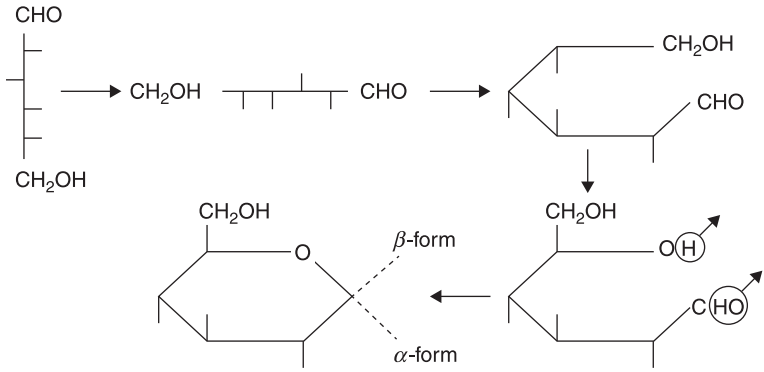

Figure 3.2 Conversion of D-glucose from straight chain to pyranose form

Polyhydroxyaldehydes or ketones are complex carbohydrates, known jointly as polysaccharides, which consist of monosaccharide chains. The shortest chains are the disaccharides, comprising only two monosaccharide units, the most common being sucrose (glucose plus fructose), lactose (glucose plus galactose) and maltose (two glucose units). Disaccharides are monosaccharides joined by α-1,4 bonds, e.g. sucrose comprises α-1,4 linked glucose and fructose (Figure 3.3).

Starch and cellulose are longer chain polysaccharides. Starch is made up from amylose and amylopectin. Amylose comprises linear glucose chains joined by α-1,4 bonds while

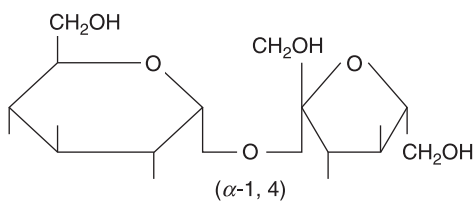

Figure 3.3 Sucrose

Published by Woodhead Publishing Limited, 2013

amylopectin is branched with α-1,6 bonds at the branch points which occur around every 25 glucose units (Figure 3.4). Glycogen[2] is similar to amylopectin, but is more highly branched.

Cellulose, in contrast to starch, comprises glucose chains where the molecules are joined by β-1,4 bonds (Figure 3.5). Hemicellulose, xylose joined by β-1,4 bonds with side chains of arabinose, is often found with cellulose bound together with lignin[3] into a stiff lignocellulosic network. Consequently, cellulose, hemicellulose and starch are metabolised by different enzymes. Cellulose is hydrolysed by one or more of a suite of enzymes, collectively known as cellulases, which

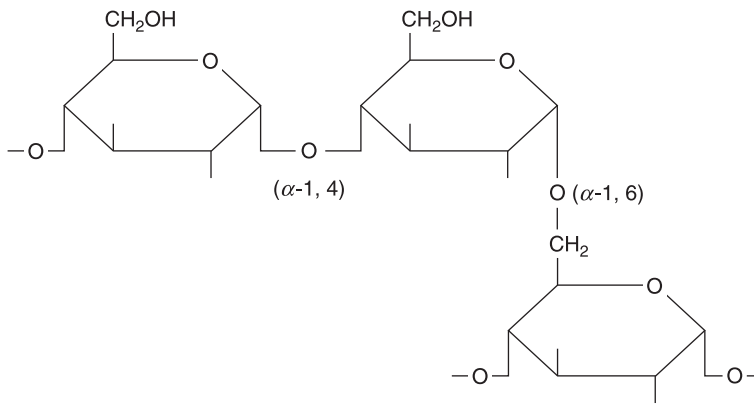

Figure 3.4 Starch

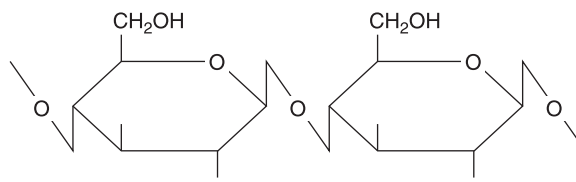

Figure 3.5 Cellulose

Published by Woodhead Publishing Limited, 2013

catalyse the hydrolysis of the β-1,4 bonds. Starch is reduced to glucose and α-1,4 and α-1,6 linked glucose units by α- and β-amylases which catalyse the hydrolysis of the α-1,4 bonds.

Amylases, produced primarily by *Bacillus* spp. as well as fungi (especially *Aspergillus*), were the first enzymes to be used industrially and today have broad based applications. Cellulases have received renewed prominence in the goal for short chain alcohols (ethanol and butanol) as renewable fuel alternatives since they release glucose from lignocellulosic materials for use as a substrate. Cellulases are normally produced by fungi, with *Trichoderma reesei* regularly the fungus of choice.

Before assimilation into metabolic pathways (Sections 5.2.1 and 5.2.2), polysaccharides are separated into their component monosaccharides by enzymic action.

3.2 Lipids

Lipids consist of a fatty acid or molecule with a fatty acid component. The fatty acids are made up of a hydrocarbon chain with a terminal carboxyl group. In living organisms, fatty acids typically have an even number of carbon atoms between 12 and 24. They are found as simple saturated (e.g. palmitic acid) or unsaturated (e.g. linoleic acid) long chain fats, or compound fats which are simple fats combined with sugars (e.g. glycolipids) or phosphates (e.g. phospholipids). Phospholipids function as structural components in the cell membrane of the microorganism (Section 2.2). The phospholipid structure comprises a hydrophilic fatty acid chain esterified to each of two adjacent hydroxyl groups on a glycerol molecule, with a phosphate group esterified to the remaining hydroxyl group on the glycerol

Published by Woodhead Publishing Limited, 2013

and an organic molecule (e.g. choline) esterified to the phosphate group.

Fatty acids provide storage of excess carbon and energy in the cell in the form of triglycerides, i.e. three fatty acids esterified to a glycerol molecule. When required, the fatty acids are metabolised through β-oxidation (Section 5.2.3) and the tricarboxylic acid cycle (TCA cycle) (Section 5.2.2) to produce energy via adenosine triphosphate (ATP) generation (Section 5.1). Some microorganisms obtain their energy directly from fats (Section 5.2.3), being unable to metabolise carbohydrates through glycolysis (Section 5.2.1). In these microorganisms, glucose is produced via a pathway known as gluconeogenesis (Section 5.3.2) which is essentially a reversal of glycolysis.

3.3 Proteins

Proteins not only form an integral structural cell constituent, they are also key to the functionality of all biochemical pathways, and so to life itself. For all enzymes are proteins, without which no reactions would take place, no metabolic pathways would be possible and life as we know it would cease to exist.

All proteins comprise a specific sequence of their basic units, the amino acids, linked together with amine bonds into polypeptide chains. Amino acids are organic molecules comprising an α-carboxyl (–COOH) and an α-amino ($-NH_2$) group but differ in the chemical nature of their side chains substituted on the α-carbon atom, each specific to one of the 20 available amino acids. Amino acids are often classified according to the polarity of their side chains. Cysteine is unusual in that it can form disulphide bonds with other cysteine residues by oxidation of its thiol groups

Published by Woodhead Publishing Limited, 2013

(–SH). This property is frequently exploited in the preparation of nutrient media for strict anaerobes; the high temperatures used for sterilisation (Section 10.1) cause the disulphide bond to form with consequent reduction of the medium.

Polypeptide chains are formed by dehydration between the amino group of a L-amino acid[4] with the carboxyl group of another. One hundred or more amino acids are linked together with covalent peptide bonds in various specific sequences in the polypeptide chain with polypeptide chains combining to form a protein. Every protein has at least one stable three-dimensional configuration. This configuration is determined by its primary and secondary structures, and where applicable, also its tertiary and quaternary structures. The primary protein structure is defined by the linear sequence of amino acids in the polypeptide chain and the secondary structure by the arrangement of these chains into pleated sheets or α-helices. The secondary structure is stabilised by H_2 bonding between the hydrogen on the amino group and oxygen on the carboxyl group of the amino acids, by oxidation of the thiol groups of the cysteine amino acids forming disulphide links, ionic bonding between the carboxyl and amide groups or by hydrocarbon side chain interaction. Proteins which are ordered into pleated sheets with parallel and extended chains are fibrous proteins with structural functions while those which exist as α-helices have biological activity. The tertiary and quaternary structures are associated with biologically active proteins (enzymes), the former referring to the convolution of the helical strand and the latter to the arrangement of several convoluted coils within a group.[5] Ultimately, then, it is the primary structure of the protein that defines its functionality.

The tertiary and quaternary enzyme structures are positioned such that the active sites are located for optimum catalytic activity. Interference of the native[6] structure of an

Published by Woodhead Publishing Limited, 2013

enzyme (or denaturation) destroys its biological activity. This is the main mechanism which underpins sterilisation (Section 10.1); the enzymes of the contaminants are denatured, the metabolic pathways come to a halt and the contaminants lyse. This is also the reason that steam sterilisation is almost exclusively the sterilisation method of choice on a large scale since protein structure is more susceptible to damage when in the hydrated form. This heat labile nature of the enzyme serves also as a red flag when processing enzymes during downstream concentration and purification programmes (Section 11.4). Extreme caution should be exercised to prevent denaturation of the enzyme (especially concerning pH and temperature limits) when deciding on appropriate unit operations, or the value of the product will be squandered.

Proteins may be classified as simple (amino acids only) or conjugated when combined with other molecules such as sugars or lipids. Conjugated proteins play a number of key roles such as the lipopeptides produced by *Bacillus* spp. These lipopeptides have in common a cyclic protein head attached to a lipid chain and exhibit strong antimicrobial activity towards bacteria and fungi (depending on the specific lipopeptide). Organisms, particularly *Bacillus* spp., producing lipopeptides are broadly used as phytotoxic agents in the agricultural industry.

3.4 Nucleosides, nucleotides and nucleic acids

3.4.1 Nucleosides and nucleotides

The basic block of a nucleotide is the nucleoside, comprising a five carbon aldose, ribose (or its deoxy form, deoxyribose),

Published by Woodhead Publishing Limited, 2013

and a nitrogenous base joined at the C_1 position on the aldose. The nitrogenous bases are derived from the parent compound, purine or pyrimidines (Figure 3.6). The pyrimidine derivatives are cytosine (4-amino-2-oxopyrimidine), thymine (5-methyly-2,4-dioxopyrimidine) and uracil (2,4-dioxopyrimidine) and the purine derivatives, adenine (6-aminopurine) and guanine (2-amino-6-oxopurine).

Nucleotides are formed from nucleosides by the esterification of inorganic phosphate to the C_5 on the aldose. Specific nucleotides, namely nicotinamide dinucleotide (NAD^+),[7] flavin adenine dinucleotide (FAD) and the adenosine phosphates, are essential to energy generation, storage and transfer (Section 5.1).

The adenosine phosphate nucleotides have ribose as the five carbon sugar and adenine as the nitrogenous base. These nucleotides differ in the number of inorganic phosphate groups phosphorylated to the ribose, which can vary from one to three. Adenosine triphosphate (ATP) contains three phosphate groups, adenosine diphosphate (ADP) two and adenosine monophosphate (AMP) one (Figure 3.7).

The NAD^+ and FAD nucleotides are actually known as dinucleotides because each of these molecules contains two nucleotides joined through phosphodiester bonds. These

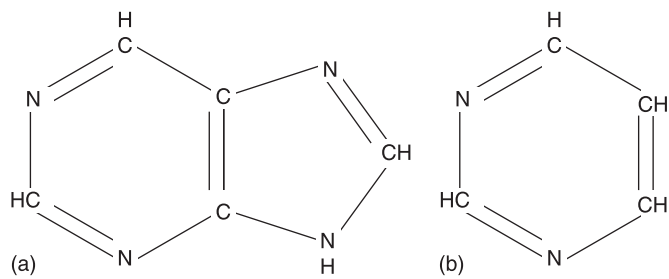

Figure 3.6 The parent purine (a) and pyrimidine (b) compounds

Published by Woodhead Publishing Limited, 2013

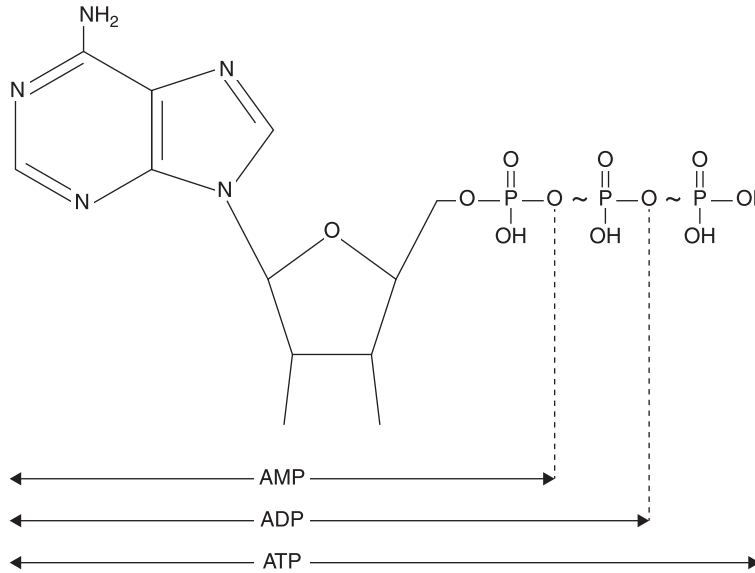

Figure 3.7 **Adenosine mono-, di- and triphosphate (~ indicates a high energy bond)**

nucleotides also contain prosthetic groups[8] which take part in reactions. In the case of NAD^+, the prosthetic group is nicotinamide, while in FAD the dimethyl alloxazine functions as the prosthetic group (Figure 3.8). The dimethyl alloxazine together with its bonded ribitol is known as riboflavin, or vitamin B2.

Another majorly important nucleotide is co-enzyme A (CoA)[9] which plays a central role in the oxidation of glucose via the TCA cycle (Section 5.2.2) and the oxidation (Section 5.2.3) and synthesis (Section 5.3.1) of fats. Adenine, ribose and pantothenic acid (vitamin B5) make up the components of CoA, but it is the terminal thiol group (–SH) which takes part directly in the metabolic reactions (Figure 3.8). Consequently, the molecule is usually abbreviated to CoA-SH.

Published by Woodhead Publishing Limited, 2013

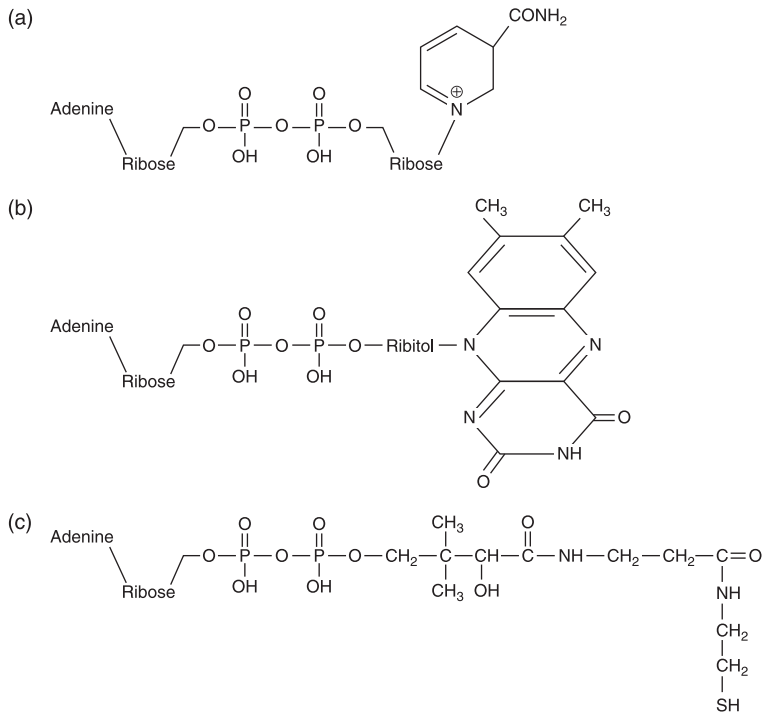

Figure 3.8 Nicotinamide adenine dinucleotide (a), flavin adenine dinucleotide (b) and co-enzyme A (c)

3.4.2 Nucleic acids

Nucleic acids comprise chains of nucleotides joined by phosphodiester bonds. There are two types of nucleic acids: ribonucleic acid (RNA) and deoxyribonucleic acid (DNA). RNA is formed from nucleotides containing ribose with adenine, guanine cytosine or uracil as a base. DNA is formed from nucleotides containing deoxyribose with likewise adenine, guanine and cytosine as bases but which have thiamine in place of uracil.

Nucleic acids are formed by the polymerisation of the nucleotides, catalysed by DNA polymerase or RNA

Published by Woodhead Publishing Limited, 2013

polymerase. The phosphodiester bond joins the 3′-carbon of one nucleotide to the 5′-carbon of the next (Figure 3.9). RNA is stable as single strands while DNA is more stable as two antiparallel strands bonded together. Two hydrogen bonds link the bases adenine and thiamine, three link cytosine and guanine. In the DNA molecule adenine and thiamine are known as complementary base pairs as are cytosine and guanine. The double stranded DNA is convoluted into a double helix at its most stable form, held together by the intermolecular hydrogen bonds of its complementary base pairs.[10]

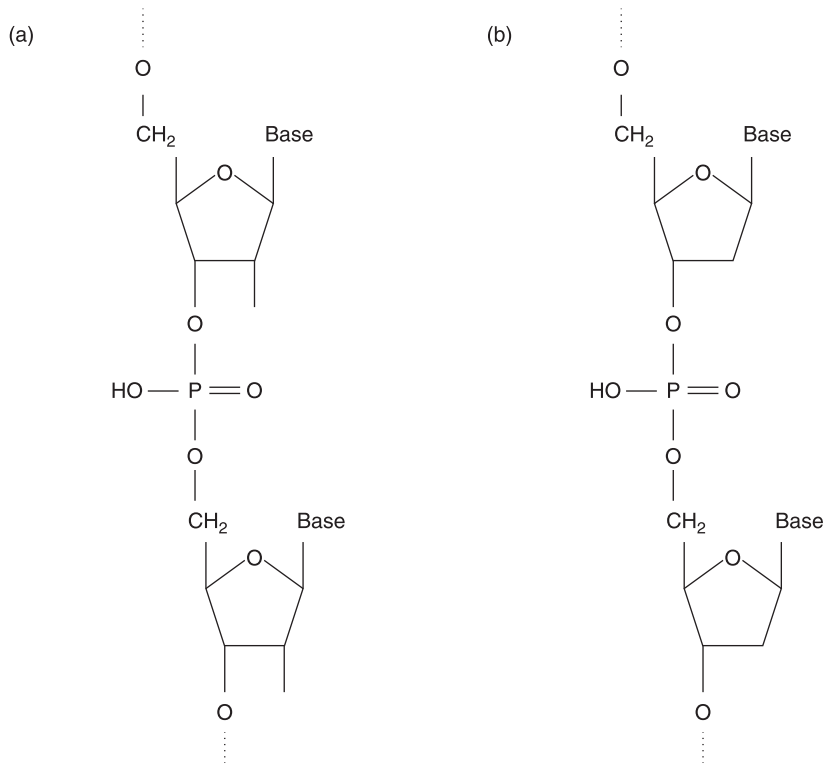

Figure 3.9 The nucleotides RNA (a) and DNA (b)

Published by Woodhead Publishing Limited, 2013

The sequence of nucleotides in the DNA is what ultimately determines the sequence of amino acids in the proteins. As all enzymes are proteins, it is the DNA in the first instance that dictates which enzymes are produced and consequently, the biochemical reactions which they catalyse. The DNA, therefore, serves to store the genetic information for the reproduction, development and functioning in all known forms of life (Section 4.1).

3.5 Notes

1. Five carbon and one oxygen form the ring structure.
2. Glycogen serves as an energy storage in eukaryotes.
3. A high molecular mass heterogeneous organic polymer.
4. Only the L-stereoisomers are found in living organisms.
5. The convolution of the helices and their grouping gives rise to a spherical or ellipsoidal protein configuration coining their naming as globular proteins.
6. Naturally most stable configuration.
7. A nucleotide analogous to NAD^+, nicotinamide dinucleotide phosphate ($NADP^+$), occurs in specific reactions. In this molecule, the ribose attached to the adenine is phosphorylated. NAD^+ and $NADP^+$ are sufficiently different as to not be interchangeable.
8. Prosthetic groups are non-protein molecules, tightly bound to enzymes, which render the enzyme biologically active.
9. Co-enzymes are non-protein molecules which render the enzyme biologically active and detach from the enzyme after reaction.
10. James Watson (b. 1928) and Francis Crick (1916–2004) deduced the double helix structure of the DNA.

Published by Woodhead Publishing Limited, 2013

4

Molecular biology

DOI: 10.1533/9781782421689.39

Abstract: The classical genetics[1] of the 1970s was the forerunner of modern molecular biology. Since its inception, molecular biology has been acknowledged as a paradigm shift in biotechnology. Today, the nucleotide sequence of entire genomes[2] of several organisms has been determined. The first sequencing was completed on *Haemophilus influenza* in 1995, the number of organisms which have had their genomes sequenced since growing almost exponentially.[3]

Certainly, the advances in molecular biology have transformed bioprocesses by *inter alia* broadening the spectrum of prospective bioproducts that can be produced and by increasing the potential of the organism for product accumulation. For this reason, it is expedient for the Bioprocess Engineer to be well positioned to embrace the opportunities afforded by the genetically modified microorganism (GMO), as well as to identify and address the process challenges introduced. The multidisciplinary nature of bioprocess engineering is no more evident than when working with GMOs and life scientists and engineers need to be able to effectively manage the attendant opportunities and challenges of the development of the process from genetic modification of the microorganism to process modification and strategy for optimum yields and productivities. In Chapter 4, the basics of molecular

Published by Woodhead Publishing Limited, 2013

biology is presented to provide a primary understanding and to facilitate meaningful interaction between the disciplines.

Key words: replication, transcription, translation, regulation, modification.

4.1 Replication, transcription and translation

4.1.1 Replication

The genetic information contained in the sequence of nucleotides in the DNA (Section 3.4.2) is transferred to the progeny during replication. During replication, the two helical strands of the parent DNA duplex uncoil[4] and separate, forming a replication fork from which synthesis of two daughter DNA strands takes place, each parent strand forming a template for a daughter strand. These daughter strands are built by linking deoxyribonucleotides to the free 3′-hydroxy end of the DNA strand with phosphodiester bonds,[5] such that the bases on the daughter DNA strands are complementary to those on the parent templates.[6] As the synthesis of each daughter strand continues, the parent DNA duplex continues to unwind. At termination, the daughter duplexes each contain one strand of the parent DNA and one strand of the newly synthesised DNA. Since the two strands of the parent duplex are complementary, the two daughter duplexes are duplicate copies of the parent duplex with identical genetic information. In this way, the DNA serves to transfer the genetic information to the next generation. This process is fast (e.g. about 10^3 nucleotides per second per fork in *E. coli*) and accurate (e.g. error occurring in $1/10^8$ to $1/10^{10}$ nucleotides).

Published by Woodhead Publishing Limited, 2013

However, in order for the genetic information contained in the DNA to be expressed in the cell, it has to undergo two further processes: transcription (Section 4.1.2) and translation (Section 4.1.3). Both transcription and translation are ultimately controlled by enzymes that recognise specific nucleotide sequences.

4.1.2 Transcription

The RNA is responsible for the implementation of the genetic information as the genetic information contained in the nucleotide sequence of the DNA is transcribed into messenger RNA (mRNA).[7] Transcription is accomplished by the synthesis of mRNA from a template strand of DNA[8] by linking ribonucleotide residues with phosphodiester bonds according to appropriate base pairing.[9] In this case, only one of the DNA strands is used as a template as mRNA is a single stranded nucleic acid.

Thus, the genetic information contained in the DNA is copied into mRNA by forming a complementary copy of the DNA sequence. The mRNA then carries this base sequence to the ribosomes where protein synthesis takes place. Here, the genetic information contained in the mRNA is translated to produce a specific polypeptide chain (Section 4.1.3).

4.1.3 Translation

The genetic information transcribed into the mRNA is expressed by means of a triplet code which is translated into a polypeptide chain by the transfer RNA (tRNA). In this code, three bases on the mRNA form a coding group (known as a codon) which codes for a specific amino acid. The tRNA

Published by Woodhead Publishing Limited, 2013

has a loop comprising three nucleotides with bases complementary to those of the codon (known as an anticodon) and, in addition, an acceptor arm which binds with the amino acid specific to that anticodon. Each tRNA functions to transport its bonded amino acid to the ribosomal RNA (rRNA),[10] the structural component of the ribosomes, for incorporation into the polypeptide chain.

The theory of the triplet code was deduced from the number of amino acids that could be coded for by four bases. Fewer than three bases would not be enough to code for 20 amino acids,[11] so the minimum number of bases had to be three. This, however, would theoretically provide 64 combinations, which means that there is some redundancy. The redundancy has been accounted for in that various codons are known to code for the same amino acid[12] and that some codons are used for punctuation to initiate or terminate an amino acid sequence.

Even before the mRNA has been completely transcribed from the DNA in the nucleus, the genetic information in the mRNA is translated into a polypeptide chain on the ribosomes (Figure 4.1). A start codon on the mRNA signals the initiation of translation with the first amino acid (usually AUG[13] which codes for the amino acid methionine). The mRNA is aligned with the P (peptidyl) site on the ribosome and the tRNA is bound to this P site and to the mRNA by hydrogen bonding between the codon of the mRNA and its anticodon. The unoccupied adjacent A (aminoacyl) site is aligned with the next codon of the mRNA and the anticodon of the next tRNA binds to the A site and to the codon of the mRNA in the site. The first amino acid is then transferred from its tRNA to form a peptide bond with the second amino acid. The mRNA advances one codon and the tRNA that was previously located at the P site is moved to the E (exit) site, from where it is released. The tRNA that was formally

Published by Woodhead Publishing Limited, 2013

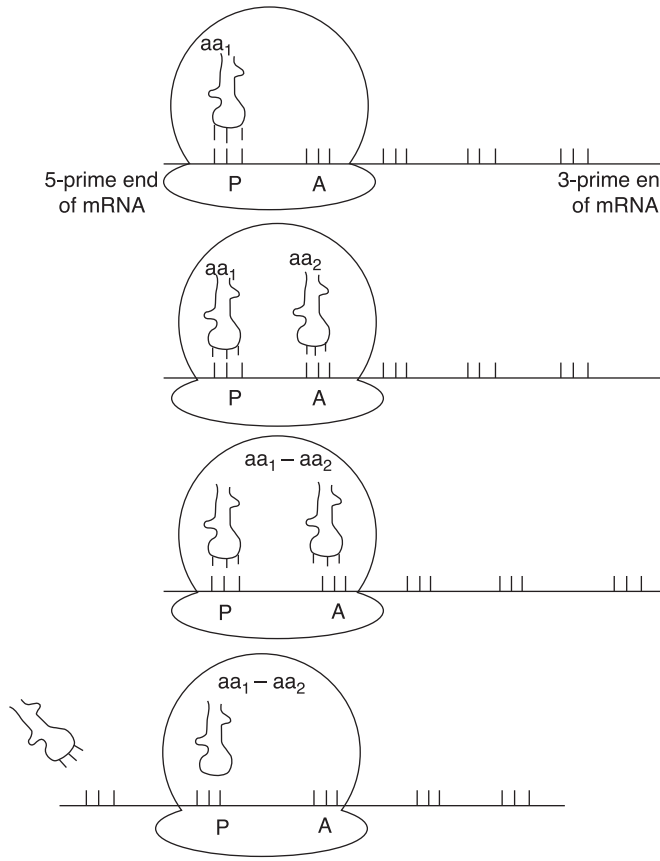

Figure 4.1 Protein synthesis

bonded to the A site now moves into the P site. The A site becomes free to attract another tRNA and the process is repeated. Elongation of the polypeptide chain continues[14] until the stop codon of the mRNA (usually UAA, UGA or UAG)[15] enters the A site, signifying the termination of translation. The polypeptide chain is released and the ribosome dissociates from the mRNA.

In this way, the genetic information contained in the DNA and transcribed into the mRNA translates into a specific

Published by Woodhead Publishing Limited, 2013

polypeptide and hence ultimately defines the functioning and regulation of the cell.

The sequence of DNA nucleotides that code for a specific polypeptide is called a gene. Adjacent genes are generally transcribed into one mRNA that may code for more than one polypeptide.

4.2 Genetic regulation

All biochemical reactions in the cell are catalysed by enzymes. To avoid chaos, hundreds of enzymes must act in a highly coordinated manner so that the cell does not waste energy or overproduce unnecessary metabolites. Consequently, the cell regulates its enzymes in response to prevailing environmental conditions to maximise its potential for survival.

While regulation is essential for the microorganism to perform optimally in its natural environment, to the Bioprocess Engineer who would prefer a wasteful microorganism, i.e. one that would overproduce the required metabolite, it is often a headache. To push the microorganism to overproduce, an understanding of the mechanisms of enzyme regulation is necessary. This understanding can inform on ways to manipulate the environmental conditions to be more conducive to overproduction.

There are two main mechanisms of enzyme regulation: regulation of enzyme activity and regulation of enzyme synthesis. The regulation of enzyme activity refers to the stimulation or inhibition of enzymes already synthesised to alter their activation energy. This is discussed later (Section 6.2). Regulation of enzyme synthesis, on the other hand, refers to the control of enzyme synthesis at the level of transcription. Enzyme synthesis can be switched on

Published by Woodhead Publishing Limited, 2013

(activated) or off (repressed), with consequent corresponding variations in enzyme concentration. The regulation of enzyme synthesis in bacteria is discussed below.

There are several distinct enzyme systems in prokaryotes: constitutive enzyme systems in which the enzymes are synthesised at constant rates regardless of the metabolic state of the cell, and adaptive enzyme systems in which the rate of synthesis is regulated by the environmental conditions. In adaptive enzyme systems, regulation is accomplished by controlling the initiation of DNA transcription by interacting with the operon on the DNA. The operon is a section of DNA containing a number of structural genes (S), a promoter gene (P) and an operator gene (O) (Figure 4.2). The structural genes contain nucleotide sequences that will be transcribed together into an mRNA strand for eventual translation into specific polypeptides. The promoter, a section of DNA upstream of the structural genes, contains a nucleotide sequence for the binding of the RNA polymerase and a sequence for the first bases to be transcribed. The structural genes are under the control of a single promoter and consequently, transcription of all the structural genes in an operon is expressed together or not at all. Transcription of the structural genes is regulated by

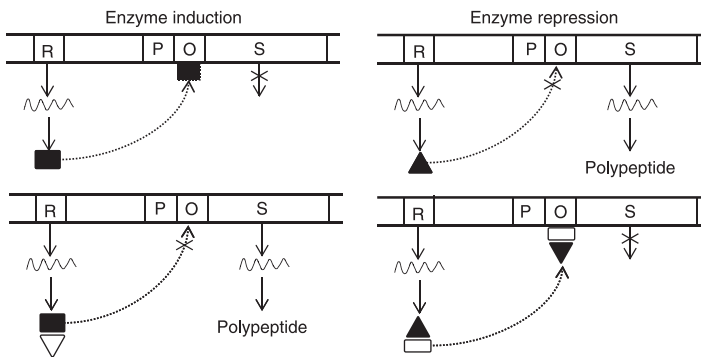

Figure 4.2 Regulation of enzyme synthesis

Published by Woodhead Publishing Limited, 2013

their common operator, a section of DNA located between the promoter and the structural genes on the operon. The operator plays no part in protein synthesis and serves solely in the regulation of transcription.

An additional gene, the regulatory gene (R), is located upstream of the operon. This regulator gene codes for a specific regulatory protein, the repressor molecule which is key to the induction or repression of enzyme synthesis. In inducible enzyme systems, an active[16] repressor protein is formed whereas in repressive systems, an inactive[17] repressor protein is produced.

In enzyme induction (Figure 4.2), the repressor diffuses from the ribosomes where it is formed and binds to the operator. This obstructs the binding of RNA polymerase to the promoter and so prevents transcription of all the structural genes in the operon. However, this repressor has an additional binding site for an inducer molecule. The inducer molecule, when bound to the repressor, changes the shape of the repressor so that it is no longer able to bind with the operator. In the presence of an inducer then, the RNA polymerase is free to bind with the promoter and the structural genes on the operon are transcribed. The inducer is often the enzyme substrate.[18] Consequently, the cell does not need to waste energy on producing enzymes when there is no substrate to metabolise, but only increases in concentration when the substrate becomes available.

The regulation of enzyme synthesis by induction is often described by reference to the lactose operon (lac operon) of *E. coli*.[19] The regulation of the lac operon enables the bacteria to use energy wisely. When no lactose is present, enzyme synthesis is repressed so that no energy is expended on synthesising enzymes to utilise this carbon source; when lactose becomes available, enzyme synthesis is induced and the bacteria synthesise the necessary enzymes.

Published by Woodhead Publishing Limited, 2013

The lac operon consists of three adjacent structural genes (*lacZ*, *lacY* and *lacA*), which together enable the effective digestion of lactose. These structural genes are transcribed into a single mRNA from the same promoter. A fourth gene, *lacI*, located just upstream of the lactose operon, codes for a repressor protein which is continuously expressed. In the absence of lactose, the lac repressor protein binds with the lac operator and physically prevents the RNA polymerase from binding to the promoter. The mRNA is not transcribed and none of the structural genes on the operon is expressed. When lactose is present, a lactose metabolite, allolactose,[20] binds with the lac repressor protein. The altered repressor is no longer able to bind with the operator, the RNA polymerase binds with the promoter and the mRNA coding for all three enzymes (β-galactosidase, lactose permease and thiogalactoside transacetylase) is transcribed.

On the other hand, in enzyme repression (Figure 4.2), the repressor protein is unable to bind with the operator until it is bound to a co-repressor. Binding with a co-repressor molecule causes a conformational change such that the repressor–co-repressor complex is able to bind with the operator, so preventing transcription of the structural genes. Co-repressor molecules are typically end products of the cell's metabolic activity. In this way, the cell does not waste energy on synthesising enzymes for products that have already been accumulated in sufficient quantities. A well-known example of this is histidine biosynthesis by *Salmonella typhimurium* which exhibits co-ordinate repression, i.e. all the enzymes which synthesise this product are repressed through the action of the end product of their activity.

Positive regulation of transcription can also occur where activator proteins promote the binding of RNA polymerase to the promoter. In this case, the promoter has two binding sites, one for the RNA polymerase and one for the

Published by Woodhead Publishing Limited, 2013

activator protein. The binding of the activator protein to the second binding site on the promoter stimulates transcription of the mRNA coding for the structural genes on the operon, and hence facilitates the subsequent expression of these genes.

The *E. coli* catabolite activator protein (CAP) is a well-known example. CAP, also known as the cAMP receptor protein, is a regulatory protein in bacteria. CAP binds with cyclic AMP (cAMP) to form a CAP–cAMP complex that binds to a promoter sequence and, through direct protein–protein interaction between CAP and RNA polymerase, activates mRNA transcription.

In lactose metabolism, the binding of the CAP–cAMP complex is essential for the transcription of the mRNA. However, in the presence of high glucose concentrations, cAMP decreases, resulting in a decrease in the CAP–cAMP complex and insufficient CAP–cAMP to promote transcription of the mRNA coding for the enzymes which metabolise lactose, even in the presence of the substrate inducer. In this manner, lactose metabolism is blocked by an elevated intracellular glucose concentration so as to allow the more readily metabolisable glucose to be utilised first.

Many enzymes are repressed by rapidly metabolisable fuel sources (other than glucose). This gives rise to the well-known diauxie effect observed during bacterial growth in nutrient media containing dual carbon sources where one nutrient is metabolised by constitutive enzymes and one by adaptive enzymes.[21] Here, a two-stage growth phase is recorded, with an intermediate lag phase during which no growth takes place. This intermediate lag phase occurs when the first carbon source has been metabolised by the constitutive enzymes and the adaptive enzymes required to metabolise the second are still being synthesised.

Published by Woodhead Publishing Limited, 2013

4.3 Genetic modification

Genetic modification (or genetic engineering) directly manipulates the organism's DNA to produce new microorganisms which code for enzymes which they previously were not able to synthesise. This is achieved by producing recombinant DNA (which codes for the desired enzymes) from the donor organism using molecular cloning techniques, and then introducing the recombinant DNA into the recipient (or host) organism so that the foreign DNA is expressed in the host. In molecular cloning, the DNA from the donor cell is treated with restriction endonucleases which cleave specific sites in DNA, generating small DNA fragments. DNA ligase is used to catalyse the combination of the DNA fragments with vector DNA, a vehicle used to transfer DNA into the host cell, e.g. plasmids (Section 2.2), to generate recombinant DNA molecules which will be replicated along with the host DNA. Probably the most significant advance in genetic modification was the development of the polymerase chain reaction (PCR) technology which facilitated the generation of millions of copies of DNA from just one or a few copies of a particular DNA sequence.[22]

One of the early, and possibly the most celebrated, processes using a genetically modified microorganism produced human insulin from modified *E. coli*, approved by the FDA[23] in the early 1980s. Today, genetic engineering is a steadily growing field with the most well-known, albeit controversial, application being the construction of genetically modified foods. Manipulation of plant DNA has facilitated higher crop yields through increased resistance to phytopathogens, insects and herbicides. New generation genetically modified plants are engineered to produce pharmaceuticals (vaccines and drugs) which can be delivered directly by ingesting the plant (quaintly known as pharming).

Published by Woodhead Publishing Limited, 2013

There is no doubt that genetic engineering continues to immeasurably broaden the range of potential bioproducts and capacity for accumulation. However, it is expedient for the Bioprocess Engineer to have some measure of understanding of the GMO in the process, especially with regards to its stability. For instance, should reversion to the wild type occur in continuous culture, the pressures imposed by this mode of operation will cause the wild type to be wholly selected with complete loss of the GMO (see Figure 7.8).

4.4 Notes

1. Gregor Mendel (1822–1884) was posthumously recognised as the founder of genetics, his work leading eventually to the concept of a gene.
2. Complete set of genes.
3. The simple prokaryote, *Escherichia coli*, has around 4.6×10^6 base pairs, compared with 4×10^9 for *Homo sapiens*.
4. Catalysed by helicase.
5. Catalysed by DNA polymerase.
6. Complementary DNA–DNA base pairs: adenine and thiamine; cytosine and guanine.
7. mRNA forms 2% of the total RNA.
8. Catalysed by RNA polymerase.
9. In the RNA strand, uracil replaces thiamine.
10. rRNA comprise about 65 weight % of the ribosomes.
11. Two bases would code for only sixteen amino acids.
12. One codon for one to six amino acids.
13. A = Adenine, U = uracil and G = guanine.
14. Elongation takes place at a rate of 15–20 amino acids per second.
15. Stop codons do not specify an amino acid and do not have a corresponding tRNA.
16. In a form which is able to prevent transcription.
17. In a form which is unable to prevent transcription.

Published by Woodhead Publishing Limited, 2013

18. Induction by a substrate molecule is referred to as substrate induction. Induction by a molecule not acted on by the enzyme is referred to as gratuitous induction.
19. The lac operon was evaluated by François Jacob (b. 1920) and Jacques Monod (1910–1976). This represented the first example of transcriptional regulation of the structural genes on an operon.
20. Combination of glucose and galactose.
21. First published by Jacques Monod in 1949 during batch culture of *E. coli* in a mixed carbon source of glucose and sorbitol.
22. Kary Banks Mullis (b. 1944), Nobel prize 1993.
23. Food and Drug Administration, USA.

Published by Woodhead Publishing Limited, 2013

5

Carbon metabolism

DOI: 10.1533/9781782421689.53

Abstract: Efficient utilisation of the carbon source impacts significantly on the ability of the microorganism to maintain its cellular integretity, to grow and reproduce and, from the process perspective, to produce the desired product. Since the majority of industrial processes utilise chemo-heterotrophs, only metabolic pathways which utilise organic compounds as their carbon and energy sources will be considered here. The metabolism of chemo- and photo-autototrophs and photo-heterotrophs can be found in specialised texts.

Energy generation and utilisation can be classified into catabolism (pathways that generate energy) and anabolism (pathways that utilise energy) such that catabolism supports anabolic cell maintenance and growth. Central to these pathways is the mechanisms of storage of the energy generated during catabolic pathways and the transfer of stored energy to anabolic pathways. This is mediated by the adenosine nucleotides (see Figure 3.7).

In Chapter 5, the main catabolic and anabolic pathways in chemo-heterotrophs are detailed and their associated energy generation and utilisation quantified. Further, the mechanisms underpinning the storage of the generated energy and the transfer of the stored energy are elucidated.

Published by Woodhead Publishing Limited, 2013

Key words: energy transfer, oxidative phosphorylation, substrate phosphorylation, glycolysis, tricarboxylic acid cycle, fat oxidation, fatty acid synthesis, gluconeogenesis.

5.1 Energy generation, storage and transfer

5.1.1 The role of adenosine triphosphate

The three key nucleotides involved in energy sequestration, storage and release are adenosine triphosphate (ATP), adenosine diphosphate (ADP) and adenosine monophosphate (AMP) containing three, two and one phosphate group(s) respectively (see Figure 3.7). ATP and ADP are most commonly involved in energy metabolism with AMP playing a much reduced role.

Energy is stored as chemical bond energy in the bonds which connect the terminal phosphate group in ATP and in ADP (Figure 5.1). ATP has two energy-rich bonds and one energy-poor bond. Energy-rich bonds may release around 10 kcal/mole on hydrolysis.

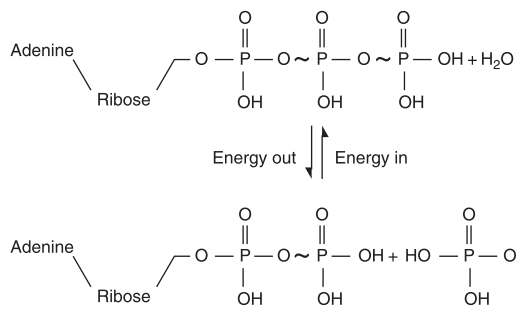

Figure 5.1 Energy release and sequestration (~ indicates a high energy bond)

Published by Woodhead Publishing Limited, 2013

When energy is required, it is released through bond breakage by hydrolysis of ATP to form ADP and inorganic phosphate (Pi) according to: $ATP + H_2O \rightarrow ADP + Pi$. To a lesser extent, ADP is involved in energy transfer processes analogous to ATP. Excess energy, on the other hand, is sequestered through bond formation by phosphorylation of ADP and inorganic phosphate to form ATP according to: $ADP + Pi \rightarrow ATP + H_2O$.

5.1.2 Oxidative and substrate level phosphorylation

The energy that is sequestered by ADP and stored in ATP is generated through catabolic oxidation[1] of metabolic intermediates by cellular respiration. The overall oxidation of glucose is analogous to its complete combustion reaction: $(CH_2O)_n + nO_2 \rightarrow nCO_2 + nH_2O$. Of course the oxidation does not take place in one step (this would release too much energy), but in a number of steps, each catalysed by a specific enzyme. Each oxidation step involves the removal of two hydrogen atoms so that the total oxidation occurs by sequential removal of hydrogen.

The liberated hydrogen atoms from each oxidation (or dehydrogenation) step are transferred along a linked chain of specific compounds, nicotinamide adenine dinucleotide (NAD^+), flavin adenine dinucleotide (FAD) and co-enzyme Q (CoQ), by sequential reduction and oxidation. The individual molecules involved in the chain are detailed in Figure 5.2 and the oxidation and reduction of the active groups of NAD^+, FAD and CoQ is shown in Figure 5.3.

The first compound in the chain is NAD^+ which is reduced according to the reversible reaction $NAD^+ + 2H \leftrightarrows NADH + H^+$ where the pyrimidine ring in its active group, nicotinamide, becomes reduced, retaining the two double

Published by Woodhead Publishing Limited, 2013

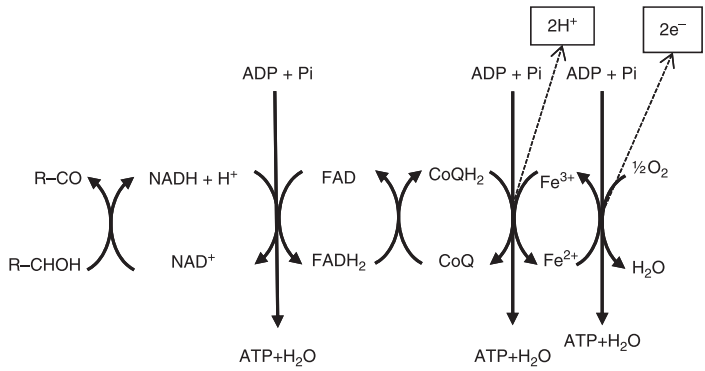

Figure 5.2 The electron transport chain or oxidative phosphorylation

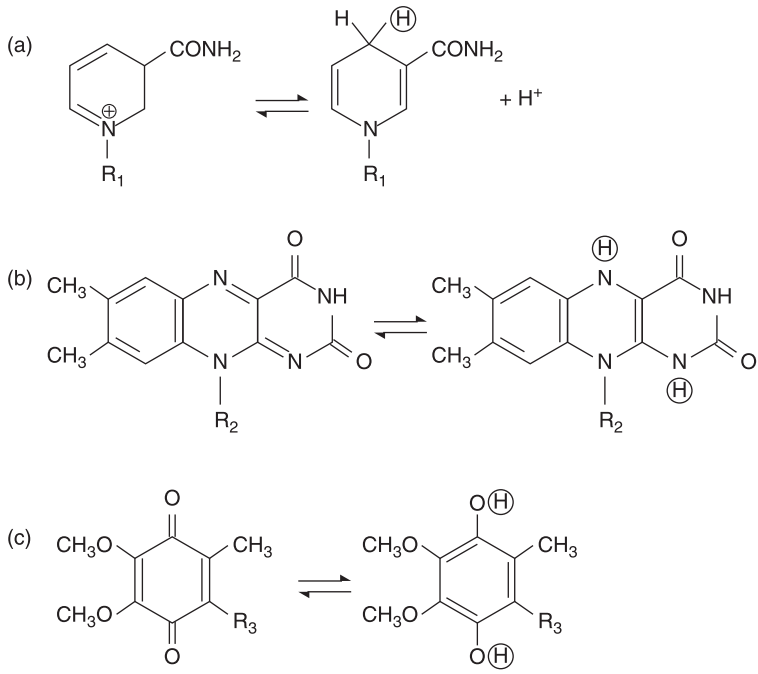

Figure 5.3 Reduction of the active groups NAD (a), FAD (b) and CoQ (c)

Published by Woodhead Publishing Limited, 2013

bonds while the nitrogen loses its positive charge. The process proceeds by the regeneration of NAD^+ by the reduction of the second compound in the chain, FAD, according to the reversible reaction $FAD + 2H \leftrightarrows FADH_2$ with reduction of the prosthetic group, dimethyl alloxazine. The FAD is regenerated by the reduction of the active group quinone on CoQ to hydroxyquinone according to: $CoQ + 2H \leftrightarrows CoQH_2$.

After reduction of CoQ, hydrogen ions are released and the electrons are transferred along a chain of iron-containing cytochromes[2] by sequential reduction and oxidation of the ion moieties (Fe^{2+} and Fe^{3+}) before themselves being released. In the presence of exogenous molecular oxygen, aerobic respiration takes place and the electrons are taken up by oxygen as the terminal electron acceptor. The oxygen combines with the electrons and hydrogen ions to form water.

The passage of hydrogen and electrons releases energy which is sequestered by the phosphorylation of ADP and Pi and stored as chemical energy in ATP. Sufficient energy is generated by the electron transport chain to form three ATP for each metabolic intermediate oxidised. The energy equation per two hydrogen atoms removed is: $3ADP + 3Pi + \frac{1}{2}O_2 \leftrightarrows 3ATP + 4H_2O$.

Since energy generation by the electron transport chain is mediated through ADP phosphorylation, this respiration process is also called oxidative phosphorylation, the oxidative phosphorylation chain or respiratory chain oxidation.

All aerobic microorganisms undergo aerobic respiration and have an obligate requirement for oxygen as the terminal electron acceptor. An oxygen level insufficient to meet the oxygen demand of aerobes results in reduced metabolism. When growth becomes primarily dependent on the oxygen

Published by Woodhead Publishing Limited, 2013

level, a situation known as oxygen limiting, the process yields and productivity decrease accordingly, irrespective of all other conditions being favourable. In the extreme case where oxygen decreases below a critical level, oxidative phosphorylation ceases and the cells lyse. It is for this reason that oxygen transfer to aerobic bioprocesses remains a major criterion for design, operation (Section 8.1) and scale up (Section 9.1).

Anaerobic microorganisms, on the other hand, undergo anaerobic respiration in the absence of exogenous molecular oxygen, using compounds other than oxygen as terminal electron acceptors, e.g. NO_3^-, SO_4^{-2}. One of the most important examples of NO_3^- being used as a terminal electron acceptor is in denitrification[3] of waste water, where the NO_3^- accepts electrons and the nitrate nitrogen is reduced to N_2, thereby removing contaminating nitrogenous compounds from the water.

Much of energy generation is via oxidative phosphorylation (aerobic or anaerobic). However, in addition to oxidative phosphorylation, microorganisms can generate ATP via substrate level phosphorylation, a mechanism which is independent of an exogenous electron acceptor. During substrate level phosphorylation, ATP is formed via phosphorylation of ADP (or in some cases GDP[4]) by direct transfer of phosphate from a reactive metabolic intermediate to ADP. Under these conditions, the NADH formed is regenerated to NAD^+ by reduction of metabolites, not by the reduction of FAD (as in oxidative phosphorylation). This mechanism is important in anaerobic fermentation processes where reduced products are formed, e.g. ethanol and lactate.

Microorganisms which produce ATP only through aerobic respiration are obligate aerobes (oxygen is obligatory). Anaerobes never use oxygen as a terminal electron acceptor. They either use anaerobic respiration (with an electron

Published by Woodhead Publishing Limited, 2013

acceptor alternate to oxygen) or anaerobic fermentation (forming reduced compounds). Facultative anaerobes can generate energy either via aerobic respiration, or anaerobic respiration or anaerobic fermentation if oxygen is not present. Aerotolerant anaerobes can tolerate the presence of oxygen, although they do not utilise it for energy generation, while obligate anaerobes are in fact destroyed by oxygen. Substrate level phosphorylation can be carried out by both aerobes and anaerobes. Obligate aerobes and strict anaerobes, in particular, can bring their own unique challenges to the optimisation of process performance.

5.2 Catabolic pathways: energy generation

A wide spectrum of chemo-heterotrophs utilise carbohydrates as their primary carbon source for energy production during catabolism. Complex carbohydrates, e.g. starch and cellulose (Section 3.1), are hydrolysed into simple carbohydrates, e.g. glucose, before being assimilated. Chemo-heterotrophs which are unable to utilise carbohydrates metabolise fats, oils or hydrocarbons as a primary energy source.

5.2.1 Glycolysis

The most primitive pathway for obtaining energy from a carbon source is the glycolytic pathway, or glycolysis. Glycolysis can occur in the complete absence of oxygen as no oxidative phosphorylation takes place; energy generation takes place by substrate level phosphorylation only. During glycolysis, glucose is oxidised to pyruvate by the removal of hydrogen with the storage of energy by the direct

Published by Woodhead Publishing Limited, 2013

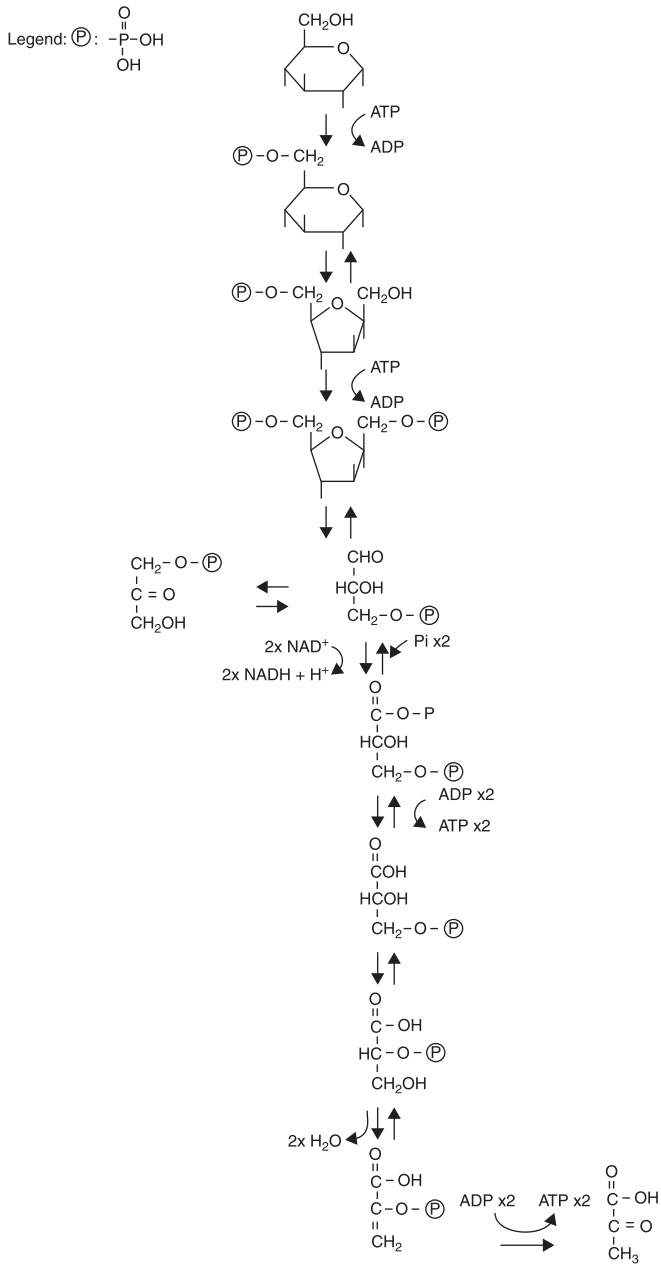

Figure 5.4 Glycolysis

Published by Woodhead Publishing Limited, 2013

incorporation of inorganic phosphate into ADP via substrate level phosphorylation (Figure 5.4). In anaerobic microorganisms, or in facultative organisms grown in the absence of oxygen (e.g. *S. cerevisiae*), this is often the sole source of energy.

Glycolysis comprises successive reactions where the conversion of glucose to pyruvate is catalysed by a group of ten enzymes where all intermediates between glucose and pyruvate are phosphorylated compounds. There are three major groups of reactions in glycolysis: (1) the energy-intensive priming stage during which two ATP are utilised to convert the 6-carbon glucose to two 3-carbon glyceraldehyde-3-phosphate molecules; (2) the oxidation of the glyceraldehyde-3-phosphate to 1,3-phosphoglyceroyl with the simultaneous uptake of inorganic phosphate and reduction of NAD^+; and (3) two subsequent substrate level phosphorylation steps in which each of the two high energy phosphate groups of 1,3-phosphoglyceroyl are utilised in the formation of ATP from ADP. Together with isomerisation and dehydration, this leads eventually to the formation of pyruvate from the 1,3-phosphoglyceroyl.

Consideration of the energy flow shows that two ATP per molecule of glucose are required to prime the pathway. Since two ATP are generated by substrate level phosphorylation per molecule of glyceraldehyde-3-phosphate, and two glyceraldehyde-3-phosphate are produced per molecule of glucose, four ATP are generated by the oxidation of glucose to pyruvate. So the overall gain is two ATP per molecule glucose oxidised to pyruvate via glycolysis (Equation 5.1).

$$\begin{aligned} &1\text{glucose} + 2\text{ADP} + 2\text{Pi} + 2\text{NAD}^+ \rightarrow \\ &2\text{pyruvate} + 2\text{ATP} + 2\text{H}_2\text{O} + 2\text{NADH} + 2\text{H}^+ \end{aligned} \qquad [5.1]$$

But the two NADH still have to be regenerated for glycolysis to continue. In an anaerobic environment, regeneration of

Published by Woodhead Publishing Limited, 2013

NAD^+ is accomplished by anaerobic fermentation where reduced compounds are formed from pyruvate. In alcoholic fermentation, the pyruvate is decarboxylated to acetaldehyde which is then reduced to ethanol (Equation 5.2). During homolactic fermentations, the pyruvate is reduced directly to lactate (Equation 5.3).

$$\text{pyruvate} + \text{NADH} + \text{H}^+ \rightarrow \text{ethanol} + \text{CO}_2 + \text{NAD}^+ \quad [5.2]$$

$$\text{pyruvate} + \text{NADH} + \text{H}^+ \rightarrow \text{lactate} + \text{NAD}^+ \quad [5.3]$$

In both cases, the overall energy balance for anaerobic fermentation to ethanol or lactate results in a total of two ATP per molecule of glucose oxidised (Equations 5.4 and 5.5).

$$1\text{glucose} + 2\text{ADP} + 2\text{Pi} \rightarrow 2\text{ethanol} + 2\text{CO}_2 + 2\text{ATP} + 2\text{H}_2\text{O} \quad [5.4]$$

$$1\text{glucose} + 2\text{ADP} + 2\text{Pi} \rightarrow 2\text{lactate} + 2\text{ATP} + 2\text{H}_2\text{O} \quad [5.5]$$

Under aerobic conditions, however, NAD^+ can be regenerated by oxidative phosphorylation and the pyruvate is completely oxidised to CO_2 and H_2O through the TCA cycle without the formation of reduced compounds (Section 5.2.2).

5.2.2 Tricarboxylic acid cycle

The TCA[5] cycle provides a common pathway for the ultimate catabolism of carbohydrates and fats, which, through its oxidative aerobic nature, generates ATP mainly[6] via oxidative phosphorylation for anabolic processes. The fuel for the TCA is acetyl-CoA, a molecule which plays a pivotal role in sugar and fat metabolism. In fat catabolism, acetyl-CoA is formed during the β-oxidation of fats (Section 5.2.3) when

Published by Woodhead Publishing Limited, 2013

fatty acids are fragmented into their acetyl-CoA components. In carbohydrate metabolism, acetyl-CoA is linked to glycolysis via the conversion of pyruvate to the thioester acetyl-CoA by incorporation of CoA (Figure 5.5). The conversion is catalysed by the pyruvate dehydrogenase complex in a series of steps during which pyruvate is

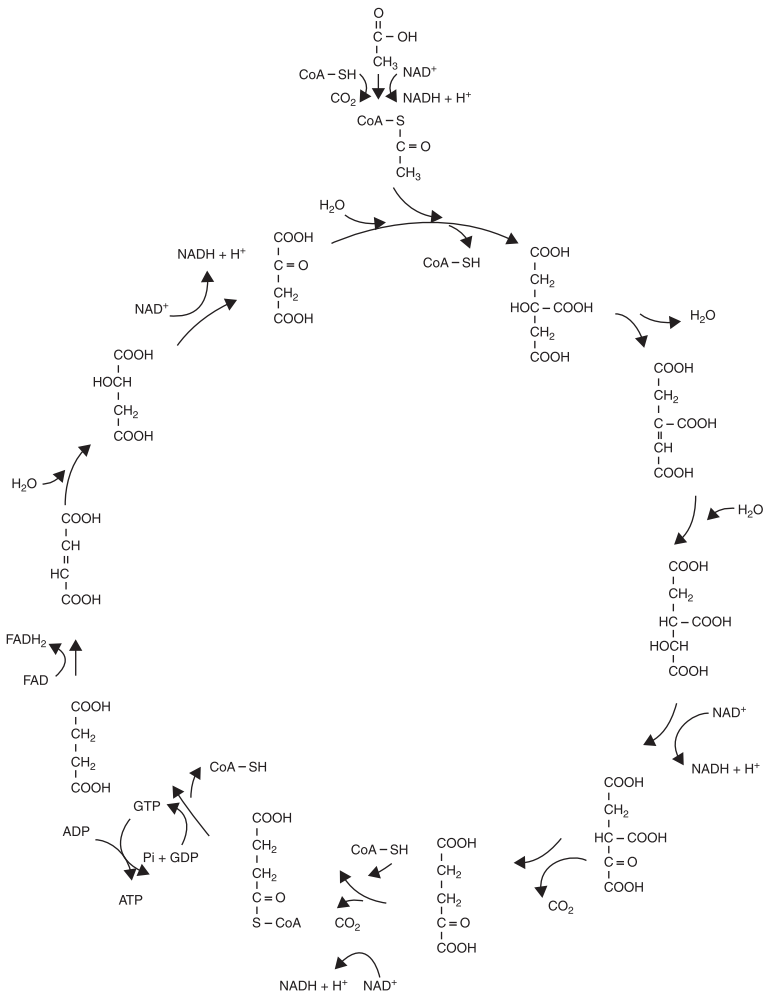

Figure 5.5 Tricarboxylic acid cycle

Published by Woodhead Publishing Limited, 2013

decarboxylated with the release of CO_2 and subsequently dehydrogenated with the reduction of NAD^+

The TCA cycle is initiated with the condensation of the acetyl-CoA with oxaloacetate to form citrate. The citrate is converted to isocitrate via addition of water across the double bond of cis-aconitate, the isocitrate is dehydrogenated to oxalosuccinate and the oxalosuccinate is decarboxylated to α-ketoglutarate. The subsequent conversion of α-ketoglutarate to succinate is mediated via the thioester, succinyl-CoA. Succinyl-CoA is first formed by decarboxylation and reduction of α-ketoglutarate, with the amalgamation of CoA, catalysed by the α-ketoglutarate dehydrogenase complex. The conversion of the succinyl-CoA to succinate features the single substrate level phosphorylation in the TCA cycle when the high energy bond in the succinyl-CoA is transferred to GDP, and subsequently to ADP, to form ATP with the incorporation of inorganic phosphate and release of CoA. Succinate is then reduced to fumarate (here FAD, rather than NAD^+ is the primary molecule as the energy released is not sufficient to include the NAD^+ step). Hydration of fumarate across the double bond yields malate, which on subsequent dehydrogenation leads back to oxaloacetate and the close of the TCA cycle.

The series of consecutive reactions during the TCA cycle forms reduced species (NADH and $FADH_2$), producing three NADH and one $FADH_2$ per acetyl-CoA molecule. NADH and $FADH_2$ then enter the respiratory chain where oxygen is incorporated as the final electron acceptor and inorganic phosphate taken up by ADP to produce ATP and H_2O as in Equations 5.6 and 5.7.

$$3ADP + 3Pi + \tfrac{1}{2}O_2 \rightarrow 3ATP + 4H_2O \text{ (per NADH)} \quad [5.6]$$

$$2ADP + 2Pi + \tfrac{1}{2}O_2 \rightarrow 2ATP + 3H_2O \text{ (per } FADH_2\text{)} \quad [5.7]$$

Published by Woodhead Publishing Limited, 2013

So, the energy balance for three NADH and one $FADH_2$ yields Equation 5.8.

$$11ADP + 11Pi + 2O_2 \rightarrow 11ATP + 15H_2O \quad [5.8]$$

Now including the substrate level phosphorylation, the energy balance becomes Equation 5.9.

$$12ADP + 12Pi + 2O_2 \rightarrow 12ATP + 15H_2O \quad [5.9]$$

During the oxidation of acetyl-CoA there is a net usage of two H_2O per molecule acetyl-CoA and a net production of two CO_2 and one CoA. So the overall equation for the complete oxidation of one molecule of acetyl-CoA can be written as Equation 5.10.

$$1acetyl - CoA + 12ADP + 12Pi + 2O_2 \rightarrow$$
$$1CoA + 12ATP + 13H_2O + 2CO_2 \quad [5.10]$$

However, one NADH was also produced and one CO_2 liberated in the decarboxylation of pyruvate to acetyl-CoA, so incorporating the energy derived from oxidation of NADH (Equation 5.6) and the liberation of CO_2, the overall equation for the complete oxidation of one molecule of pyruvate can be written as Equation 5.11.

$$1pyruvate + 15ADP + 15Pi + 2½O_2 \rightarrow$$
$$15ATP + 17H_2O + 3CO_2 \quad [5.11]$$

The overall energy balance from glucose under aerobic conditions, however, also has to incorporate the energy produced during glycolysis. Under aerobic conditions, the NADH produced during glycolysis will enter the oxidative phosphorylation chain, each NADH producing three ATP according to Equation 5.6. Two NADH are produced per glucose during glycolysis to yield an additional six ATP per glucose molecule. This, in addition to the net two ATP per molecule of glucose produced by substrate level

Published by Woodhead Publishing Limited, 2013

phosphorylation during glycolysis, gives an overall balance of glucose to pyruvate under aerobic conditions (noting that two H_2O are produced per glucose during glycolysis) according to Equation 5.12.

$$1\text{glucose} + 8\text{ADP} + 8\text{Pi} + \text{O}_2 \rightarrow 2\text{pyruvate} + 8\text{ATP} + 10\text{H}_2\text{O} \quad [5.12]$$

Combining the contributions from glycolysis (Equation 5.12) and the TCA cycle (Equation 5.11) under aerobic conditions yields 38 ATP for the complete oxidation of one molecule of glucose to CO_2 and H_2O (Equation 5.13).

$$1\text{glucose} + 38\text{ADP} + 38\text{Pi} + 6\text{O}_2 \rightarrow 2\text{pyruvate} + 38\text{ATP} + 44\text{H}_2\text{O} + 6\text{CO}_2 \quad [5.13]$$

The 38 ATP produced from glucose under aerobic conditions (Equation 5.13) is in stark contrast to the two ATP produced from glucose (Equations 5.4 and 5.5) by anaerobic fermentation. Clearly, glucose utilisation is far more energy efficient when reduced compounds are not formed.

An understanding of the underlying principles of the metabolism and energy generation is always important from a process viewpoint, especially when dealing with facultative microorganisms[7] in aerobic bioprocesses. Poor mixing can lead to pockets of depleted oxygen in large scale bioreactors. During passage through the anaerobic pockets, microbial metabolism will change from aerobic to anaerobic with consequent alteration of yields and productivities.

Arguably, the most well documented industrial example of the impact of underlying metabolism on process performance is in the production of the facultative yeast, *S. cerevisiae*, the mainstay of the baking and brewing industries. Efficient glucose utilisation provides optimum performance for growth of *S. cerevisiae* so process conditions should prevent glucose being diverted to ethanol and consequent reduction

Published by Woodhead Publishing Limited, 2013

of ATP per molecule of glucose. However, under high concentrations of glucose, the TCA cycle enzymes are inhibited and energy production takes place by substrate level phosphorylation only, despite adequate oxygen supply.[8]

To maximise the carbon conversion to yeast, a process strategy known as fed-batch (see Section 7.4) is used. Here the glucose is fed to the process at a rate that maintains the glucose concentration below the inhibitory level. This manipulation of process strategy to optimise process kinetics is a classic example of the synergism between life science and engineering where the success of the process depends on both an understanding of fed-batch process design equations and the regulation of enzyme synthesis which underpins the microbial behaviour.

The major function of the TCA cycle is to provide energy in the form of ATP in anabolic pathways. In addition, the TCA cycle also serves as a pool of intermediates and/or precursors for anabolic functions, e.g. amino acid biosynthesis.[9] However, if TCA cycle intermediates are used in this way, they have to be replenished by other reactions for energy generation to continue. These reactions are called anaplerotic reactions. One of the most important anaplerotic reactions is the reversible carboxylation of pyruvate to oxaloacetate at the expense of ATP which facilitates the start of gluconeogenesis (Section 5.3.2).

In some microorganisms, the TCA cycle is modified to eliminate those reactions which release CO_2. This modified pathway, called the glyoxylate shunt, functions to conserve carbon. Conservation of carbon is particularly important in microorganisms which grow only on fats where acetyl-CoA serves not only to provide energy, but also as a carbon source. In the glyoxylate shunt, the isocitrate splits into glyoxylate and succinate. The glyoxylate then combines with acetyl-CoA to form malate which re-enters the TCA cycle. The

Published by Woodhead Publishing Limited, 2013

shunt through glyoxylate eliminates two steps in the TCA cycle which liberate CO_2, hence carbon is conserved.

5.2.3 β-Oxidation of fats

Fatty acids are stored in the cell as triglycerides (Section 3.2) and oxidised to produce energy in the form of ATP when required. Triglycerides are first separated into their component fatty acids with the release of glycerol, after which the fatty acids are oxidised to acetyl-CoA via the β-oxidation pathway. Subsequently, complete oxidation of acetyl-CoA to CO_2 and H_2O takes place via the TCA cycle (Section 5.2.2).

Triglycerides are stored in the extra mitochondrial cytoplasm. However, the respiratory enzymes catalysing β-oxidation and the TCA cycle reside in the mitochondria (Figure 2.2). Consequently, the initial steps function to move the fatty acid from the extra mitochondrial cytoplasm into the mitochondria. In order for a long chain fatty acid to cross the mitochondrial membrane, it has to be combined with the carnitine molecule. This is achieved by activating the fatty acid by the ATP-driven ($2ATP + 2H_2O \rightarrow 2ADP + 2Pi$) esterification of extra mitochondrial CoA to yield fatty acyl-CoA. The acyl group from the fatty acyl-CoA is then transferred to the carrier group, carnitine, to form fatty acyl-carnitine. Fatty acyl-carnitine is able to pass through the membrane into the mitochondria where it is converted back to fatty acyl-CoA by the incorporation of inter mitochondrial CoA. This fatty acyl-CoA is then in position to undergo β-oxidation within the mitochondria (Figure 5.6).

During β-oxidation, the fatty acyl-CoA is oxidised to α,β-transenoyl-CoA, hydrated to 3-hydroxyacyl-CoA and oxidised again to 3-ketoacyl-CoA. Thiolase then catalyses the cleavage of 3-ketoacyl-CoA into acetyl-CoA and a

Published by Woodhead Publishing Limited, 2013

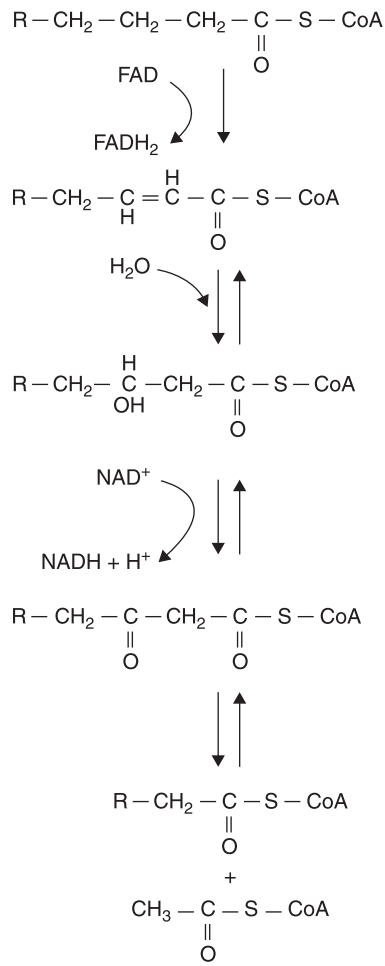

Figure 5.6 *β*-Oxidation of fats

thioester which is two carbons shorter than the original chain. The thioester then re-enters *β*-oxidation and the process is repeated, each time lopping off an acetyl-CoA molecule, until only acetyl-CoA remains.

The energy produced from a fatty acid depends on the number of acetyl-CoA molecules that are removed, i.e. it depends on the number of carbons in the original fatty acid

Published by Woodhead Publishing Limited, 2013

chain. Palmitic acid (16 carbons) is one of the most commonly found fatty acids and a suitable illustration of the energy produced. In this case, the breakdown of the fatty acyl-CoA into acetyl-CoA requires seven cycles. In each cycle, one NADH and one $FADH_2$ are formed, together producing five ATP (Equations 5.6 and 5.7) according to Equation 5.14.

$$5ADP + 5Pi + O_2 \rightarrow 5ATP + 7H_2O \quad [5.14]$$

Since H_2O is also taken up during this process, the removal of seven acetyl-CoAs from the C_{16} fatty acyl-CoA can be written as Equation 5.15.

$$C_{16}\text{ fatty acyl-CoA} + 7CoA + 35ADP + 35Pi + 7O_2 \rightarrow 8\text{acetyl-CoA} + 35ATP + 42H_2O \quad [5.15]$$

Each acetyl-CoA enters the TCA cycle producing a further 12 ATP from three NADHs, one $FADH_2$ and one substrate level phosphorylation, according to Equation 5.10. So, for eight acetyl-CoAs, Equation 5.16 holds.

$$8\text{acetyl-CoA} + 96ADP + 96Pi + 16O_2 \rightarrow 8CoA + 96ATP + 104H_2O + 16CO_2 \quad [5.16]$$

Combining Equations 5.15 and 5.16 yields the overall balance for conversion of C_{16} fatty acyl-CoA to eight acetyl-CoA according to Equation 5.17.

$$C_{16}\text{ fatty acyl-CoA} + 131ADP + 131Pi + 23O_2 \rightarrow CoA + 131ATP + 146H_2O + 16CO_2 \quad [5.17]$$

Note though, that the formation of C_{16} fatty acyl-CoA from palmitic acid required two ATP and one H_2O, so the overall balance for conversion of C_{16} fatty acid to eight acetyl-CoA is given by Equation 5.18.

$$C_{16}\text{ fatty acid} + 23O_2 + 129ADP + 129Pi \rightarrow 145H_2O + 16CO_2 + 129ATP \quad [5.18]$$

Published by Woodhead Publishing Limited, 2013

Although the energy released from fats is dependent on chain length, it can be more than 30-fold greater than that from glucose. (For palmitic acid, it calculates as 34-fold.) Additionally, an increased intracellular level of acetyl-CoA (as produced during β-oxidation) generally favours the accumulation of lipophilic products. So from a process perspective, production of, for example, carotenoids, steroids and co-enzyme Q are likely to be enhanced when fatty acids are used as a carbon source, even though these products are also able to be formed from carbohydrates. Of particular interest here are the polyhydroxyalkonates, a range of lipophilic polymers which have significant potential as biodegradable plastic.

A similar case can be made for use of hydrocarbons such as alkanes. Alkanes are converted to fatty acids (through fatty alcohol and fatty aldehyde compounds) which are subsequently metabolised into acetyl-CoA molecules as described. A wide range of microorganisms utilise hydrocarbons efficiently, including bacteria (e.g. *Microbacterium hydrocarbonoxydans*) and yeast (e.g. *Yarrowia lipolytica*). These microorganisms are key to unlocking the potential of conversion of chemically resistant alkanes to a wide variety of value-added products while simultaneously decreasing the pool of waste by-products produced from gas to liquid fuel technologies.

5.3 Anabolic pathways: energy utilisation

5.3.1 Fatty acid synthesis

Fatty acid synthesis and subsequent formation of triglycerides (Section 3.2) enables the storage of energy in the form of

Published by Woodhead Publishing Limited, 2013

ATP. Fatty acids are synthesised from individual acetyl-CoA molecules residing in the extra mitochondrial cytoplasm. In this way the cell separates the anabolic fatty acid synthesis (catalysed in the extra mitochondrial cytoplasm) from the catabolic fatty acid oxidation (catalysed in the mitochondria) although acetyl-CoA plays a central role in both.

The initial step is to move the acetyl-CoA from the mitochondria, the site of the respiratory enzymes (see Figure 2.2) and formation of acetyl-CoA from β-oxidation and glycolysis, to the extra mitochondrial cytoplasm where fatty acid synthesis takes place. This occurs through the condensation of inter mitochondrial acetyl-CoA with oxaloacetate (a TCA cycle intermediate) to form citrate. The citrate passes through the mitochondrial membrane into the extra mitochondrial cytoplasm where, with the input of ATP, it is cleaved back into its (now extra mitochondrial) acetyl-CoA and oxaloacetate components. This extra mitochondrial acetyl-CoA is then carboxylated to malonyl-CoA.

The priming reaction for fatty acid synthesis is the esterification of the acyl intermediates to a sulfhydryl group (–SH) on the prosthetic group of ACP,[10] and acetyl-ACP and malonyl-ACP are formed from acetyl-CoA and malonyl-CoA respectively. The 2-carbon acetyl-ACP and 3-carbon malonyl-ACP combine to form the 4-carbon 3-keto acyl-ACP with the release of CO_2. Reduction of 3-ketoacyl-ACP with nicotinamide adenine dinucleotide phosphate (NADPH) yields β-hydroxybutyryl-ACP, dehydration of β-hydroxybutyryl-ACP forms 3-crotonyl-ACP and reduction again yields butyryl-ACP which is two carbons longer than the original acetyl-CoA.

The butyryl-ACP is then in position to accept another malonyl-ACP to form a 6-carbon 3-keto acyl-ACP and the process continues by the progressive addition of malonyl-ACP, thus increasing the fatty acyl-ACP chain by two carbon

Published by Woodhead Publishing Limited, 2013

lengths at each addition until the required number of carbons is incorporated. At this point, the ACP is released with the formation of the free fatty acid.

5.3.2 *Gluconeogenesis*

Microorganisms which are unable to metabolise fats, produce glucose via gluconeogenesis. This pathway is the central biosynthetic route from such precursors as pyruvate. While the overall oxidation of glucose to pyruvate is essentially irreversible, most of the reaction steps have a small energy change and so can proceed in the reverse direction to form the synthesis of glucose and glycogen if needed. Exceptions are the conversion of pyruvate to phosphoenolpyruvate and fructose-1,6-diphosphate to fructose-6-phosphate. In gluconeogenesis, alternative enzymes are used which catalyse the conversion of pyruvate to phosphoenolpyruvate (via oxaloacetate as intermediate) and the dephosphorylation of fructose-1,6-diphosphate to fructose-6-phosphate.

5.4 Notes

1. Often referred to as dehydrogenation, referring to oxidation via the removal of hydrogen.
2. Proteins containing iron-porphyrin prosthetic groups which undergo $Fe^{++} \leftrightharpoons Fe^{+++}$.
3. Removal of nitrogen generally from sewage and waste water.
4. Guanidine diphosphate (in these cases, the GTP formed is converted to ATP).
5. The TCA cycle is also known as the Krebs cycle after Hans Krebs (1900–1981) who received a Nobel prize in 1953 for its identification.
6. In one instance substrate level phosphorylation does take place in the TCA cycle.

Published by Woodhead Publishing Limited, 2013

7. Microorganisms able to switch between aerobic and anaerobic metabolism, depending on the level of oxygen present.
8. The Crabtree Effect, published by Herbert Grace Crabtree in 1928. Complete aerobic respiration via the TCA cycle takes place only at glucose concentrations less than 0.5%.
9. E.g. The formation of analine and α-ketoglutarate from pyruvate and glutamate.
10. Acyl carrier protein.

Published by Woodhead Publishing Limited, 2013

6

Enzymes as biocatalysts

DOI: 10.1533/9781782421689.75

Abstract: Every biochemical reaction in the cell is catalysed by specific enzymes. Enzymes function in the same manner as do chemical catalysts, namely to lower the activation energy. Isolation of enzymes, either in a crude or purified form, permits biotransformation directly without the need for whole cells. In fact, biotransformations with isolated enzymes rather than cells as biocatalysts confer several advantages. High selectivity can be obtained with enzyme biocatalysts, because fewer by-products are produced, and many enzymes confer high degrees of regioselectivity.

By far the most common enzymes utilised in enzyme engineering to date have been extracellular and almost exclusively hydrolytic. These are relatively simple to extract and require little in the way of purification (Section 11.4). Even today, amylases[1] and proteases[2] are widely used in the food and beverage and detergent industries respectively.

Probably the first intracellular enzyme to be used was glucose isomerase. This was mainly used in conjunction with amylase in the production of high fructose sweet syrups and jams from starch. Isomerisation of the glucose (produced from the hydrolysis of starch by amylase) produced fructose, which, with its 1.5-fold sweetening power compared with glucose, provided a correspondingly sweeter syrup for the same quantity of starch.

Published by Woodhead Publishing Limited, 2013

The first major usage of an enzyme other than that for food or detergents was penicillin amidase. Penicillin amidase, which catalyses the formation of 6-amino penicillanic acid, the precursor of synthetic penicillin, heralded the start of the synthetic pharmaceutical industry. Today the use of enzymes as biocatalysts is widespread in diverse industries, with advances in genetic engineering contributing significantly to the pool of enzymes available. In many instances, the cost of the enzyme is high and the Bioprocess Engineer is tasked to optimise the design of the enzyme reactor.

Enzyme reactor design requires a fundamental understanding of enzyme kinetics. In Chapter 6, the conceptual mechanisms which underpin the kinetic behaviour of enzymes is discussed and kinetic models which enable prediction of reaction velocity are developed. Both basic enzyme kinetics in the absence of inhibition as well as kinetics which exhibit competitive, uncompetitive and non-competitive inhibitory kinetics are included. The simpler kinetic models are used in the development of process design equations for different process strategies, including continuous immobilised enzyme reactors.

Key words: enzyme kinetics, competitive inhibition, uncompetitive inhibition, mixed inhibition, immobilised enzymes, enzyme reactors.

6.1 Enzyme kinetics with no inhibition

The basic enzyme kinetics in the absence of inhibition can be understood by considering the equilibrium between the free enzyme (E), substrate (S), enzyme–substrate complex (ES) and products (P) in an enzymic reaction as represented by

Published by Woodhead Publishing Limited, 2013

Equation 6.1. In this reaction, the rate constants k_1 and k_2 refer to the forward and reverse reactions respectively.

The rate of formation of the enzyme–substrate complex is then represented by $k_1[E][S]$ and the rate of destruction of the enzyme–substrate complex by $k_2[ES] + k_3[ES]$.[3] Since the rate of change of the enzyme–substrate complex is negligible,[4] the relationship between the rates of formation and destruction of the enzyme–substrate complex can be equated to give Equation 6.2 where K_m is known as the Michaelis–Menten[5] constant.

$$E + S \overset{k_1 k_2}{\longleftrightarrow} ES \overset{k_3}{\rightarrow} P + E \qquad [6.1]$$

$$\frac{k_2 + k_3}{k_1} = \frac{[E][S]}{[ES]} = k = K_m \qquad [6.2]$$

At equilibrium, the rate of product formation is the limiting step such that the overall velocity of reaction (v) is determined by this rate (Equation 6.3).

$$v = k_3[ES] \qquad [6.3]$$

The maximum velocity for a given quantity of enzyme is that which is achieved when the entire enzyme is in the form of the enzyme–substrate complex, i.e. the velocity which relates to the total quantity of enzyme initially available (Equation 6.4).

$$v_{max} = k_3([E] + [ES]) \qquad [6.4]$$

Combining Equations 6.2, 6.3 and 6.4 yields the well-known Michaelis–Menten equation for prediction of the reaction velocity, and is expressed in terms of the Michaelis–Menten constant (Equation 6.5). This function represents a typical saturation curve where K_m equates to the substrate concentration when the velocity is half the maximum and serves to indicate the rate at which maximum velocity is reached (i.e. high K_m means a slow rate and vice versa).

Published by Woodhead Publishing Limited, 2013

$$v = \frac{v_{max}[S]}{K_m + [S]} \quad [6.5]$$

The prediction of the velocity of reaction via Equation 6.5, however, requires quantification of the kinetic constants, v_{max} and K_m. Traditionally this is carried out by means of inversion of the Michaelis–Menten equation (Equation 6.6) and plotting the reciprocal of the substrate concentration (x-axis) versus the reciprocal velocity (y-axis) to yield the reciprocal of v_{max} as the y-intercept and the reciprocal of $-K_m$ as the x-intercept.[6]

$$\frac{1}{v} = \frac{K_m}{v_{max}}\frac{1}{[S]} + \frac{1}{v_{max}} \quad [6.6]$$

Equation 6.6 is known as the Lineweaver–Burk[7] relationship and is used ubiquitously as the standard plot for the calculation of the kinetic constants. However, it should be used only with extreme caution as it places most reliance on the few points obtained at low substrate concentrations and, therefore, the points with the least accuracy. A considerably more reliable approach is to use the Eadie–Hofstee relationship (Equation 6.7) in which the Michaelis–Menten equation (Equation 6.5) is rearranged so that a plot of $v/[S]$ (x-axis) versus v (y-axis) will yield a gradient of $-K_m$ and a y-intercept of v_{max}.

$$v = -K_m\frac{v}{[S]} + v_{max} \quad [6.7]$$

6.2 Enzyme kinetics with inhibition

The activity of many enzymes is regulatory in nature. Regulation of enzyme activity is achieved by a number of inhibitory mechanisms, all of which relate to the reversible binding of an inhibitor to the enzyme, enzyme–substrate

Published by Woodhead Publishing Limited, 2013

complex, or both.[8] Three enzyme inhibition mechanisms have been defined: competitive inhibition, uncompetitive inhibition and mixed inhibition, with non-competitive inhibition a specific case of mixed inhibition.

6.2.1 Competitive inhibition kinetics

Competitive inhibition involves an inhibitor, often similar in structure to the substrate molecule, which has an affinity for the active site on the enzyme. Under these conditions, the inhibitor (I) competes with the substrate for access to the active site to form an enzyme–inhibitor complex (EI) according to Equation 6.8, where the rate constants k_4 and k_5 refer to the forward and reverse reactions respectively. Since the rate of change of the enzyme–inhibitor complex is negligible, the relationship between the rates of formation and destruction of the enzyme–inhibitor complex can be equated to give Equation 6.9 where K_I is known as the inhibition or dissociation constant. K_I represents the degree of dissociation of the enzyme–inhibitor complex and hence indicates the potency of the inhibitor. A small K_I implies $[EI] > [E][I]$ and high inhibition. On the contrary, a large K_I implies $[E][I] > [EI]$, indicating comparatively less inhibition.

$$E + I \overset{k_4 k_5}{\longleftrightarrow} EI \qquad [6.8]$$

$$\frac{[E][I]}{[EI]} = \frac{k_5}{k_4} = K_I \qquad [6.9]$$

The maximum velocity, again expressed in terms of the given quantity of enzyme, now includes both the enzyme–substrate and enzyme–inhibitor complexes according to Equation 6.10.

Published by Woodhead Publishing Limited, 2013

$$v_{max} = k_3([E] + [ES] + [EI]) \quad [6.10]$$

Combining Equations 6.2, 6.3, 6.9 and 6.10 yields the well-known Michaelis–Menten equation for prediction of the reaction velocity under conditions of competitive inhibition, expressed in terms of the Michaelis–Menten constant and the inhibition constant (Equation 6.11). This predicts a reduction in the velocity of product formation in the presence of an inhibitor. Further, the reduction in velocity is exacerbated for small K_I[9] and higher inhibitor concentrations.[10] The lower velocity with an identical v_{max} results in an increased K_m. This makes conceptual sense because a higher substrate concentration will be required for the velocity to reach half its maximum value.

$$v = \frac{v_{max}[S]}{K_m + [S] + \frac{K_m[I]}{K_I}} = \frac{v_{max}[S]}{K_m\left(1 + \frac{[I]}{K_I}\right) + [S]} \quad [6.11]$$

The situation is, however, different at high substrate concentrations. Here, the substrate out-competes the inhibitor such that the effect of the inhibitor is largely negated and the maximum velocity for a given quantity of enzyme remains the same as that under conditions of no inhibition. This is reflected in Equation 6.11 for substrate concentrations very much larger than $\frac{K_m[I]}{K_I}$ when the velocity approximates Equation 6.5, i.e. the velocity of product formation in the absence of an inhibitor.

The constants can be evaluated by using one of the standard plots. For instance, for competitive inhibition, a Lineweaver–Burk relationship will yield a gradient of $\frac{K_m}{v_{max}}\left(1 + \frac{[I]}{K_I}\right)$, y-intercept $\frac{1}{v_{max}}$ and an x-intercept of

Published by Woodhead Publishing Limited, 2013

$-\frac{1}{K_m\left(1+\frac{[I]}{K_I}\right)}$, from which the constants K_m, v_{max} and K_I can be calculated.

6.2.2 Uncompetitive inhibition kinetics

Uncompetitive inhibition results from the binding of an inhibitor with the enzyme–substrate complex to form an enzyme–substrate–inhibitor complex (ESI), according to Equation 6.12, where the rate constants k'_4 and k'_5 refer to the forward and reverse reactions respectively. Since the rate of change of ESI is negligible, the relationship between the rates of formation and dissociation of the enzyme–substrate–inhibitor complex can be equated to give K'_I, the dissociation constant (Equation 6.13). Again, a small K'_I indicates little dissociation of the complex with correspondingly high inhibition (and vice versa).

$$ES + I \overset{k'_4 k'_5}{\longleftrightarrow} ESI \qquad [6.12]$$

$$\frac{[ES][I]}{[ESI]} = \frac{k'_5}{k'_4} = K'_I \qquad [6.13]$$

The maximum velocity, again expressed in terms of the given quantity of enzyme, now includes both the enzyme–substrate and enzyme–substrate–inhibitor complexes according to Equation 6.14.

$$v_{max} = k_3([E] + [ES] + [ESI]) \qquad [6.14]$$

Combining Equations 6.2, 6.3, 6.13 and 6.14 yields the Michaelis–Menten equation for prediction of the reaction velocity under conditions of uncompetitive inhibition, expressed in terms of the Michaelis–Menten constant and

Published by Woodhead Publishing Limited, 2013

the inhibition constant (Equation 6.15). As with competitive inhibition, the velocity of product formation is decreased in the presence of an inhibitor, especially for small K_I[11] and higher inhibitor concentrations.[12]

$$v = \frac{v_{max}[S]}{K_m + [S] + \frac{[S][I]}{K'_I}} = \frac{v_{max}[S]}{K_m + [S]\left(1 + \frac{[I]}{K'_I}\right)} \qquad [6.15]$$

Unlike competitive inhibition, in uncompetitive inhibition, the maximum velocity for a given quantity of enzyme is lowered, even at high substrate concentration. The bonding of the enzyme–substrate complex with the inhibitor reduces the effective concentration of the enzyme–substrate complex, ultimately resulting in a decrease of v_{max}. Nevertheless, the reduction in the concentration of the enzyme–substrate complex also increases the enzyme's affinity for the substrate according to Le Chatelier's Principle[13] and K_m is lowered.

The constants can be evaluated from a Lineweaver–Burk relationship. A gradient of $\frac{K_m}{v_{max}}$, y-intercept $\frac{1 + \frac{[I]}{K'_I}}{v_{max}}$ and an x-intercept of $-\frac{1 + \frac{[I]}{K'_I}}{K_m}$, yields the constants K_m, v_{max} and K'_I.

6.2.3 Mixed inhibition kinetics

In competitive inhibition, the inhibitor cannot bind if the substrate has already bound to the enzyme, whereas in uncompetitive inhibition, the inhibitor can only bind if the substrate has already bound to the enzyme. A third type of inhibition, mixed inhibition, exists in which the inhibitor can bind whether or not the substrate has already bound to the enzyme.[14] This is a consequence of the availability of two binding sites, where the binding site for the inhibitor is

Published by Woodhead Publishing Limited, 2013

distinct from the active site to which the substrate binds. The site to which the inhibitor binds is termed an allosteric site and the enzyme, an allosteric enzyme.

So binding of the inhibitor can take place either directly with the free enzyme, according to Equation 6.16, or with the enzyme–substrate complex according to Equation 6.17.

$$E + I \overset{k_4 k_5}{\longleftrightarrow} EI \qquad [6.16]$$

$$ES + I \overset{k'_4 k'_5}{\longleftrightarrow} ESI \qquad [6.17]$$

Since the allosteric site is different from the active site, the substrate can still bind to the enzyme–inhibitor complex, according to Equation 6.18, where k′ is defined according to Equation 6.19.

$$EI + S \overset{k'_1 k'_2}{\longleftrightarrow} ESI \qquad [6.18]$$

$$\frac{[EI][S]}{[ESI]} = \frac{k'_2}{k'_1} = k' \qquad [6.19]$$

The maximum velocity, again expressed in terms of the given quantity of enzyme, now includes the enzyme–substrate, enzyme–inhibitor and enzyme–substrate–inhibitor complexes according to Equation 6.20.

$$v_{max} = k_3([E] + [ES] + [EI] + [ESI]) \qquad [6.20]$$

The binding of the inhibitor to the allosteric site alters the overall charge distribution on the enzyme, and hence the affinity of the substrate for the active site, resulting in negative or positive modulation. Positive modulation increases the affinity of the substrate for the active site (and so decreases K_m), while negative modulation decreases the affinity of the substrate for the active site (and so increases K_m). In either event, the binding of the inhibitor to the

Published by Woodhead Publishing Limited, 2013

allosteric site prevents the enzyme substrate complex from functioning so v_{max} is lowered.

A special case of mixed inhibition exists where the binding of the inhibitor to the allosteric site and the binding of the substrate to the active site is independent, so $k = k'$ (k given by Equation 6.2[15] and k′ by Equation 6.19) and $K_I = K'_I$ (K_I given by Equation 6.9 and K'_I by Equation 6.13). This is called non-competitive inhibition where K_m remains constant.

In consideration of the above equalities in the rate constants, a combination of Equations 6.2, 6.3, 6.13, 6.19 and 6.20 yields the Michaelis–Menten equation for prediction of the reaction velocity under conditions of non-competitive inhibition, expressed in terms of the Michaelis–Menten constant and inhibition constant (Equation 6.21).

$$v = \frac{v_{max}[S]}{K_m + [S] + \frac{K_m[I]}{K_I} + \frac{[S][I]}{K_I}} = \frac{v_{max}[S]}{K_m\left(1 + {}^{[I]}\!/\!_{K_I}\right) + [S]\left(1 + {}^{[I]}\!/\!_{K_I}\right)} \quad [6.21]$$

Equation 6.21 predicts that the effect of non-competitive inhibition is to decrease the velocity. As for uncompetitive inhibition, the maximum attainable velocity is also decreased.

The constants can be evaluated from a Lineweaver–Burk relationship. A gradient of $\frac{K_m}{v_{max}}\left(1 + \frac{[I]}{K_I}\right)$, y-intercept $\frac{1 + \frac{[I]}{K_I}}{v_{max}}$ and an x-intercept of $-\frac{1}{K_m}$, yields the constants K_m, v_{max} and K_I.

6.3 Enzyme reactors with soluble enzymes

Batch enzyme reactors generally use soluble enzymes. In this case, the process design equations can be developed directly

Published by Woodhead Publishing Limited, 2013

from the velocity as defined in the Michaelis–Menten equation. The following development of the process design equations assumes no inhibition. If the kinetics exhibit some form of inhibition, the design equation should be modified by incorporating the appropriate kinetic equation derived above (Section 6.2).

To formulate the design equation, consider a batch enzymic process where the initial substrate concentration (S_0) at time zero is decreased to S at time t, with a velocity as given by Equation 6.5. Separation of variables and integration over the entire time of batch operation (Equation 6.22) yields Equation 6.23.[16]

$$\int_{S_0}^{S} -\frac{K_m + S}{S}\, dS = \int_0^t v_{max}\, dt \qquad [6.22]$$

$$K_m \ln\frac{S_0}{S} + (S_0 - S) = v_{max}\, t \qquad [6.23]$$

This can also be written in terms of conversion (x), where conversion respresents the amount of substrate used realtive to the intial amount available (Equation 6.24).

$$-K_m \ln(1 - x) + xS_0 = v_{max} t \qquad [6.24]$$

This, however, assumes that the enzyme retains its activity in entirety for the duration of the batch operation. But enzymes generally do not remain stable; they lose activity with time at a rate depending on their half-lives. Many enzymes have been found to exhibit a first order decay that can be represented by Equation 6.25, where k_d is the enzyme decay constant. Separation of variables and integration yields an expression for the enzyme concentration at time t in terms of the initial enzyme concentration (E_i) (Equation 6.26).

$$\frac{dE}{dt} = -k_d E \qquad [6.25]$$

Published by Woodhead Publishing Limited, 2013

$$E = E_i \exp(-k_d t) \quad [6.26]$$

Substitution of Equation 6.26 into Equation 6.22 results in Equation 6.27. Finally, intergration yields the design equation for a batch enzyme reactor under conditions of no inhibition where the enzyme experiences a first order decay (Equation 6.28).

$$\int_{S_0}^{S} -\frac{K_m + S}{S}\, dS = \int_0^t k_3 E_i \exp(-k_d t)\, dt \quad [6.27]$$

$$-K_m \ln(1-x) + xS_0 = \frac{k_3 E_i}{k_d}\{1 - \exp(-k_d t)\} \quad [6.28]$$

6.4 Enzyme reactors with immobilised enzymes

6.4.1 Immobilisation techniques

Continuous enzyme processes only become economically viable if the enzyme can be recovered and re-used. This is especially important in the case of purified isolates, more so if these isolates are obtained from GMOs. In practice, continuous enzyme processes incorporate some sort of enzyme retention in the system to facilitate enzyme re-use.

Enzyme retention may take the form of *ex situ* enzyme separation using an ultrafiltration membrane with a molecular weight cut off smaller than that of the enzyme to be retained (see Section 11.4.2), and recycle of the retentate back to the reactor. Or an *in situ* ultrafiltration membrane can be used directly to retain the enzyme within the reactor. Retention of the enzymes within the reactor also allows for greater product purity and eliminates expensive purification steps to remove impurities (Section 11.4).

Published by Woodhead Publishing Limited, 2013

Alternatively, enzyme immobilisation can be mediated through immobilisation of the enzyme in the reactor. Several immobilisation matrices have been developed, almost all of which rely on adsorption onto or entrapment into a solid phase. Adsorption onto a solid surface is the oldest immobilisation process. Many supports, both inorganic and organic may be used as the adsorption matrix; glass is common. Unfortunately some enzyme loss can occur through desorption, although this also means that regeneration of the support is relatively easy. Covalent linking to the solid surface has also been used to secure the enzyme but activity may be lost.

Entrapment commonly makes use of calcium or barium alginate or agarose beads, although other matrices have been found to be suitable. This method of immobilisation is similarly unlikely to deactivate the enzyme but may pose mass transfer limitation problems as the substrate diffuses into, and the product out of, the bead so that the reaction may become transport rather than kinetically controlled. A novel method of entrapment is the immobilisation of the enzyme inside the porous support of a ceramic membrane with a molecular weight cut off that prevents the enzyme from passing through (Section 11.4.2).

Enzyme adsorption and entrapment takes place under moderate conditions so immobilisation by either of these methods is unlikely to cause enzyme deactivation. In fact, these types of immobilisation generally improve the enzyme stability such that enzymic processes become feasible with the half-life of the enzyme measured in terms of months rather than days.

A more recently developed enzyme immobilisation procedure, cross-linked enzyme aggregates (CLEAs), have enjoyed increasing popularity. CLEAs are produced by precipitation of the enzyme from solution as amorphous

Published by Woodhead Publishing Limited, 2013

aggregates of enzyme molecules (Section 11.4.1) which are subsequently cross-linked to render them permanently insoluble. Since precipitation essentially purifies the enzyme, this technique has the added advantage that it does not require a highly purified enzyme for its execution.

Immobilised enzyme configurations can be used in both continuous stirred tank reactor (CSTR) and continuous plug flow reactor (CPFR) configurations. A laboratory membrane reactor for continuous operation using enzymes immobilised in a ceramic matrix is shown in Plate 6.1.

6.4.2 Continuous enzyme processes with kinetically controlled reaction

Immobilised enzymes in either a CSTR or a CPFR introduce a solid matrix which changes the system to a heterogeneous one. In heterogeneous systems, the reaction

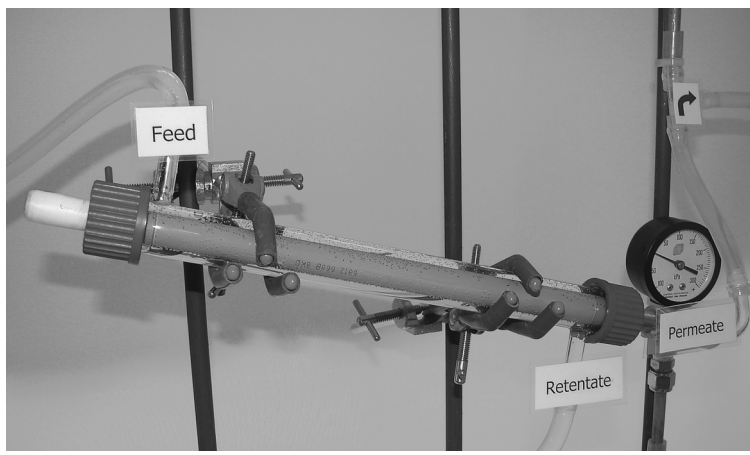

Plate 6.1 **A laboratory membrane reactor housing a ceramic support for enzyme immobilisation. Substrate fed into shell side, product from lumen side as permeate. Photo: R du Preez**

Published by Woodhead Publishing Limited, 2013

takes place in the liquid volume (V_L) only, while the total enzyme concentration (E_T) is related to the total volume (V_T). The different volumes need to be accounted for in the development of the design equations for each of these reactor configurations.

The design equation for the CSTR is developed from a substrate balance over the reactor at steady state[17] where F refers to the volumetric flow rate and S_R to the substrate in the feed reservoir (Figure 6.1). The substrate balance equates the substrate entering the reactor by flow with the substrate leaving by flow plus the substrate utilised in the reaction (Equation 6.29),

$$FS_R = FS + vV_L \qquad [6.29]$$

Inserting the expression for velocity, assuming no inhibition (Equation 6.5), and the expression for v_{max} (Equation 6.4) results in Equation 6.30, where $\in$ is the voidage (V_L/V_T). Rearrangement yields Equation 6.31. The design equation which predicts conversion in a CSTR enzyme reactor in terms of residence time (τ) is given in Equation 6.32.

$$F(S_R - S) = \frac{k_3(E_T / V_T)S}{K_m + S} V_L = \frac{k_3 E_T \in S}{K_m + S} \qquad [6.30]$$

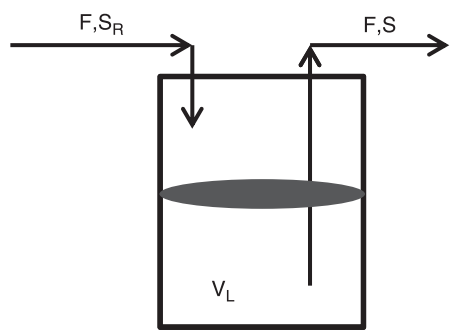

Figure 6.1 CSTR schematic

$$K_m\left(\frac{S_R - S}{S}\right) + (S_R - S) = \frac{k_3 E_T \in}{F} \quad [6.31]$$

$$K_m\left(\frac{x}{1-x}\right) + xS_R = \frac{k_3 E_T \in \tau}{V_L} \quad [6.32]$$

The design equation for the PFR is developed from a substrate balance over a differential volume element dV_L in the reactor at steady state where F refers to the volumetric flow rate and dS to the differential change in substrate concentration in dV_L (Figure 6.2).

A substrate balance equates the substrate entering the element by flow with the substrate leaving by flow plus the substrate utilised in the reaction (Equation 6.33).

$$FS = F(S + dS) + vdV_L \quad [6.33]$$

Inserting the expression for velocity in the absence of inhibition (Equation 6.5), and the expression for v_{max} (Equation 6.4) results in Equation 6.34.

$$-FdS = \frac{k_3\left(E_T / V_T\right)S}{K_m + S} dV_L \quad [6.34]$$

Separation of variables and integration over the entire PFR as in Equation 6.35, results in Equation 6.36. The design equation which predicts conversion in a plug flow enzyme reactor in terms of residence time (τ) is given in Equation 6.37.

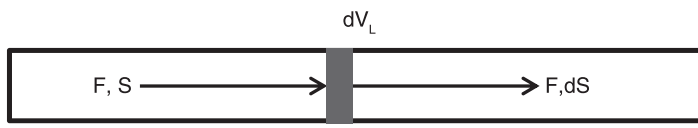

Figure 6.2 CPFR schematic

Published by Woodhead Publishing Limited, 2013

$$\int_{S_R}^{S} -\frac{K_m + S}{S} dS = \int_0^{V_L} \frac{k_3 \left(E_T / V_T\right)}{F} dV_L \quad [6.35]$$

$$K_m \ln \frac{S_R}{S} + (S_R - S) = \frac{k_3 E_T \in}{F} \quad [6.36]$$

$$-K_m \ln(1-x) + xS_R = \frac{k_3 E_T \in \tau}{V_L} \quad [6.37]$$

The process performance of immobilised enzyme reactors is usually measured in terms of conversion (and, less frequently, in terms of productivity). The parameters which majorly influence conversion in immobilised enzyme systems are the enzyme concentration in the reactor and the time during which the enzyme is in contact with the substrate. Since the reaction is theoretically independent of reactor volume, the influences of enzyme concentration and residence time may be assessed in terms of the total amount of enzyme and the volumetric flow rate respectively. Comparison between the process performance of CSTRs and CPFRs can, therefore, be assessed in terms of these parameters.

Comparison of the volumetric flow rates in a CSTR (Equation 6.38) and a CPFR (Equation 6.39) shows that, for the same conversion, the flow rate in the CSTR will be lower than that in the CPFR. This implies that for the same flow rate, the conversion in the CSTR will be less than that in the CPFR. But this difference in conversion decreases as the ratio S_R/K_m increases. In most industrial processes, the difference in conversion is negligible as S_R is usually much larger than K_m.

$$F_{CSTR} = \frac{k_3 E_T \in}{K_m \left(\frac{x}{1-x}\right) + xS_R} \quad [6.38]$$

Published by Woodhead Publishing Limited, 2013

$$F_{CPFR} = \frac{k_3 E_T \in}{-K_m \ln(1-x) + x S_R} \quad [6.39]$$

Comparison of the amounts of enzyme required for the same conversion in the CSTR (Equation 6.40) and the CPFR (Equation 6.41) shows that more enzyme is required in the CSTR. However, the voidage in a CSTR is usually slightly larger (0.95–0.99) than that in a CPFR (0.7–0.8) which reduces the difference somewhat. The difference in enzyme amounts is also lower at high S_R/K_m as in most industrial processes.[18]

$$E_T = \frac{F}{k_3 \in}\left[K_m\left(\frac{x}{1-x}\right) + x S_R\right] \quad [6.40]$$

$$E_T = \frac{F}{k_3 \in}\left[-K_m \ln(1-x) + x S_R\right] \quad [6.41]$$

These process design equations developed here for immobilised enzyme CSTRs (Equation 6.32) and CPFRs (Equation 6.37) present only the most basic of models. They do not take into account enzyme decay or enzyme inhibition. To include these more complex scenarios, enzyme decay models, such as first order decay (Equation 6.25) and the appropriate inhibition kinetics (Section 6.2) would need to be included in the derivation, where applicable. In the case of enzymes which are subject to product inhibition, the CPFR will give a greater conversion than the CSTR, while in the case of substrate inhibited enzymes, the conversion in the CSTR will be greater, all other conditions being equal.

6.4.3 Continuous enzyme processes with transport controlled reaction

In the discussion on immobilised enzyme reactors (Section 6.4), it has been assumed that the reaction rate is

Published by Woodhead Publishing Limited, 2013

controlled by Michaelis–Menten kinetics. However, in immobilised systems, where the enzymes are attached on or in a support matrix, the substrate must diffuse into a relatively stagnant layer around the support, and in the latter case, into the pores of the support itself. Under these conditions, the enzymes may be subject to diffusional limitations of one or more substrates (e.g. carbon source and oxygen) such that the velocity of reaction becomes limited by the rate of transfer of the substrate(s) to the active sites on the enzymes. This loss of kinetic control has serious negative consequences with regard to reactor performance.

For enzymes bound to a non-porous matrix, external mass transfer limitation may occur when the substrate concentration at the matrix surface (S_s), i.e. the substrate in contact with the enzyme, will be significantly less than the substrate concentration in the bulk fluid (S_b). In order to apply Michaelis–Menten kinetics, an expression for S_s in terms of S_b needs to be obtained. This is achieved by considering the rate of substrate transport to the matrix surface.

The most common model describing substrate transport to the matrix surface is based on a mechanism which assumes that a stagnant liquid layer or film forms on the surface of the matrix in which all the resistance to mass transfer resides. Since this is a stagnant liquid film, transport takes place by molecular diffusion only and consequently, the molar flux (the rate of transfer per unit area) is proportional to the concentration gradient across the stagnant film. This is represented by Equation 6.42 where S_b is the substrate concentration in the bulk fluid and S_s the substrate concentration on the matrix surface. K is the proportionality constant and has the physical significance of the inverse of the resistance in the stagnant film; it is known as the mass transfer coefficient.[19]

$$\text{Flux} = K_L(S_b - S_s) \qquad [6.42]$$

Published by Woodhead Publishing Limited, 2013

However, the flux represents a molar rate in terms of area which is inconsistent with reaction velocity which is a molar rate in terms of volume. To convert the flux to a velocity base, an additional parameter is introduced. This parameter is the ratio of the interfacial area per unit liquid volume and is designated 'a'. Multiplying both sides of Equation 6.42 by 'a' results in the expression for reaction velocity (Equation 6.43) where $K_L a$ is a lumped parameter referred to as the overall volumetric mass transfer coefficient.

$$v = K_L a(S_b - S_s) \qquad [6.43]$$

From Equation 6.43 the substrate concentration at the surface can be deduced (Equation 6.44). Inserting this expression into the Michaelis–Menten equation (Equation 6.5) yields Equation 6.45.

$$S_s = S_b - v/K_L a \qquad [6.44]$$

$$v = \frac{v_{max}\left(S_b - v/K_L a\right)}{K_m + \left(S_b - v/K_L a\right)} \qquad [6.45]$$

The transfer limitation will be most severe at low flow rates where fluid turbulence is lowest. Here the stagnant film will be relatively thick, thereby imposing a high resistance (i.e. small K_L). On the other hand, the limitation is reduced at high substrate concentrations in the bulk fluid. In practice, a trade-off between substrate wastage and reduced reaction velocity needs to be made.

In this (Equation 6.45) and previous Michaelis–Menten expressions, the K_m has represented the intrinsic value. However, in situations where the velocity is transport controlled, the observed or apparent value is larger than the

Published by Woodhead Publishing Limited, 2013

intrinsic value and is represented as K'_m. To account for the change in this value, the Michaelis–Menten equation (Equation 6.5) is frequently written as Equation 6.46 where the reaction velocity is transport controlled.

$$v = \frac{v_{max} S_b}{K'_m + S_b} \quad [6.46]$$

In the case of enzymes which are bound to a porous support, internal mass transfer limitation may also occur. In order to determine whether the reactor is operating in a kinetics or transport limited regime, a parameter known as the Thiele modulus (Φ), given by Equation 6.47 is used. Here D is the effective diffusivity and R the radius of the support. In the case of membrane supports, R represents the membrane thickness.

$$\Phi = R\left(\frac{v_{max}}{K_m D}\right)^{0.5} \quad [6.47]$$

The Thiele modulus is related to an effectiveness factor (η) which defines the ratio of the velocity of reaction with pore diffusion to the velocity of reaction in the absence of pore diffusion according to Equation 6.48. The effectiveness factor can be developed from first principles and the solutions obtained via numerical integration. The relationship of the effectiveness factor and the Thiele modulus is frequently presented graphically with S/K_m as a third parameter. These graphs show that if the Thiele modulus is less than 0.3, then the effectiveness factor is approximately unity (i.e. no diffusional limitations). Thiele moduli greater than 0.3 indicate diffusion limited reaction rates. However, as S/K_m increases, the effect of pore diffusion is lessened.

$$\eta = \frac{\text{observed rate}}{\text{intrinsic rate}} \quad [6.48]$$

Published by Woodhead Publishing Limited, 2013

6.5 Notes

1. α- and β-amylases break down α-1,4 linkages in starch.
2. Proteases hydrolyse the peptide bonds that link amino acids together in polypeptide chains.
3. Square brackets indicate concentrations.
4. Enzymes are very large molecules so will be present in small amounts, as will the enzyme complex.
5. Leonor Michaelis (1875–1949) and Maud Menten (1879–1960).
6. The gradient of K_m/v_{max} can alternatively be used in the calculations.
7. Hans Lineweaver (1907–2009) and Dean Burk (1904–1988).
8. Note that this is very different from the regulation of enzyme synthesis which takes place at the level of the gene.
9. This correlates with a lower dissociation of the enzyme inhibitor complex.
10. This correlates with a decrease in the available binding sites for the substrate.
11. This correlates with a lower dissociation of the enzyme–substrate–inhibitor complex.
12. This correlates with an increase in the formation of enzyme–substrate–inhibitor complex according to Le Chatelier's Principle.
13. Henry Louis Le Chatelier (1850–1936) formulated the principle: 'If a chemical system at equilibrium experiences a change in concentration, temperature, volume or partial pressure, then the equilibrium shifts to counteract the imposed change and a new equilibrium is established.'
14. Mixed inhibition is conceptually seen as a 'mixture' of competitive and uncompetitive inhibition.
15. The derivation can be simplified by assuming K_m approximates k; this is valid since k_3 is small (rate limiting).
16. The square brackets have been omitted for convenience.
17. Steady state implies no accumulation or depletion in the system with time.
18. This comparison of total amounts of enzyme has assumed comparable activity and stability in the different systems.
19. The subscript L indicates that the resistance resides within the liquid. Note the similarity to oxygen transfer.

Published by Woodhead Publishing Limited, 2013

7

Microbial kinetics during batch, continuous and fed-batch processes

DOI: 10.1533/9781782421689.97

Abstract: To grow microorganisms successfully, whether the desired product is a metabolic intermediate or the cells themselves, the necessary nutrients required for growth and maintenance need to be provided in sufficient quantities. Without these, the microorganism would be unable to synthesise the macromolecules for reproduction and maintenance of cellular structure or for fuel storage. Nor would they be able to carry out respiratory, fermentative or photosynthetic pathways to provide energy.

An appropriate nutrient medium then, together with suitable environmental conditions of, for example, pH, temperature and oxygen availability, are the process conditions which define the minimum requirement for all bioprocesses. Bioprocesses, in addition, are designated according to the strategy under which they operate. The simplest and most widely used operational bioprocess strategy is batch culture (Section 7.2). Other strategies, namely continuous culture (Section 7.3) and fed-batch culture (Section 7.4) are also extensively used and are preferred under certain specific instances. The development of the appropriate process strategy and the formulation of optimal process conditions are singly and together essential

Published by Woodhead Publishing Limited, 2013

for the maximisation of the potential of the biocatalyst for product formation. This responsibility sits largely on the shoulders of the Bioprocess Engineer.

Chapter 7 begins with a discussion of suitable process conditions for microbial culture, specifically appropriate nutrient medium formulation and an analysis of the effects of environmental conditions, such as pH and temperature, on cell growth (Section 7.1). The supply of adequate oxygen for aerobic respiration is dealt with in a separate chapter (Chapter 8).

Following this, the kinetic bases for cell growth and substrate utilisation during batch culture are elucidated and expressed mathematically. These mathematical expressions are then applied to continuous and fed-batch systems in the development of the appropriate mathematical design equations for these process strategies.

Key words: batch reactor kinetics, continuous reactor kinetics, fed-batch reactor kinetics, endogenous metabolism, energy of maintenance.

7.1 The nutrient medium

To understand the nutrient requirements of a microorganism, the elemental components that make up the living matter need to be defined. This is not necessarily simple, as different microorganisms will differ in their elemental compositions, with larger discrepancies between different categories of microorganisms, for example, heterotrophs and autotrophs. Considering chemo-heterotrophs only (the most common type in commercial microbial processes), studies have shown that these microbial cells comprise mainly (about 99%) of the elements carbon, oxygen, hydrogen, nitrogen, phosphorous and sulphur. Elements such as Fe, Mg and Ca

Published by Woodhead Publishing Limited, 2013

are present in trace amounts only. Carbon makes up about 50% of the elements and, together with oxygen (about 20%) and hydrogen (about 8%), is ubiquitous in the cell. Nitrogen (about 15%) is *inter alia* an essential element in proteins and nucleic acids, phosphorous (about 3%) in nucleotides and sulphur (about 1%) in some amino acids and vitamins. Trace elements have various functions, notably as metal cofactors, such as Fe which serves as an electron carrier during respiratory or photosynthetic pathways.

An appropriate nutrient medium, therefore, will contain salts of these elements in proportions required by the cells. Carbon requirements are met by some form of carbohydrate, fat or hydrocarbon, depending on the metabolism of the microorganism. Carbon supplied as carbohydrate also meets about 66% of the oxygen demand of an aerobic microorganism. The remainder of the oxygen required, however, has to be transferred to the medium by continuous aeration and agitation because of its low solubility (Section 8.1). When the nutrients supply negligible oxygen (e.g. when a hydrocarbon source is utilised), all the oxygen has to be transferred to the aerobe via aeration and agitation.

Nitrogen is usually added as an ammonium or nitrate salt. Some organisms are reported to prefer one or the other form but this may be in part due to a pH effect. Metabolism of a nitrogen-containing cation (e.g. NH_4^+ from $(NH_4)_2SO_4$) would result in a pH decrease and growth inhibition (depending on the severity of the decrease). On the other hand, metabolism of a nitrogen-containing anion (e.g. NO_3^- from $NaNO_3$) would tend to increase the pH and possibly avoid pH inhibition of growth. Bioreactors with pH control facilities can of course avoid pH inhibition by maintaining the pH above the inhibitory level through controlled feeding of an alkaline solution. Alkaline solutions that contain nitrogen, such as NH_4OH, also serve as an additional nitrogen supply.

Published by Woodhead Publishing Limited, 2013

In some microorganisms, however, inorganic nitrogen sources may not be sufficient to meet the particular metabolic demands. For instance, these microorganisms may not be able to synthesise specific amino acids or vitamins themselves. In these cases, an organic nitrogen source must be incorporated to provide the amino acids or vitamins. Organic nitrogen may be supplied as yeast extract (about 10% nitrogen) or peptone (about 15% nitrogen), both of which are good sources of amino acids, although generally only economically viable on the smaller scale.

Phosphorous is commonly added as a potassium or sodium salt. In view of the importance of the pH of the medium on the microbial viability, K_2HPO_4 and KH_2PO_4 (or Na equivalents) can be added in a ratio which provides buffering capacity at a required pH. This is particularly important in processes without pH control. However, care should be taken so as not to overdo the addition of buffer salts as some microorganisms can be inhibited by elevated concentrations of sodium, potassium and/or phosphorous. To reduce sodium or potassium levels, the K_2HPO_4 and KH_2PO_4 (or Na equivalents) can be substituted by NH_4PO_4, which supplies both phosphates and nitrogen.

These principles provide only a guideline for formulating a simple medium. Different requirements by different microorganisms and different process conditions, which may alter nutrient requirements, should be taken into account. The change from an aerobic to anaerobic process condition during culture of the facultative *Bacillus subtilis* is a typical example. When oxygen is no longer available, *B. subtilis* substitutes nitrate for oxygen as an electron acceptor, and so is likely to need more nitrogen under anaerobic conditions. Moreover, product formation may also introduce the need for media modifications, for instance a requirement for additional compounds or precursors for product formation,

Published by Woodhead Publishing Limited, 2013

or the addition of an inducer in the case of enzymes subject to control.

On the small scale, and particularly in the research laboratory, each media component, and the ratios of elements in each of the components, is typically defined. However, in large scale industrial processes where raw materials may constitute 50% or more of manufacturing costs, the media tend to be complex and substitutes for expensive components (especially vitamins and amino acids) are made. Cheaper sources of amino acids can be sourced from, for example, whey, a by-product of the cheese industry.

To reduce carbon costs, refined sugars have been replaced by raw molasses, sugar hydrolysates, or where possible, wastes containing fermentable carbon. The burgeoning research into production of renewable fuels from hydrolysed lignocellulosic wastes is one such example of using waste as a raw material. Here a key issue is the ability to metabolise the 5-carbon sugars present in lignocellulosic wastes (together with the 6-carbon sugars) which generally requires either bacterial or fungal GMOs. Another is the bioconversion of alkane by-products, accumulating worldwide from the flourishing gas to liquid technologies. More recently perhaps is the conversion of wastes to hydrogen for use in fuel cells. Nevertheless, the impression should not be created that the use of wastes is a new idea; we have long since explored the opportunities of eliminating waste while producing a useful bioproduct, to name only a couple: skins and pips from the wine industry and sludge from municipal sewage.

7.2 Batch process design equations

Batch cultures are sometimes preferred over other operating strategies, especially in the case of high cost products. Here

Published by Woodhead Publishing Limited, 2013

the product is often highly specialised and/or produced in low yields, making maximal product concentrations, rather than maximal productivities the measure of success. A maximal product concentration minimises the number of unit operations required in the product recovery programme (Section 11.1), and so reduces the overall production cost when downstream processing is taken into account. Importantly, batch operation is advantageous in that it facilitates flexibility in product volume and type and so is well positioned to meet changing market demands.

Batch culture is most often conducted in a stirred tank reactor (STR). A STR is a cylindrical reactor, agitated by means of impellers, and usually fitted with baffles to increase turbulence and mixing efficiency. In aerobic bioprocesses, air is sparged from an outlet below the bottom impeller. To increase the oxygen transfer to the microorganisms, the impeller in an aerobic process is usually a turbine impeller as the radial flow is best suited for breakup of air bubbles which improves oxygen transfer. The bubble density distribution is typically highest in the vicinity of the impellers (Plate 7.1).

In view of the widespread use and importance of batch operation, it is expedient to determine and analyse kinetic data for cell growth, substrate utilisation and product formation during batch bioprocesses and to predict performance through process design equations.

7.2.1 The rate of microbial growth

Some of the most fundamental questions asked in bioprocess development is how fast do the microorganisms metabolise the nutrients (more specifically, the limiting nutrient[1]), how fast do they grow on the limiting nutrient, how fast do they form product and what is the yield of product formed? To answer these questions, we need to develop mathematical

Published by Woodhead Publishing Limited, 2013

Plate 7.1 Aeration showing bubble intensity highest around impellers. Photo: L. Correia

models which quantify the respective rates of growth, substrate utilisation and product formation, models which can then be used to predict the process kinetics.

Batch culture may be carried out at the millilitre scale on the lab bench, typically in Erlenmeyer flasks (Plate 7.2), or litre scale in laboratory reactors (Plate 7.3) to up to tens of thousands of litres at the industrial scale. The batch culture is initiated by the introduction of a small volume (1–10% v/v) of an actively growing culture (called an inoculum) into the sterile nutrient medium in the flask or

Published by Woodhead Publishing Limited, 2013

Plate 7.2 Flask cultures in a shaker incubator on the lab bench. Photo: J. van Rooyen

reactor where it is allowed to grow, as far as possible for the specific system, under optimum environmental conditions. The inoculum itself is developed originally from a stock microbial culture (perhaps freeze dried or in a frozen glycerol solution), revived in a suitable nutrient medium and sequentially transferred into successively larger volumes of nutrient medium until it is of sufficient volume for use as an inoculum.

The characteristic microbial phases of growth during batch culture were first quantified with bacterial cells in the pioneering work of Robert Buchanan.[2] Years later, Jacques Monod[3] developed and expanded these concepts in his PhD thesis (1942) and later publications (from 1947).

The growth phases are defined in terms of the rate of change of cell concentration from the time of inoculation

Published by Woodhead Publishing Limited, 2013

Plate 7.3 **Instrumented laboratory stirred tank reactor**

Published by Woodhead Publishing Limited, 2013

(time zero) to the time of cell lysis (Figure 7.1). After inoculation, the cell concentration often undergoes a period of stasis; this is called the lag phase and represents a time when the cells are adapting to their environment and may also involve the synthesis of adaptive enzymes. The length of the lag phase depends on both the changes in nutrient composition experienced by the cells after transfer and the age and size of the inoculum. In general, the lag phase can be minimised by ensuring that the culture medium used to grow the inoculum is as close as possible to the final full scale process composition and by using actively growing cells as the inoculum culture.

At the end of the lag phase, the population of microorganisms is well adjusted to its new environment and the cells begin to multiply rapidly. This is the acceleration phase in which the cell concentration begins to increase. Eventually the cell numbers multiply at their maximum rate and divide at regular intervals. Here the cell numbers increase exponentially with time and the growth is said to be in the exponential growth phase (between 5 and 16 hours in Figure 7.1).

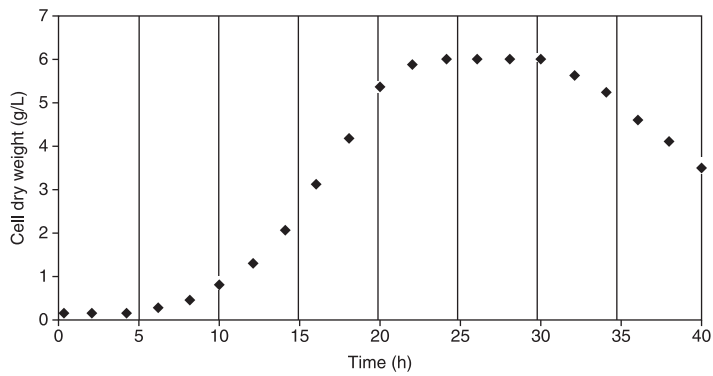

Figure 7.1 Characteristic microbial growth phases

Published by Woodhead Publishing Limited, 2013

As the nutrients for cell growth (including oxygen) become depleted in the culture medium and/or inhibitory metabolic products accumulate, the cell growth rate is retarded and the cell concentration tails off, giving rise to the de-acceleration phase. The cell growth rate continues to fall until the rate of cell growth equals the rate of cell lysis and the cell concentration remains constant, at which point the stationary phase has been reached (between 20 and 24 hours in Figure 7.1). Cells in the stationary phase are known as resting cells. A death phase may also occur during which starvation and/or stress becomes significant and cell numbers decline. Occasionally the death rate is so rapid that an exponential decline is observed.

The exponential growth phase is a consequence of unhindered replication, i.e. when all nutrients are in excess and no products have accumulated beyond a toxic threshold. Under these conditions, the growth of a single bacterial cell can be approximated by considering sequential division of one cell and its progeny in the following manner (Figure 7.2).

One cell will divide to produce two progeny after a certain time. The time taken to produce two cells from one cell is called the doubling time (t_D), or as the progeny represent the

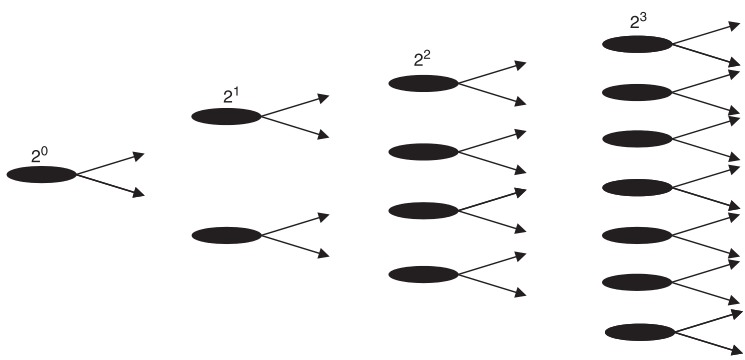

Figure 7.2 Exponential growth of a single bacterial cell

Published by Woodhead Publishing Limited, 2013

next generation, the generation time (g).[4] Each progeny then divides to form the cells of the following generation. After one generation, 2^1 cells are formed; after two generations, 2^2 cells are formed, after three generations, 2^3 cells are formed and so on. Assuming a mean generation time, in time t, we have t/g generations and, correspondingly, $2^{t/g}$ cells formed.

When quantifying the cells accumulated in time t, the cells introduced by the inoculum as well as those formed during this time have to be considered. Say the small concentration of cells introduced via the inoculum at the start is x_0, the cell concentration at time t is given by Equation 7.1.

$$x = 2^{t/g} x_0 \qquad [7.1]$$

The early researchers chose to write the cells formed at time t in terms of $\log_2$ (Equation 7.2). Later researchers expressed this is terms of natural logs and today the most common form is given in Equation 7.3, where μ represents the number of 'e-fold' generations in time t. μ is known as the specific growth rate and has units of reciprocal time.

The mathematical relationship between the specific growth rate and the generation time is revealed by writing Equation 7.1 in terms of natural logs ($\ln x = \ln x_0 + {}^{1}/_{g} \ln 2$) and comparing this directly with Equation 7.3. The relationship may be written in terms of the generation time or the doubling time (Equation 7.4).

$$\log_2 x = \log_2 x_0 + {}^{1}/_{g} t \qquad [7.2]$$

$$\ln x = \ln x_0 + \mu t \qquad [7.3]$$

$$\mu = {}^{\ln 2}/_{g} \text{ or } \mu = {}^{\ln 2}/_{t_D} \qquad [7.4]$$

Differentiation of Equation 7.3 yields the equation for microbial growth (Equation 7.5). This is known as Monod

Published by Woodhead Publishing Limited, 2013

growth kinetics and is used ubiquitously to quantify cell growth.

$$\frac{dx}{dt} = \mu x \qquad [7.5]$$

During the exponential growth phase, when the cells are dividing at their maximum rate (corresponding to the shortest generation time), the specific growth rate is the maximum value possible[5] and is, therefore, a constant. This is referred to as balanced growth because theoretically the cells in the exponential growth phase have a constant or steady composition. It is important to note that here it is the *composition* of the cells that is assumed constant, not the *concentration* of the cells. In fact, during balanced growth, the cell concentration is increasing exponentially![6]

This maximum specific growth rate is written as μ_{max} or $\hat{\mu}$. $\hat{\mu}$ is easily calculated from empirical cell concentration data during exponential growth. During this growth phase, a linear correlation of ln x versus t exists which, according to Equation 7.3, yields a gradient equal to $\hat{\mu}$ and an intercept ln x_0.

There are several methods available to gather empirical cell concentration data. The few that are in common usage are the quantification of cell numbers, cell dry weight, concentration of a cellular component (e.g. DNA, RNA, protein) and optical density[7] of the cell suspension. The methods which determine the cell numbers and cell dry weight are direct methods. Cell numbers are counted directly from a suitably diluted sample on a haemocytometer (or counting chamber) under a microscope; cell dry weight is measured directly from a dried cell pellet, obtained by centrifugation or filtration of a suitable sample volume. The methods which determine cellular components and optical density are indirect methods which should be calibrated against either cell numbers or cell dry weight.

While it is mathematically simple to calculate $\hat{\mu}$ from cell concentration data, care must be taken in the interpretation of the result as $\hat{\mu}$ can vary significantly depending on the method used to measure the cell concentration. In indirect methods, for instance, the quantity of internal cellular components per cell is unlikely to remain constant throughout all batch phases. DNA/cell is the most accurate but it would seem that protein/cell is the most commonly used.

Even the direct methods can yield anomalous behaviour. Consider the batch growth curve of the eukaryote *S. cerevisiae* (Figure 7.3).[8] During the exponential growth phase, the yeast rapidly produces buds and the ratio of buds to parent cells is high, so there are many small cells. As the stationary phase is approached, the budding rate decreases and the proportion of the larger parent cells increases, so there are fewer but larger cells in the stationary phase relative to the exponential growth phase. Because cell counts determine the number of cells, and cell dry weight determines the mass of cells, the ratio of cell numbers to cell dry weight is likely to be greater in the exponential growth phase than in the stationary phase. This, in general, will give rise to different growth curves. Specifically, since the rate of increase of cell numbers exceeds the rate of increase of

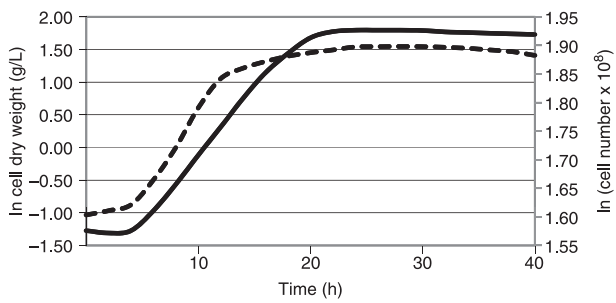

Figure 7.3 Batch growth curves determined from cell dry weight (—) and cell numbers (----)

Published by Woodhead Publishing Limited, 2013

cell mass during the exponential growth phase, this is also likely to give rise to different values of $\hat{\mu}$. It should be noted though, that this anomalous behaviour occurs only when there is a change of morphology during the culture. Cultures of prokaryotes which tend to have a constant cell number to cell dry weight through the batch phases will exhibit parallel curves.

The specific growth rate is of course not constant during phases other than the exponential growth phase, but varies with the gradient of the ln x versus t curve. During the lag and stationary phases the specific growth rate is zero, during acceleration and deacceleration the specific growth rate is positive, but increases with time in the former and decreases in the latter. On the other hand, the specific growth rate is negative during the death phases. Any value of the specific growth rate (albeit not very accurate) can be determined from the gradient of the curve taken over a small time interval.

Monod growth kinetics have wide application but should be used with caution with bioprocesses with filamentous fungi. Recall that the fundamental assumption on which Monod growth kinetics was developed is that growth takes place solely by cell division. While this assumption is certainly appropriate in the case of prokaryotes,[9] it is not necessarily valid for eukaryotic replication, even when considering only vegetative growth forms. In the case of yeasts which multiply by cell budding, Monod growth kinetics is a fair approximation. However, filamentous fungi grow by extension and branching of hyphal lengths, a growth pattern which may be more accurately described by linear rather than exponential equations. This should be taken into account when using Monod growth kinetics to predict cell growth under these conditions.

Published by Woodhead Publishing Limited, 2013

7.2.2 The dependence of microbial growth rate on substrate concentration

Monod also evaluated the dependence of the specific growth rate on the substrate concentration (s).[10] In his experiments, he eliminated the lag phase[11] such that the exponential growth phase was initiated immediately. His empirical observations of the relationship between the specific growth rate and substrate concentration during the exponential growth phase and deacceleration phase in batch culture remains the basis of the majority of biokinetic studies to this day and can be defined and explained as follows.

At high initial substrate concentrations, exponential growth is supported and the specific growth rate remains at its maximum value. However, as cells continue to grow and utilise the substrate, the substrate concentration decreases. Eventually the substrate reaches a concentration at which it is no longer able to support exponential growth. At this limiting substrate concentration, the specific growth rate begins to decrease, reaching zero at substrate exhaustion.

This relationship can be quantified by determining values of the specific growth rate from gradients of the ln x versus t curve at discrete time intervals during the exponential growth phase and deacceleration phase, and relating these to the values of substrate concentration at the midpoint of the corresponding time intervals. The data take the form of a typical saturation function from zero specific growth at zero substrate to maximum specific growth rate at high (non growth limiting) substrate concentrations (Figure 7.4).

The equation representing this saturation function is given by Equation 7.6 which is known simply as the Monod Model. K_s, the saturation constant, represents the substrate concentration at which $\mu = \frac{1}{2}\hat{\mu}$. K_s gives an indication as to

Published by Woodhead Publishing Limited, 2013

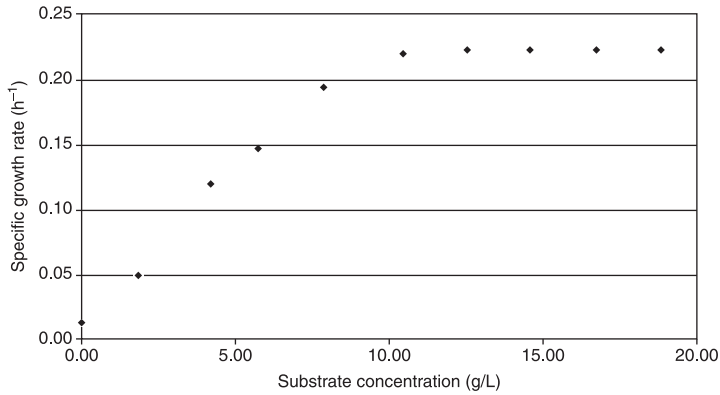

Figure 7.4 The effect of substrate concentration on specific growth rate

how fast (or slowly) the microbial growth ceases after the limiting substrate concentration has been reached. This value is different for different microorganisms, and varies widely with different substrates, being of the order of mg/L for sugars and μg/L to ng/L for amino acids. K_s also depends on the pH, osmotic pressure and, to some extent, other medium constituents. The K_s of facultative microorganisms will also vary depending on whether the organism is growing aerobically or anaerobically. In situations where K_s is particularly large, curious growth dynamics without a proper exponential growth phase may be observed.

$$\mu = \frac{\hat{\mu}s}{K_s + s} \qquad [7.6]$$

The Monod Model was developed from exponential and deaccelerating phase data only and, therefore, is strictly valid for these growth phases only. Nevertheless, it has been very widely used for decades and arguably forms the basis of most kinetic models in its basic form (Equation 7.6) or a modification thereof. Several modifications exist, probably the most

Published by Woodhead Publishing Limited, 2013

common being the modification to incorporate substrate inhibition of growth at high substrate concentrations (Equation 7.7). This equation successfully models a specific growth rate which decreases when substrate concentrations become toxic. Toxicity is often a function of concentration, e.g. for many sugars where toxicity at high concentrations is due to high osmotic pressure. Another case in point is phenol. This substance serves well as a growth substrate for a surprisingly wide range of microorganisms, but acts as a bacterial poison at high concentrations. Other elements (such as phosphate) can also exhibit substrate inhibition. Note the red flag when adding phosphate buffer to a medium for pH stabilisation!

$$\mu = \frac{\hat{\mu} s}{K_s + s + {}^{s^2}\!/_{K_I}} \qquad [7.7]$$

The Monod Model, and its various formulations, can be used to predict the specific growth rate of an organism at any substrate concentration provided the kinetic constants K_s and $\hat{\mu}$ are known. These constants are commonly obtained in the first instance from empirically determined values of the specific growth rate at defined substrate concentrations. Inversion of the Monod Model yields the familiar Lineweaver–Burk relationship between the reciprocal values of these data (Equation 7.8) with slope $\frac{K_s}{\hat{\mu}}$ and y-intercept $\frac{1}{\hat{\mu}}$ from which K_s and $\hat{\mu}$ can be calculated. Although the Lineweaver–Burk relationship is most commonly used to determine the kinetic constants, it is not recommended. The accuracy relies most heavily on the data at the lowest substrate concentrations where inaccuracies are most likely to occur. A more reliable method is to use the Eadie–Hofstee relationship (Equation 7.9), derived from the Monod Model, and which provides K_s as the negative gradient and $\hat{\mu}$ as the y-intercept.

Published by Woodhead Publishing Limited, 2013

$$\frac{1}{\mu} = \frac{K_s}{\hat{\mu}}\frac{1}{s} + \frac{1}{\hat{\mu}} \quad [7.8]$$

$$\mu = -K_s\frac{\mu}{s} + \hat{\mu} \quad [7.9]$$

7.2.3 The rate of substrate utilisation and product formation

Substrate utilisation may be related to cell growth via a yield coefficient, $Y_{x/s}$, where $Y_{x/s}$ relates the cells produced directly to the substrate utilised for cell production (Equation 7.10). The yield coefficient is generally assumed to be a constant and it often is, especially at high specific growth rates. Integration of Equation 7.10 allows calculation of the constant $Y_{x/s}$ from the gradient of $(x\text{-}x_0)/(s_0\text{-}s)$ where x_0 and s_0 refer to initial conditions. (Later, a variable yield coefficient, Y, will be introduced (Sections 7.3.3 and 7.3.4).)

$$Y_{x/s} = \frac{dx/dt}{ds/dt} \quad [7.10]$$

Product formation has likewise been related to substrate utilisation through a yield coefficient, $Y_{p/s}$, where $Y_{p/s}$ relates the product formed directly to the substrate utilised (Equation 7.11). Combining Equation 7.10 and Equation 7.11 further results in a yield coefficient, $Y_{p/x}$, which relates the product formed directly to the cells produced (Equation 7.12).

$$Y_{p/s} = \frac{dp/dt}{ds/dt} \quad [7.11]$$

$$Y_{p/x} = \frac{dp/dt}{dx/dt} = \frac{Y_{p/s}}{Y_{x/s}} \quad [7.12]$$

Relationships between product formation and other variables are complex and generally cannot be reduced to such simple

direct proportionality. Direct proportionality would typically be limited to a straightforward fermentation producing a primary metabolite where the rate of product formation is directly related to cell growth, but would not be applicable to, for instance, bioprocesses with secondary metabolites (e.g. penicillin production) or consecutive product formation (e.g. acetone and butanol production). Even with primary metabolites, caution should be exercised when assuming such a relationship. A case in point is the simple fermentation of sugar to ethanol as a primary metabolite which has nevertheless been demonstrated to be both a function of cell growth and cell concentration according to Equation 7.13.[12]

$$\frac{dp}{dt} = \alpha \frac{dx}{dt} + \beta x \qquad [7.13]$$

7.3 Continuous process design equations

Continuous culture is undeniably the most appropriate mode of operation for large volume products whose production costs are significantly reduced by high productivities. Non-potable ethanol and butanol production for the purpose of energy supplementation are typical examples of such processes. Biological treatment of domestic sewage is another. Further, any process which produces a product which inhibits growth would benefit from continuous operation since product concentrations are considerably lower in a continuous reactor than in a batch reactor.

Continuous operation can be conducted with one of many reactor types, the most common being the continuous stirred tank reactor (CSTR) and the continuous bubble column reactor (CBCR). The CSTR is similar to the STR (Section 7.2), but modified to incorporate inlet and outlet flows. In a CBCR

Published by Woodhead Publishing Limited, 2013

there are no impellers and mixing is facilitated solely by gas sparging. Aeration takes place through air sparge and sparger design becomes critical. Several different CBCR designs are available for specific purposes, one of the most common being the air lift reactor which incorporates a draft tube used to improve bubble distribution and enhance oxygen transfer, especially important in bioprocesses exhibiting a high oxygen demand. An instrumented laboratory scale CBCR with a sintered disc sparge with efficient oxygen transfer characteristics is shown in Plate 7.4.

Process design equations developed here are based on the CSTR type since these are very common in biological continuous culture. Basic process design equations for the prediction of process performance in continuous systems (Section 7.3.1) have been based on the kinetic behaviour which underpins microbial growth and substrate utilisation. Observed deviations of kinetic behaviour from this basic model during continuous operation at low flow rates have been explained conceptually and the design equations modified accordingly to more accurately predict the kinetic behaviour under these conditions (Sections 7.3.2, 7.3.3 and 7.3.4).

7.3.1 Development of the basic model equations

Development of the basic process design equations describing process performance during continuous culture requires consideration of the simplest continuous culture system, here using a CSTR for example (Figure 7.5). The CSTR is fed with a nutrient medium (almost always sterile, but depending on the process) through a pump and the culture is withdrawn from the CSTR at the same flow rate. During the time that the nutrient medium stays in the CSTR (the residence time), the nutrients are metabolised by the microorganisms and cell

Published by Woodhead Publishing Limited, 2013

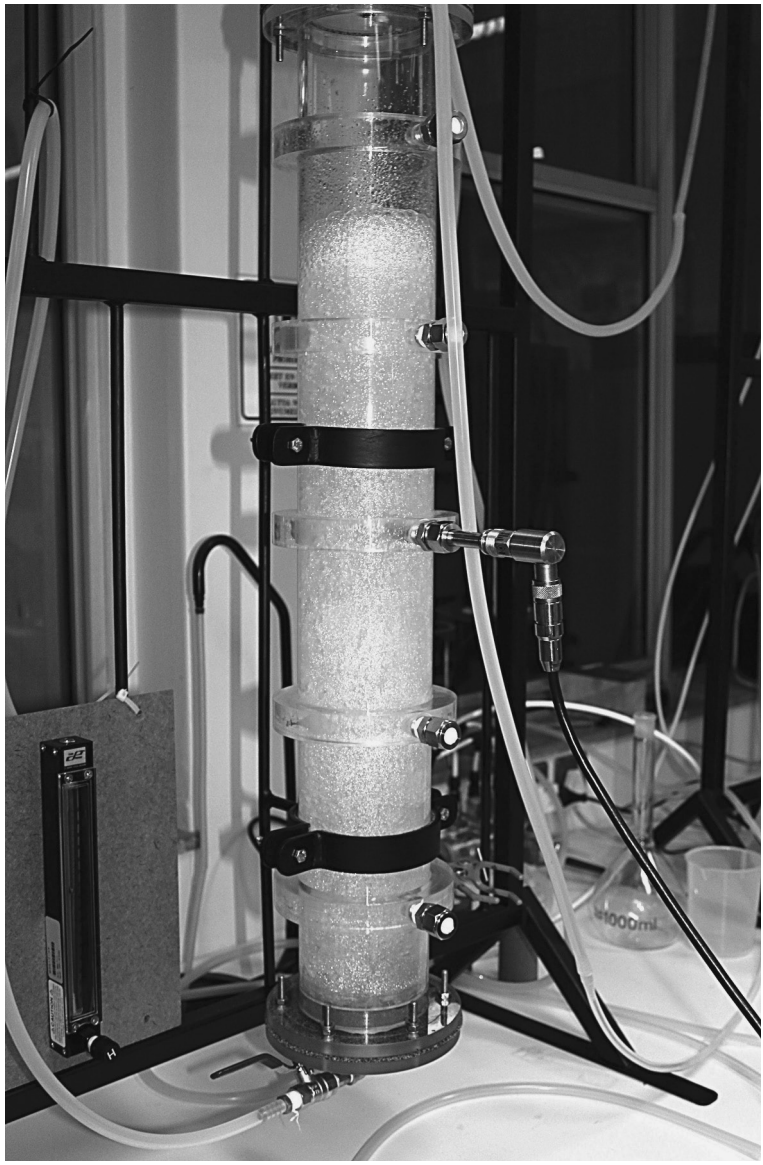

Plate 7.4 A laboratory scale bubble column reactor. Photo: A. Garlick and G. Pretorius

Published by Woodhead Publishing Limited, 2013

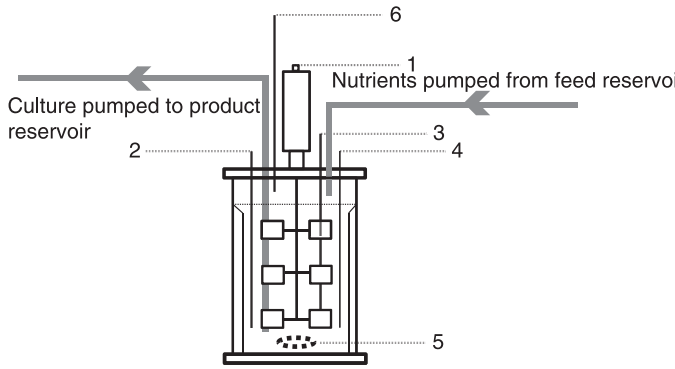

Key: 1: agitation control; 2: Temperature control; 3: pH control; 4: Dissolved oxygen measurement; 5: gas inlet and sparger; 6: gas outlet and condenser.

Figure 7.5 **A simple continuous culture system incorporating a CSTR**

growth, substrate utilisation and product formation takes place. In a properly instrumented CSTR, the environment can be maintained at the conditions (temperature, pH, dissolved oxygen) optimal for these kinetic processes.

The residence time is used universally in chemical kinetics to denote the time spent by the liquid in a reactor. It is, however, seldom used in biological kinetics. In biological kinetics, a term called the dilution rate (D) is used instead, where the dilution rate is the inverse of the residence time. Conceptually, the dilution rate is thought of as the rate at which the system's volume is diluted by the addition of the nutrient feed. As an example, a system which has a residence time of 4 h will have a dilution rate of 0.25 h^{-1}. That is, 0.25 of the system's volume will be diluted every hour, or, as is more commonly expressed, the system will undergo 0.25 'volume changes' every hour.

In continuous culture operated with a constant nutrient feed, the concentration of nutrients and products in the reactor can be kept constant, unlike in batch culture where

Published by Woodhead Publishing Limited, 2013

these concentrations vary with time. A continuous system under constant controlled environmental conditions with a constant nutrient feed is generally considered to eventually reach a state in which *all concentrations remain constant*. This is dubbed the steady state.

The validity of the steady state assumption can be shown by considering an unsteady state situation such as the time after inoculation. At this time, the substrate concentration in the reactor is high and approximately equal to that in the feed reservoir. At a high substrate concentration, the specific growth rate is high, according to the Monod Model (Equation 7.6), i.e. greater than the dilution rate, and so the cell concentration in the reactor increases. But as the cell concentration increases, the substrate concentration will decrease, thereby decreasing the specific growth rate, again according to the Monod Model. Thereafter the specific growth rate will continue to decrease until it equals the dilution rate and there is no further tendency to change.

The rule of thumb dictates that a steady state will be reached after the system has undergone at least four volume changes. This is valid for many continuous systems but caution is advised when dealing with more complex systems exhibiting metabolic control, especially those which experience morphological shifts depending on the microbial physiology, such as in the continuous culture of *C. acetobutylicum* for butanol production.[13]

The basic process design equations are formulated[14] according to the law of conservation of mass (i.e. that mass is conserved in the system), where mass refers to cell mass or mass of substrate. In the development of these equations, a number of assumptions are made. These assumptions are that the nutrient medium fed to the CSTR is sterile, that a steady state is eventually reached, that the reactor is perfectly mixed, that a single nutrient limits the cell growth, that the

Published by Woodhead Publishing Limited, 2013

process is kinetically controlled[15] and that cell death and cell maintenance is negligible.[16] In this analysis, product formation (other than cells) will not be incorporated.

Considering first the cell mass in the continuous system, the conservation of cell mass dictates the following conceptual balance (Equation 7.14).

cells entering in nutrient feed + cells generated in the system – cells leaving in outflow = cells accumulated in the system [7.14]

Written mathematically, Equation 7.14 becomes Equation 7.15 where $\left(\frac{dx}{dt}\right)_g$ and $\left(\frac{dx}{dt}\right)_a$ refer to the rate of change of cell concentration due to growth and to accumulation in the system respectively. F is the volumetric flow rate, V the working volume and x_f the concentration of cells in the nutrient feed.

$$Fx_f - Fx + V\left(\frac{dx}{dt}\right)_g = V\left(\frac{dx}{dt}\right)_a \quad [7.15]$$

The feed is assumed to be sterile,[17] so x_f is zero. Also, the steady state assumption means that the cell concentration remains constant, i.e. that there is no accumulation of cells in the system with time, so $\left(\frac{dx}{dt}\right)_a = 0$. Consequently,

$$-Fx + V\left(\frac{dx}{dt}\right)_g = 0 \quad [7.16]$$

Incorporating Monod growth kinetics (Equation 7.5) yields Equation 7.17, which, after division by the volume, results in Equation 7.18.[18]

$$-Fx + V\mu x = 0 \quad [7.17]$$

Published by Woodhead Publishing Limited, 2013

$$-\frac{F}{V}x+\mu x=0 \qquad [7.18]$$

But $\frac{F}{V}$ is the inverse residence time, or the dilution rate, D, so Equation 7.18 reduces to Equation 7.19.

$$\mu=D \qquad [7.19]$$

Equation 7.19 is the simplest equation mathematically, but immense in its implication. This equation predicts that, if you operate a continuous culture at a constant dilution rate, you will force the culture to grow at a constant specific growth rate. Not only will this specific growth rate be constant, it will also equal the value of the dilution rate that you choose to impose on the system. Theoretically then, the culture could be grown at any constant specific growth rate of choice (providing it was within the capabilities of the microorganism) just by choosing a particular flow rate. Moreover, this specific growth rate could be maintained indefinitely by maintaining this flow rate.

Maintenance of a specific growth rate of choice has enormous potential both for production and for research purposes. For production purposes, the system can be operated at the specific growth rate most favourable for product formation. For instance, in processes where the rate of cell production is key, the dilution rate at which this rate is maximum (D_{max}) can be calculated and the processes can be operated indefinitely at this value.[19]

For research purposes, the value of being able to maintain constant conditions facilitates the most rigorous kinetic analysis when one parameter can be varied at a time whilst keeping all others constant. In this manner, any change in performance can be attributed solely to the change in that one parameter. If that parameter is the specific growth rate, precise data can be accumulated on the impact of different

Published by Woodhead Publishing Limited, 2013

specific growth rates on performance, data which will then inform on optimal strategy for production.

Moreover, continuous culture at steady state facilitates physiological control with respect to control of precursor, inducer, repressor, etc. concentrations, which potentially provides invaluable data on the metabolic control of the microorganism.

This equation (Equation 7.19) leads directly to the expression to predict the substrate concentration at steady state. Substitution of the dilution rate for the specific growth rate in the Monod Model (Equation 7.6) yields Equation 7.20 which can be solved to predict the substrate concentration, s, in the system at steady state for any dilution rate (Equation 7.21).

$$D = \frac{\hat{\mu} s}{K_s + s} \qquad [7.20]$$

$$s = \frac{DK_s}{\hat{\mu} - D} \qquad [7.21]$$

Interestingly, the steady state substrate concentration is a function of only the dilution rate and is independent of the substrate concentration in the feed. Provided then that the kinetic constants K_s and $\hat{\mu}$ have been calculated, the substrate concentration at any imposed dilution rate can be predicted from Equation 7.21 under steady state conditions. K_s and $\hat{\mu}$ can be calculated using the Lineweaver–Burk relationship (Equation 7.8) or Eadie–Hofstee relationship (Equation 7.9) as described for batch culture data, where the specific growth rate is replaced by the dilution rate. Calculation of these constants using continuous culture is to be preferred over batch culture since the changing parameters during batch culture make it difficult to obtain accurate specific growth rate data. (Although it must be admitted that the route to

Published by Woodhead Publishing Limited, 2013

these constants via continuous culture is far more of an inconvenience than via batch culture.)

To obtain an analogous equation for the cell concentration in a continuous system at steady state, it is necessary to consider the balance of substrate mass in the system. The following conceptual balance describes this (Equation 7.22).

substrate entering in nutrient feed + substrate utilised in the system – substrate leaving in outflow = substrate accumulated in the system [7.22]

Written mathematically, Equation 7.22 becomes Equation 7.23 where $\left(\frac{ds}{dt}\right)_g$ and $\left(\frac{ds}{dt}\right)_a$ refer to the rate of change of substrate concentration due to growth and accumulation respectively. The concentration of the feed is denoted s_f.

$$Fs_f - Fs + V\left(\frac{ds}{dt}\right)_g = V\left(\frac{ds}{dt}\right)_a \quad [7.23]$$

Again assuming steady state is reached when the substrate concentration remains constant, i.e. there is no accumulation or depletion of substrate in the system with time, $\left(\frac{ds}{dt}\right)_a = 0$. Now incorporating the yield constant $Y_{x/s}$ from Equation 7.10, Equation 7.23 becomes Equation 7.24.

$$F(s_f - s) - V\frac{\mu x}{Y_{x/s}} = 0 \quad [7.24]$$

Dividing by V, noting that $\mu = D$ (Equation 7.19) and rearranging, results in Equation 7.25 which predicts the cell concentration, x, in the system at steady state for any dilution rate.

$$x = Y_{x/s}(s_f - s) \quad [7.25]$$

This equation predicts that the steady state concentration of cells is dependent on the substrate concentration in the

Published by Woodhead Publishing Limited, 2013

nutrient feed as well as the dilution rate, unlike the equation which predicts the steady state concentration of substrate as independent of the substrate concentration in the nutrient feed and dependent only on the dilution rate. In any event, calculation of the kinetic constants K_s, $\hat{\mu}$ and $Y_{x/s}$ allows determination of the steady state cell concentration (via the steady state substrate concentration).

Steady state predictions for cell concentration (Equation 7.25) and substrate concentration (Equation 7.21) as a function of the dilution rate yield characteristic curves (Figure 7.6). At a dilution rate of zero, no nutrient is fed into the reactor (i.e. zero flow rate) so the substrate concentration in the reactor is zero. At this stage, the cell concentration is at its maximum value $\left(Y_{x/s}s_f\right)$ according to Equation 7.25. As the dilution rate increases (i.e. flow rate increases), the substrate concentration increases according to Equation 7.21 with a corresponding decrease in the cell concentration according to Equation 7.25. This scenario continues until the dilution rate has increased to the critical dilution rate, D_c, above which the rate of cell growth cannot keep pace with the rate of cells flowing out of the system. At the critical dilution rate the cells are effectively washed out of the system

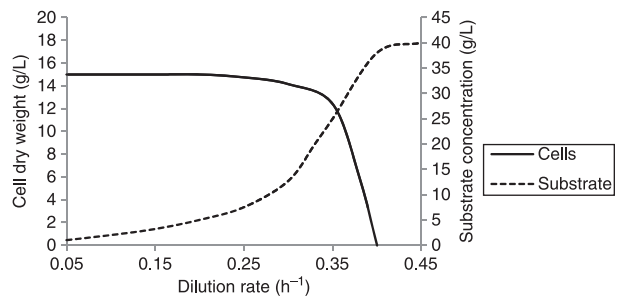

Figure 7.6 **Predictions of cell and substrate concentrations in a continuous system at steady state with a single feed concentration**

Published by Woodhead Publishing Limited, 2013

and the cell concentration falls to zero. Correspondingly, at cell washout, the substrate concentration equals that in feed because there are no more cells in the reactor to metabolise it.

There is a common misconception that washout occurs when the dilution rate reaches the value of the specific growth rate. In fact, washout occurs slightly before this happens. The critical dilution rate can be simply calculated from Equation 7.20 by setting $s = s_f$, as occurs at washout. The resultant dilution rate, i.e. D_c, is given by Equation 7.26. K_s and s_f are always both positive, so D_c must always be less than $\hat{\mu}$ (but only slightly).

$$D_c = \frac{\hat{\mu} s_f}{K_s + s_f} \qquad [7.26]$$

These characteristic curves, however, apply to a single concentration of substrate in the feed. Characteristic curves for multiple feed substrate concentrations are illustrated in Figure 7.7. Since the substrate concentration is a function of the dilution rate only, it can be expected that the shape of the curve predicting the substrate concentration will be the same irrespective of the substrate concentration in the feed.

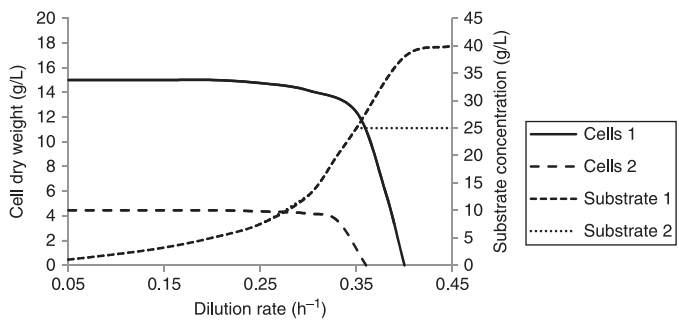

Figure 7.7 **Predictions of cell and substrate concentrations in a continuous system at steady state with multiple feed concentrations**

Published by Woodhead Publishing Limited, 2013

Obviously though, the substrate concentration curve will terminate at the corresponding value in the feed, since it can never be larger than that in the feed.

On the other hand, the cell concentration curves can be expected to differ with different feed concentrations. The maximum value of the cell concentration at zero dilution rate will depend directly on the feed substrate concentration according to Equation 7.25, increasing proportionately as the feed substrate concentration increases. Moreover, cell washout, and hence the critical dilution rate, will occur at values progressively less than the maximum specific growth rate as the feed substrate concentration decreases, according to Equation 7.26.

Determination of the cell concentration also allows for the calculation of the maximum rate of cell production (Dx) and the dilution rate at which this occurs. As the dilution rate increases, the cell concentration decreases such that the rate of cell production reaches a maximum value at a specific dilution rate (D_{max}) between zero and D_c. At this maximum value, the slope of the curve is zero, i.e. $\frac{d(Dx)}{dD} = 0$. Multiplication of the cell concentration (Equation 7.25) by the dilution rate, and differentiating this product with respect to the dilution rate, will yield the equation for D_{max} (Equation 7.27) under the condition where $\frac{d(Dx)}{dD} = 0$.[20]

$$D_{max} = \hat{\mu}\left(1 - \sqrt{\frac{K_s}{K_s + s_f}}\right) \qquad [7.27]$$

7.3.2 Empirical deviations from the predictions of the basic model equations

The basic models developed to predict the steady state concentrations of cell and substrate concentrations have

found application in a wide range of continuous bioprocesses. However, the assumptions made in the derivation of these models do not always apply and, in these cases, the kinetic behaviour cannot be predicted by these equations. There are a number of deviations to the predictions afforded by the basic models which are observed in practice. Seven of these are outlined below.

Microorganisms may attach to the walls of the reactor and the inner structures (e.g. impellers and baffles). This is frequently observed in microorganisms which produce extracellular polysaccharides, or slime layers, which cause the microorganisms to adhere strongly to surfaces, a phenomenon referred to as wall growth. Microorganisms are retained in the system as a result of the wall growth and consequently washout occurs later than at the calculated critical dilution rate. Since microorganisms remain in the system at the calculated critical dilution rate, substrate utilisation still takes place and the feed substrate concentration will not be reached. Thus, at the critical dilution rate, the cell concentration will be higher and the substrate concentration lower than the values predicted by the basic models.

Deviations similar to those obtained with wall growth are likely to also be observed with poor mixing. Inadequate mixing can result in a distribution of concentrations in the reactor. This negates the assumption of perfect mixing made in the development of the basic models and its implication that the cell and substrate concentrations in the reactor are identical to those in the outlet flow. Hence, imperfect mixing results in cell and substrate concentrations at the critical dilution rate which are not compatible with the basic models. Imperfect mixing is generally not a problem on the small scale where bioreactors tend to be overmixed. However, on the larger scale, where heterogeneity may exist, poor mixing may be problematic. Accordingly, maintenance of adequate

Published by Woodhead Publishing Limited, 2013

mixing is one of the major criteria for successful scale up of bioreactors (Section 9.2).

Similar deviations from the basic models will be observed with GMOs should the microorganism lose the ability conferred by the mutation and revert to a wild type with more favourable growth kinetics. This is a problem where the wild type has a lower K_s and higher $\hat{\mu}$ than the GMO. The alteration of the kinetics can best be understood in terms of the Monod Model (Equation 7.6). Suppose that the continuous culture of the GMO is being operated at a dilution rate which sets its specific growth rate, μ_{GMO}, to a value identical to that of the dilution rate ($0.15\,h^{-1}$ in Figure 7.8). This μ_{GMO} corresponds to a certain value of substrate concentration, according to the Monod Model for the GMO. At this substrate concentration, however, a wild type with a lower K_s will exhibit a higher specific growth rate, say μ_{WT} ($0.18\,h^{-1}$ in Figure 7.8). Since μ_{WT} is greater than the dilution rate, the substrate concentration will decrease until μ_{WT} equals the dilution rate. At this new (lower) substrate concentration, μ_{GMO} is less than the dilution rate

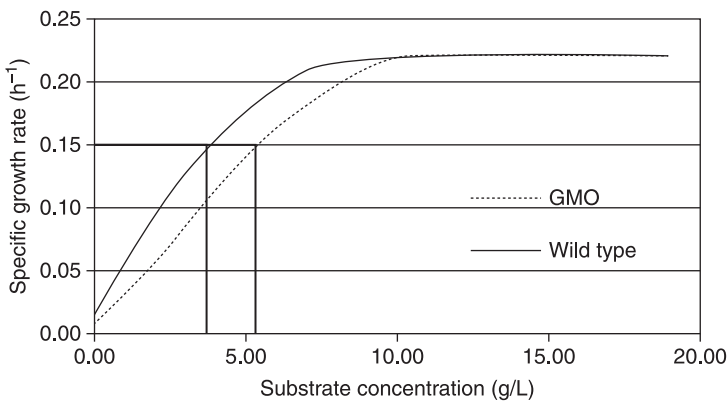

Figure 7.8 **Selection of wild type during continuous culture of genetically modified organisms with reversion**

Published by Woodhead Publishing Limited, 2013

and so the GMO will wash out, leaving the system with only the wild type (with its higher critical dilution rate relative to that of the GMO). This is referred to as the selective pressure of continuous culture and should be taken into consideration when using a GMO in a continuous process.

Deviations from the basic model may also be observed when using complex media. In these media, the limiting substrate could change from one nutrient to another with change in dilution rate. This contravenes the assumption of a single limiting substrate applied in the development of the basic equations and leads to an alteration of the shape of the predicted curves. It is not possible to guess the actual alteration that takes place as this will depend on the specific medium under consideration. Suffice to say that caution is advised when using the basic model to predict cell and substrate concentrations in complex media.

Another observed deviation is not so much an actual deviation, but an artefact of the methodology used to measure the cell concentration. Supposing cell mass was used to quantify the cell concentration in a continuous culture which was under nitrogen or sulphur limitation. Such a substrate limitation implies excess carbon which would typically be stored in the cell as carbohydrates or lipids, thereby increasing the cell mass. The effect of an increase in cell mass due to carbon storage would be most marked at low dilution rates where the increase in cell mass due to growth is less than at high dilution rates, resulting in a higher cell concentration at low dilution rates than is predicted by the basic model. However, should cell numbers have been used to quantify cell concentration, it is probable that no deviation would have occurred because this method does not distinguish between carbon-heavy and carbon-light cells.

A similar increase in cell concentration at low dilution rates above that predicted by the basic model has also been

Published by Woodhead Publishing Limited, 2013

observed under substrate limitation with magnesium, phosphate or potassium, but for a different reason. Magnesium, phosphate and potassium are required for RNA synthesis, so a limitation of any of these nutrients will limit RNA production. But slow growing cells require less RNA than fast growing cells, so the ratio of cell concentration to RNA at low dilution rates is greater than the ratio at high dilution rates. Therefore, cell concentrations limited by RNA content would be proportionally higher at low dilution rates. However, should RNA content have been used directly as a measure of cell concentration, no deviation would have been observed.

Finally and probably most importantly, is the deviation of the basic model resulting in an observed decrease in cell concentration at low dilution rates. This is of particular concern in bioprocesses which operate at low dilution rates because it can reduce the capacity of the continuous system significantly. The low cell concentration at low dilution rates has specific significance in biological treatment of sewage where a low dilution rate is used so as to minimise the substrate concentration (in this case the substrate concentration is the pollutant). Under these conditions, recycle of the microbial sludge to increase the system's capacity for pollutant removal is mandatory.

In view of the importance of this observation, especially with respect to sewage treatment, the basic model has been revised to provide two modified models, each of which is able to mathematically predict the decline in cell concentration at low dilution rates. In these models, the assumptions relating to cell death and cell maintenance of the basic model were not made. The first model incorporates a term for cell death, while the second model instead incorporates a term for substrate diversion for cell maintenance. These modified models were developed separately from different conceptual

bases, but nevertheless arrive at the same mathematical prediction and both are equally successful in describing the observed deviation. For clarity, the development of the modified models will be explained separately (Sections 7.3.3 and 7.3.4). Subsequently, the individual models will be compared and their interrelation defined.

7.3.3 Modified model equations incorporating endogenous metabolism

The first model is based on the concept of endogenous metabolism (sometimes called endogenous respiration). Endogenous metabolism refers to metabolism that occurs when no exogenous substrate is present. It has been confirmed by the observation of a decrease in oxygen level (through respiration) under these conditions. In essence, the microorganism facilitates respiration by utilising its own internal (endogenous) reserves, and will continue to do so until no more internal reserves remain, at which stage the cell lyses. Simply put, the organism starves until it dies. No wonder then, that endogenous metabolism is defined mathematically as a death rate, $\left(\frac{dx}{dt}\right)_e$.

Thus the cell mass balance in the basic model (Equation 7.15) is modified to incorporate a rate of cell death to give Equation 7.28.

$$Fx_f - Fx + V\left(\frac{dx}{dt}\right)_g + V\left(\frac{dx}{dt}\right)_e = V\left(\frac{dx}{dt}\right)_a \qquad [7.28]$$

As a simplifying assumption, the cell death rate is assumed to be independent of the dilution rate. It is related to the cell concentration via a constant called the endogenous respiration constant, or k_e. Incorporation of k_e into Equation

Published by Woodhead Publishing Limited, 2013

7.28 yields Equation 7.29 at steady state which, when divided by V and rearranged, results in Equation 7.30.

$$-Fx + V\mu x - Vk_e x = 0 \quad [7.29]$$

$$\mu = D + k_e \quad [7.30]$$

Substitution of $(D + k_e)$ for μ in the Monod Model (Equation 7.6) now yields Equation 7.31 and on rearranging, an expression for the substrate concentration at steady state under conditions in which endogenous metabolism has been taken into account (Equation 7.32). Note that for $k_e = 0$, Equation 7.32 reduces to the model for s without consideration of endogenous metabolism (Equation 7.21).

$$D + k_e = \frac{\hat{\mu} s}{K_s + s} \quad [7.31]$$

$$s = \frac{(D + k_e)K_s}{\hat{\mu} - (D + k_e)} \quad [7.32]$$

In this modification of the basic model, no assumptions regarding the substrate have been changed and so the substrate mass balance for the basic model applies (Equation 7.23). However, μ in this equation must now be substituted with $D + k_e$ according to Equation 7.30. This results in a modified model for the steady state cell concentration (Equation 7.33). Note that for $k_e = 0$, Equation 7.33 reduces to the model for cell concentration without consideration of endogenous metabolism (Equation 7.25).

$$x = \frac{D}{D + k_e} Y_{x/s}\left(s_f - s\right) \quad [7.33]$$

As with the basic model, the model which incorporates the effect of endogenous metabolism presents steady state predictions for cell and substrate concentrations, where the substrate concentration is a function of the dilution rate only

Published by Woodhead Publishing Limited, 2013

and the cell concentration depends on both the dilution rate and the substrate concentration in the feed. Provided the kinetic constants $Y_{x/s}$, k_e, K_s and $\hat{\mu}$ have been determined from kinetic data, both the cell and substrate concentrations under conditions where endogenous metabolism is significant can be predicted. $Y_{x/s}$ and k_e can be determined by rearranging Equation 7.33 and inverting to yield Equation 7.34 with gradient $\frac{k_e}{Y_{x/s}}$ and y-intercept $\frac{1}{Y_{x/s}}$. Knowing k_e, K_s and $\hat{\mu}$ can then be determined from Equation 7.8 or Equation 7.9 with $\mu = D + k_e$.

$$\frac{s_f - s}{x} = \frac{k_e}{Y_{x/s}}\frac{1}{D} + \frac{1}{Y_{x/s}} \qquad [7.34]$$

This model has been shown to accurately predict empirical data over the entire range of dilution rates in continuous cultures which exhibit a decrease in cell concentration at low dilution rates and is used extensively in biological treatment of waste waters.

Mathematically it is fairly simple to understand how this expression will account for decreased cell concentration at low dilution rates. Consider the term $\frac{D}{D + k_e}$ in Equation 7.33. Empirically, k_e has been found to be at least an order of magnitude smaller than all but the lowest dilution rates,[21] and since k_e is constant irrespective of the dilution rate (recall assumption), at high dilution rates k_e is negligible and the denominator $(D + k_e)$ in the term reduces to D, thus cancelling with the numerator. Hence, Equation 7.33 reduces to the equation for cell concentration in the basic model which does not consider endogenous metabolism (Equation 7.25). Consequently, cell concentration in both the basic and modified model is the same value at high dilution rates. The situation is,

Published by Woodhead Publishing Limited, 2013

however, quite different at low dilution rates. Here k_e becomes significant in comparison to D and the denominator becomes significantly larger than the numerator in this term. Thus, the cell concentration predicted by the modified model at low dilution rates is significantly lower than that predicted by the basic model at the corresponding dilution rate.

This expression also predicts that the observed cell yield will not be constant[22] but will decrease at low dilution rates. This is shown in the term $\frac{DY_{x/s}}{D+k_e}$ which represents the observed yield. At low dilution rates, k_e becomes significant and this term becomes less than $Y_{x/s}$.

7.3.4 Modified model equations incorporating energy of maintenance

The second model is based on the concept of an energy of maintenance. The energy of maintenance refers to the energy that is required to maintain metabolic functions (as distinct from that which is required for growth). This implies that substrate is required for maintenance purposes as well as for growth. In this modified model then, the substrate mass balance is modified to account for part of the substrate being diverted for cell maintenance purposes. Incorporation of the additional substrate utilised for cell maintenance into Equation 7.23 yields Equation 7.35.

$$Fs_f - Fs + V\left(\frac{ds}{dt}\right)_g + V\left(\frac{ds}{dt}\right)_m = V\left(\frac{ds}{dt}\right)_a \qquad [7.35]$$

The rate of substrate utilised for cell maintenance is assumed to be independent of the dilution rate (in much the same way that the rate of cell death was assumed to be independent of dilution rate in the model based on endogenous metabolism

Published by Woodhead Publishing Limited, 2013

(Section 7.3.3)). The rate of substrate utilised for maintenance is related to the cell concentration via a constant called the maintenance coefficient, or m. Incorporation of m into Equation 7.35 yields Equation 7.36 which, when divided by the volume and rearranged, results in the expression for the steady state cell concentration in the modified model where energy of maintenance has been taken into consideration (Equation 7.37).

$$F(s_f - s) - V\frac{\mu x}{Y_{x/s}} - Vmx = 0 \qquad [7.36]$$

$$x = \frac{D}{D+mY_{x/s}} Y_{x/s}\left(s_f - s\right) \qquad [7.37]$$

It is important to note that in this modification, there are is no change to the cell mass balance of the basic model which still results in $\mu = D$ (Equation 7.19). Consequently, substitution of D into the Monod Model (Equation 7.6) and rearranging produces the identical expression for the substrate concentration at steady state as for the basic model (Equation 7.21).

The model modified to incorporate the energy of maintenance can then be used to predict cell and substrate concentrations at steady state over the entire range of dilution rates. Again, the substrate concentration is a function of the dilution rate only and the cell concentration a function of both the dilution rate and the feed substrate concentration. These predictions similarly require that that the kinetic constants $Y_{x/s}$, m, K_s and $\hat{\mu}$ are determined from kinetic data. Since $\mu = D$ in this model, K_s and $\hat{\mu}$ can be calculated exactly as is done for the basic model (Equation 7.8 or Equation 7.9) while $Y_{x/s}$ and m are calculated by rearranging Equation 7.37 and inverting to yield Equation 7.38 with gradient m and y-intercept $\frac{1}{Y_{x/s}}$.

Published by Woodhead Publishing Limited, 2013

$$\frac{s_f - s}{x} = \frac{m}{D} + \frac{1}{Y_{x/s}} \qquad [7.38]$$

The explanation as to how the expression for cell concentration in this model results in a decreased value at low dilution rates is analogous to that when considering the model modified according to the concept of endogenous metabolism. Empirically, m has been found to be at least an order of magnitude smaller than all but the lowest dilution rates,[23] and since it is a constant value irrespective of dilution rate (recall assumption), at high dilution rates, m is negligible. Thus, the denominator $\frac{D}{D+mY_{x/s}}$ in Equation 7.37 reduces to D and the term approximates unity. Under these conditions, Equation 7.37 reduces to Equation 7.25, the prediction for cell concentration in the basic model. Consequently, the steady state cell concentration in both the basic model and in the model which includes energy of maintenance has the same value at high dilution rates. On the other hand, at low dilution rates, m becomes significant in comparison to D and the term becomes significantly less than unity. Thus, cell concentrations predicted by this modified model at low dilution rates are significantly lower than that predicted by the basic model at the corresponding dilution rate.

Similar to endogenous metabolism, energy of maintenance also predicts that the observed cell yield will not be constant but will decrease at low dilution rates. This is shown in the term $\frac{DY_{x/s}}{D+mY_{x/s}}$ which represents the observed yield. At low dilution rates, m becomes significant and this term becomes less than $Y_{x/s}$.

So while the endogenous metabolism model and the energy of maintenance model are based on completely different conceptual reasoning and mathematical development, both

Published by Woodhead Publishing Limited, 2013

predict kinetic performance in continuous culture equally well, and one or the other can be used with confidence provided a steady state can be assured. This is actually not surprising when comparing the expressions for cell concentrations in the two models (Equations 7.33 and 7.37); equating these expressions reveals a direct relationship between k_e and m according to Equation 7.39.

$$k_e = mY_{x/s} \quad [7.39]$$

7.3.5 Customised continuous culture configurations

Continuous culture can be operated in different configurations for one of many specialised purposes. Use of two bioreactors in series is a particularly attractive process strategy for production of secondary metabolites when high productivities are of major importance, above that of high yield. In this manner, growth rate and environmental and/or physiological conditions can be optimised individually to enhance the production of actively growing cells in the first reactor as feed to the second reactor with conditions optimised for production of the secondary metabolite in the second reactor. Growth rate is readily manipulated by changing the working volume: a relatively small volume in the first reactor will ensure actively growing cells (high dilution rate) while a comparatively larger working volume in the second reactor will impose the low growth rate (low dilution rate) associated with secondary metabolite accumulation.

Additionally, continuous systems can be modified to enhance the production capability of the system by incorporating some means of microbial retention, either by retention in the reactor itself, or by microbial separation in a unit external to the reactor coupled with recycle of the

Published by Woodhead Publishing Limited, 2013

microbial mass. Direct retention is enabled through use of one or other matrices, generally by absorption or adsorption of the microorganisms to the matrix. Conventional matrices include organic beads (e.g. agarose gels) or inorganic solids (e.g. glass) while more novel designs incorporate ultra- and micro-filtration membranes as absorption matrices. Direct retention can also be facilitated by an internal membrane which acts as a filter through which the microorganisms cannot pass, rather than a matrix for microbial absorption.

Microbial retention through separation and recycle comprises various configurations. Ultra- and micro-filtration membranes can also be used as external separation units for the purposes of recycle. On the other end of the scale (and where asepsis is not required) settling tanks are used as the separation unit; this technique is universal in biological treatment of domestic waste water for concentration of microbial mass (sludge) from the reactors (activated sludge tanks). Under conditions where a separator is used for the purpose of cell recycle, the continuous process design equations would need to be modified to incorporate the recycle ratio, separate hydraulic and solid retention times in the system,[24] as well as the dual clarified and concentrated flows from the separator. For biological waste water treatment, the equations would in addition need to include the effect of endogenous metabolism as these plants are operated at low dilution rates (where endogenous metabolism is significant) in order to minimise pollution (substrate) in the out flow.[25]

A further configuration of importance relates to *in situ* product removal which functions both to reduce downstream processing requirements and, importantly, to increase production capacity, especially in the case of an inhibitory product, where product removal will result in lowered (or negligible) product inhibition. *In situ* product removal can be conducted via *in situ* filtration, liquid–liquid extraction or

foam removal. *In situ* liquid–liquid extraction is a suitable methodology if the product is more soluble in a discontinuous hydrophobic phase; *in situ* foam removal becomes feasible when the product is a surface active molecule which not only produces foam but resides predominantly in it.

The appropriate continuous culture configuration will depend on the nature of the bioprocess with the range of appropriate configurations probably limited only by the degree of innovation of the Bioprocess Engineer. The few configurations described above are meant only to illustrate some of the possibilities.

7.4 Fed-batch bioprocess design equations

Fed-batch culture is, in practice, a strategy midway between batch and continuous culture. In fed-batch mode, a batch culture with an initial low working to total volume ratio is supplied with a nutrient feed. Unlike continuous culture, though, no culture is removed from the reactor during operation and the fed-batch culture is terminated when the volume has reached the maximum possible. In function, however, the fed-batch mode has very specific purposes and fills a niche role which cannot be realised by either batch or continuous strategies. One of the most well documented uses of fed-batch culture is to produce a high cell mass. This is achieved under pseudo (quasi) steady state conditions during which the cell concentration remains constant. (The relevant equations are derived later in this section.)

Fed-batch culture is in general very useful if it is appropriate to prolong a particular phase of batch culture for optimal product formation. This is particularly true of products which are secondary metabolites whose formation is induced

Published by Woodhead Publishing Limited, 2013

or enhanced by a particular precursor, inducer or substrate limitation (e.g. nitrogen or phosphate). Using a fed-batch strategy, the rate of cell growth can be maximised in a rich nutrient medium during the initial batch phase and, once an acceptable cell concentration has been reached, the change to optimal product formation can be initiated by feeding an appropriate nutrient.

Fed-batch culture is also used extensively when a substrate concentration threshold exists above which product formation is inhibited or repressed. In fact, the use of fed-batch culture for the production of yeast probably constitutes the most widespread industrial use of this mode of operation. In yeast production, aerobic respiration is repressed above the threshold concentration of glucose, irrespective of a supply of adequate oxygen. This repression results in the diversion of the carbon source to the by-product ethanol (Section 5.2.1). Fed-batch culture, however, avoids both the waste of carbon source and maximises product (yeast) accumulation by applying a feed composition and rate which maintains the glucose concentration in the reactor to just below the threshold value.

Fed-batch operation can also be useful when the substrate concentration is so high as to exert detrimental osmotic effects on the microorganism. For instance, during ethanol production, 10% ethanol is considered an acceptable product concentration. With a product yield on substrate of about 0.5 (w/w), 20% glucose would be required. But glucose concentrations above 10% (w/w) could exert too high an osmotic pressure, so fed-batch operation is practised so that the sugar concentration does not rise above 10%.

Several control strategies to optimise the rate of feed of specified nutrient concentrations have been devised for fed-batch culture. The simplest strategy is to attempt to balance substrate feed with demand based on historical or predicted

Published by Woodhead Publishing Limited, 2013

data. This is somewhat limited as it does not allow for feedback correction. More accurate control of substrate feed is affected through on-line control of parameters such as pH, dissolved oxygen and off gas composition. One innovative on-line control strategy involves control of the respiratory quotient (RQ). The RQ is a dimensionless number which relates the carbon dioxide produced to oxygen consumed. So, for example, in yeast production, RQ is indicative of the ratio of anaerobic fermentation to aerobic respiration (the lower the RQ, the more aerobic the culture). By adjusting the glucose feed rate to maintain a constant RQ at a specified value which optimally favours aerobic respiration, maximal yeast accumulation can be achieved with minimal wastage of raw material.

Process design equations for fed-batch culture can be derived as for continuous culture with outlet flow equal to zero. Generally, the effect of endogenous metabolism or energy of maintenance can be neglected because fed-batch is operated at dilution rates significantly greater than the coefficients k_e and m.

The cell mass balance for fed-batch can therefore be written as Equation 7.40 which is the same as that for continuous culture (Equation 7.15) except that the time dependence of the volume during fed-batch is taken into account.[26] Good mixing has again been assumed. With a sterile feed and no outflow, Equation 7.40 becomes Equation 7.41 and, after substitution, Equation 7.42. Finally, rearrangement and substitution of D for $\frac{F}{V}$ yields Equation 7.43.

$$Fx_f - Fx + V\left(\frac{dx}{dt}\right)_g = \left(\frac{d(xV)}{dt}\right)_a \qquad [7.40]$$

$$V\left(\frac{dx}{dt}\right)_g = V\left(\frac{dx}{dt}\right)_a + x\left(\frac{dV}{dt}\right)_a \qquad [7.41]$$

Published by Woodhead Publishing Limited, 2013

$$V\mu x = V\left(\frac{dx}{dt}\right)_a + xF \qquad [7.42]$$

$$\left(\frac{dx}{dt}\right)_a = (\mu - D)x \qquad [7.43]$$

Similarly, the substrate mass balance is the same as that for continuous culture (Equation 7.23) with volume as a time-dependant variable, as in Equation 7.44. With substitution of the relationship between substrate utilisation and cell growth (Equation 7.10) and elimination of the outflow, Equation 7.44 becomes Equation 7.45. Finally, rearrangement and substitution of D for $\frac{F}{V}$ yields Equation 7.46.

$$Fs_f - Fs + V\left(\frac{ds}{dt}\right)_g = V\left(\frac{d(sV)}{dt}\right)_a \qquad [7.44]$$

$$Fs_f + V\frac{\mu x}{Y_{x/s}} = V\left(\frac{ds}{dt}\right)_a + s\left(\frac{dV}{dt}\right)_a \qquad [7.45]$$

$$\left(\frac{ds}{dt}\right)_a = D\left(s_f - s\right) + \frac{\mu x}{Y_{x/s}} \qquad [7.46]$$

The reactor can be operated under pseudo steady state conditions where the substrate is almost completely utilised and $\left(\frac{dx}{dt}\right)_a$ and $\left(\frac{ds}{dt}\right)_a$ both approximate zero (i.e. the cell and substrate concentrations are both constant). Under these conditions, $\mu = D$ (from Equation 7.43) and so obviously substitution of D into the Monod Model (Equation 7.6) must yield the same expression for substrate concentration as that obtained in the basic equation for the substrate concentration in continuous culture at steady state (Equation 7.21). Additionally, with $\mu = D$, Equation 7.46 reduces to the same expression for cell concentration as that obtained in the basic equation for continuous culture at steady state

Published by Woodhead Publishing Limited, 2013

(Equation 7.25). It evident (from Equation 7.25) that if fed-batch is operated at a very low substrate concentration (i.e. very much less than the feed substrate concentration), the cell concentration can be maintained very close to its maximum value of $s_f Y_{x/s}$.

It is important to note that while the cell concentration is effectively constant during pseudo steady state operation, the total mass of cells increases in proportion to the increase in volume. Consider the rate of increase of total cell mass, X, where $X = xV$ (Equation 7.47). Under pseudo steady state conditions Equation 7.47 reduces to Equation 7.48, and further to Equation 7.49 at very low substrate concentrations. Now integration of Equation 7.49 with $X = X_0$ at the start of flow and t_{fb}, the time of feeding, allows calculation of the cell mass reached at any time during feeding (Equation 7.50).

$$\left(\frac{d(X)}{dt}\right)_a = V\left(\frac{dx}{dt}\right)_a + x\left(\frac{dV}{dt}\right)_a \quad [7.47]$$

$$\left(\frac{dX}{dt}\right)_a = xF \quad [7.48]$$

$$\left(\frac{d(x)}{dt}\right)_a = s_f Y_{x/s} F \quad [7.49]$$

$$X = X_0 + (s_f Y_{x/s} F)t_{fb} \quad [7.50]$$

Cyclic fed-batch operation may also be practised where the process can (theoretically) be repeated indefinitely. During cyclic fed-batch operation, about 90% of the culture is removed and sent to downstream processing, leaving enough cells to act as an inoculum as the process is started again.

Published by Woodhead Publishing Limited, 2013

7.5 Notes

1. The limiting nutrient is that nutrient in the medium which limits the cell growth.
2. Robert Earle Buchanan (1883–1973).
3. Jacques Lucien Monod (1910–1976).
4. Typical doubling times of *E. coli* and *S. cerevisiae* are about 20 and 75 minutes respectively.
5. The maximum specific growth rate depends on the particular organism and the specific operating conditions.
6. This is very different from the steady state reached during continuous culture where the cell concentration remains constant.
7. Samples should be diluted to give optical densities below 0.8, above which a linear relationship between optical density and cell concentration cannot be assumed.
8. A semi-log plot is a convenient representation as it enables visual comparison of the $\hat{\mu}$ values (gradients) obtained using different measurements for cell concentration.
9. Ignoring sporulation.
10. The limiting nutrient is usually referred to as the substrate.
11. The lag phase can be reduced or eliminated by using a large inoculum volume with the same medium as the test culture.
12. The well-known Luedeking and Piret Model.
13. In complex bioprocesses, interaction between physiological and morphological changes may cause oscillatory behaviour which precludes the attainment of steady state.
14. First developed by Herbert, Elsworth and Telling in 1956.
15. Assuming no mass or heat transfer limitations.
16. This last assumption will not be made in the modification to the basic equations.
17. The nutrient feed is sterile in most bioprocesses. Even in sewage treatment where the feed is clearly not sterile, x_f is mostly still assumed to be zero since the cell concentration in the feed relative to that in the activated sludge tank (reactor) is small and considered to be insignificant.
18. The assumption of perfect mixing results in the cell concentration in the reactor being equal to that in the outlet flow.

Published by Woodhead Publishing Limited, 2013

19. The dilution rate corresponding to the maximum rate of cell production is given in Equation 7.27.
20. The derivation is left to the reader.
21. Typically $k_e = 0.01\,h^{-1}$ while D can increase up to about $0.45\,h^{-1}$.
22. In the basic model, the yield was constant and equal to $Y_{x/s}$.
23. Typically $m = 0.03\,h^{-1}$ while D can increase up to about $0.45\,h^{-1}$.
24. These could be very different, for example in biological waste treatment the hydraulic residence time is measured in hours (about 6 to 12) while the sludge usually spends about 5 to 7 days in the activated sludge tank.
25. Traditionally the concept of endogenous metabolism, rather than energy of maintenance, has been used in biological waste water treatment, but either model would be suitable.
26. In continuous culture, the volume is constant.

Published by Woodhead Publishing Limited, 2013

8

The oxygen transfer rate and overall volumetric oxygen transfer coefficient

DOI: 10.1533/9781782421689.147

Abstract: During aerobic microbial growth, oxygen is required by microorganisms as a final electron acceptor for energy production during oxidative phosphorylation (Section 5.1.2). Should the oxygen in the culture decrease below that sufficient for oxidative phosphorylation, the metabolism of the organism will be limited by the oxygen concentration and the specific growth rate will decrease according to the Monod Model (Equation 7.6). In this manner cell growth and product formation will become transport rather than kinetically controlled, leading to a decline in the yield and productivity of the process.

Provision of adequate oxygen is especially challenging because of low oxygen solubility. Oxygen solubility in water is around 8 mg/L at room temperature and this is further decreased in the culture medium due to the presence of dissolved solutes and the relatively higher fermentation temperatures. This low level of solubility can be appreciated as critical when considering the specific oxygen utilisation rate of microorganisms. Filamentous fungi require about 3 mmoles O_2/g cells/h, yeasts about 4–8 mmoles O_2/g cells/h, while bacteria may require up to 12 mmoles O_2/g cells/h. Taking an extreme case, say 10 g/L

Published by Woodhead Publishing Limited, 2013

bacteria with a specific oxygen utilisation rate of 12 mmoles O_2/g cells/h, this equates to a total oxygen utilisation rate (OUR) of 3840 mg O_2/L/h; so 8 mg/L oxygen would disappear in only 7.5 seconds! Therefore it is imperative that oxygen be continuously transferred to the culture if the metabolic needs of the microorganism are to be met.

In bioprocesses containing hydrocarbons, rather than carbohydrates, as the sole carbon source, the effect of low oxygen solubility on the adequacy of oxygen supply may be exacerbated. The carbohydrate molecule contributes around two thirds of the required oxygen through its intrinsic oxygen content. However, unlike carbohydrates, hydrocarbons tend to be deficient in oxygen and so all the required oxygen has to be supplied through direct transfer into the culture. Moreover, the increased fluid viscosity brought about by the hydrocarbon in suspension makes efficient transfer more difficult. Although some relief is afforded by the considerably higher oxygen solubility in the hydrocarbon relative to that in an aqueous phase, this is not always sufficient to off-set the difficulties generated by the increased requirement for oxygen transfer and the increased resistance to transfer in viscous systems.

In view of the above considerations, the oxygen transfer rate (OTR) is fundamental to the successful design, operation and scale up of aerobic bioprocesses and accordingly, several mathematical expressions which predict OTR behaviour have been developed. These include both empirical correlations and semi-fundamental models. The empirical models incorporate parameters which influence the fluid dynamics (power per unit volume, superficial gas velocity) and sometimes also include the fluid properties (viscosity, surface tension), the latter usually only when viscous substances[1] are present. As with all empirical expressions, however, these are limited in application to the conditions under which they were

Published by Woodhead Publishing Limited, 2013

derived, such as the operating conditions and scale of the operation, and will not be discussed further.

A number of semi-fundamental models have been developed, each based on a distinct conceptual mechanism. These models have been used both in the prediction and in the measurement of OTR and are defined and discussed in Chapter 8. The different methodologies for OTR measurement are also elucidated and evaluated in Chapter 8, and their constraints and limitations discussed.

Key words: oxygen transfer rate, overall volumetric coefficient, probe response, measurement methodologies.

8.1 Oxygen transfer design equations

A number of models to predict OTR have been developed, three of which have been the most widely documented, namely the Two Film Theory (TFT), the Penetration Theory (PT) and the Surface Renewal Theory (SRT). The TFT has by far been the most commonly used and is well documented in biotechnology texts dealing with oxygen transfer. The mathematical development is fairly lengthy so complete derivations are not given here. Rather, the conceptual development is explained and supported by key mathematical expressions.

The TFT is based on the assumption that a stagnant film will form on either side of any phase interface, that all resistance to oxygen transfer resides within the stagnant films and that transfer of oxygen through these stagnant films takes place by molecular diffusion only. Thus, in an aqueous medium, during its transfer from inside the gas bubble to the site of respiratory oxidation in the microorganism, the oxygen molecule will theoretically meet

Published by Woodhead Publishing Limited, 2013

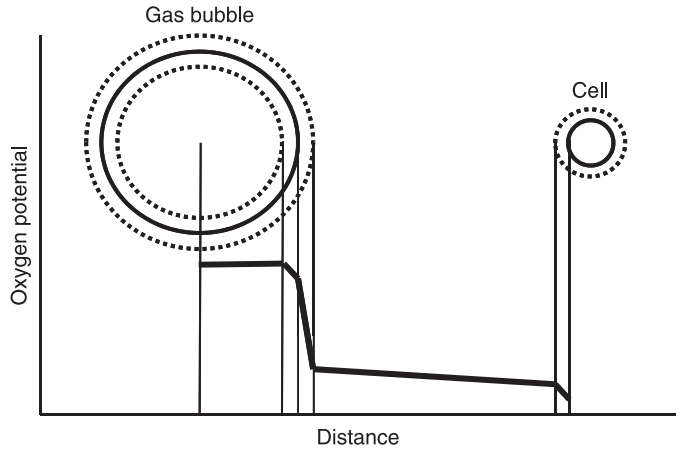

Figure 8.1 Possible resistances to oxygen transfer according to the Two Film Theory model

with resistance to transfer within the stagnant films in the gas and liquid phases at the gas–liquid interface and in the liquid phase around the cell (Figure 8.1). In this analysis, the bulk liquid is assumed to be sufficiently well mixed so that the resistance to oxygen transfer in this liquid is negligible. Further, a negligible resistance is attributed to the transfer through the gas–liquid interface itself.[2]

When considering the low oxygen solubility in the liquid phase and its high diffusivity in the gas phase, the resistance to transfer in the stagnant gas film at the gas–liquid interface is insignificant when compared with the resistance to transfer in the stagnant liquid film at the gas–liquid interface. Further, when considering the relative diameters of the gas bubble and the individual microorganisms, it is clear that the resistance in the liquid film around the gas bubble is significantly more than that in the liquid film around the microorganism.[3] Thus, OTR through the stagnant liquid film surrounding the bubble becomes the rate-controlling step in the mechanism. Therefore the OTR, by molecular

Published by Woodhead Publishing Limited, 2013

diffusion across this stagnant liquid film, defines the OTR from the bubble to the microorganism.

Molecular diffusion has been well-defined by Fick's Law as proportional to the concentration difference driving the diffusion and inversely proportional to the thickness of the stagnant film through which the diffusion takes place. In terms of oxygen diffusing through the stagnant liquid film surrounding the bubble, a molar flux of oxygen per unit area (J) can be defined as proportional to the oxygen concentration gradient across the stagnant liquid film around the gas bubble and inversely proportional to the thickness of this film, according to Equation 8.1, where the diffusivity of oxygen in the liquid (D) is assumed constant.

$$J = -D\frac{dC}{dz} \qquad [8.1]$$

Integration of Equation 8.1 yields the molar oxygen flux from bubble to microorganism (Equation 8.2), where C is the bulk oxygen concentration in the liquid, C_{sat} is the oxygen concentration in the liquid that would be in equilibrium with that in the gas phase (i.e. oxygen solubility) and δ is the thickness of the stagnant film.

$$J = \frac{D}{\delta}\left(C_{sat} - C\right) \qquad [8.2]$$

The molar flux in terms of unit transfer area (i.e. bubble surface) is, however, difficult to measure. To overcome this, the molar flux has traditionally been measured in terms of a molar flux per unit volume (N). N is obtained from J by the incorporation of the interfacial area per unit volume (a) (Equation 8.3).

$$N = \frac{D}{\delta}a\left(C_{sat} - C\right) \qquad [8.3]$$

Published by Woodhead Publishing Limited, 2013

The term $\frac{D}{\delta}$ corresponds to an inverse resistance to diffusion in the stagnant liquid film and is represented by the oxygen transfer coefficient (K_L). In models describing the OTR, K_L and a are lumped into an overall volumetric oxygen transfer coefficient (K_La), as in Equation 8.4, before equating N and OTR.

$$OTR = K_La\ (C_{sat} - C) \qquad [8.4]$$

The lumped K_La parameter is used universally, mainly because of the challenges associated with measurement of the interfacial area per unit volume. However, although not done routinely, measurement of the interfacial area per unit volume has been carried out very successfully by means of high-speed photography and image analysis. In this manner, the projected areas of the bubbles can be measured and the Sauter mean diameters determined. The Sauter mean diameters, together with gas hold up measurements, facilitate the calculation of the total interfacial area per unit volume. Plate 8.1 shows high-speed photography of the bubbles in a bubble column reactor while Plate 8.2 shows an image of the bubbles after image analysis has been performed. These measurements are particularly useful in determining the impact of the interfacial transfer area per unit volume on the OTR.

A major criticism of the TFT is, however, that it predicts a linear relationship between K_L and diffusivity while experimental results suggest a square-root dependence. The predicted linear relationship is a consequence of the implicit assumption of the establishment of a steady gradient from the instant of gas–liquid contact. In reality, at the first instance of contact, the oxygen in the film equals that in the bulk liquid and a transient period follows during which a gradient is initiated and only later reaches a steady state.

Published by Woodhead Publishing Limited, 2013

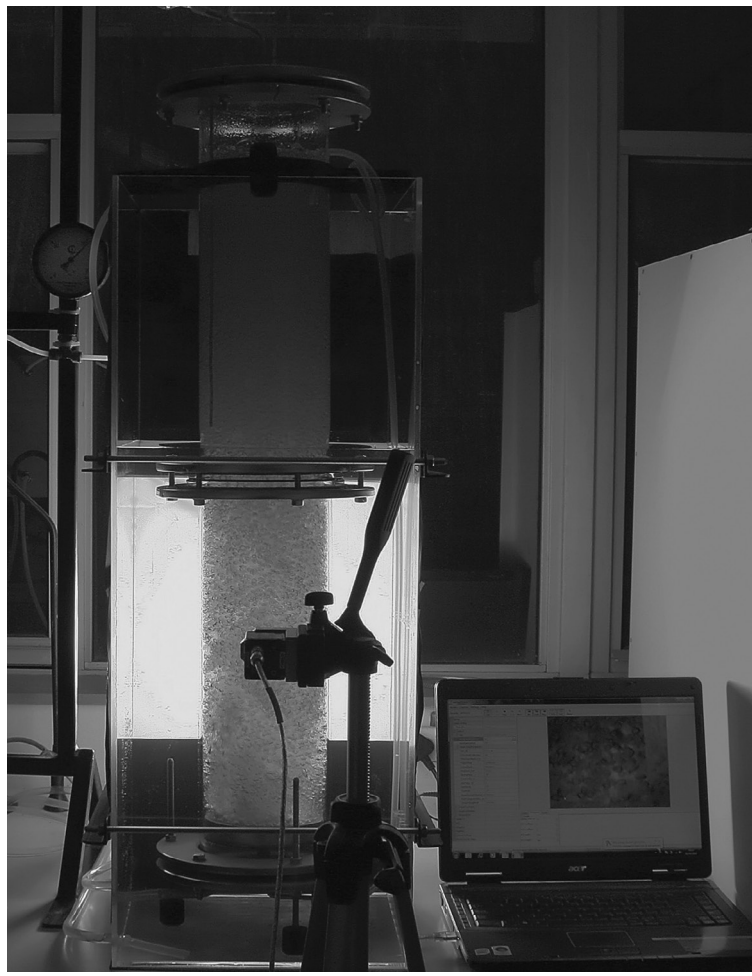

Plate 8.1 **High speed photography of bubble diameter and size distribution in a bubble column reactor (camera at front). Photo: W. Burger**

The steady state assumption of the TFT was addressed in the PT by considering unsteady state diffusion where turbulence extends to the gas–liquid interface. This approach is more appropriate in a well-mixed vessel, where eddy currents continually expose fresh liquid surfaces to the

Published by Woodhead Publishing Limited, 2013

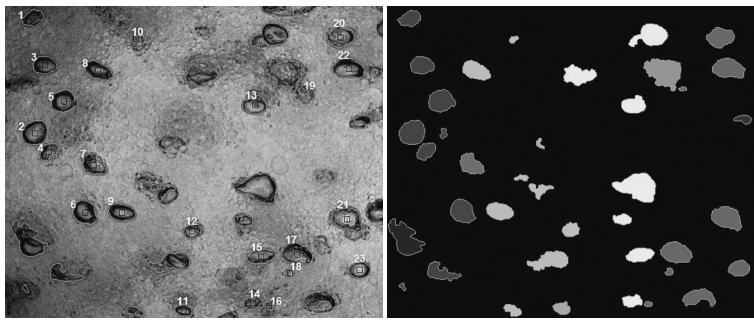

Plate 8.2 Edge detection on original image and contrast mapping of detected bubbles. Photo: W. Burger

oxygen and a steady state concentration gradient in a stagnant film at the interface is less likely. The PT assumes that unsteady state diffusion takes place in each liquid element during its time in contact with the gas–liquid interface (where contact times are assumed identical). The PT therefore considers unsteady state diffusion where the change in oxygen concentration with time is defined by Fick's Second Law (Equation 8.5). From this, an instantaneous molar flux per unit area can be obtained (Equation 8.6) which, when integrated, yields the total molar flux per unit area (Equation 8.7).

$$\frac{dC}{dt} = D\frac{d^2C}{dz^2} \qquad [8.5]$$

$$J_t = \sqrt{\frac{D}{\pi t}}\left(C_{sat} - C\right) \qquad [8.6]$$

$$J = 2\sqrt{\frac{D}{\pi t}}\left(C_{sat} - C\right) \qquad [8.7]$$

As with the TFT, the molar flux per unit area is combined with the interfacial area per unit volume to give the molar flux per unit volume (Equation 8.8).

Published by Woodhead Publishing Limited, 2013

$$N = 2\sqrt{\frac{D}{\pi t}}\, a \left(C_{sat} - C\right) \qquad [8.8]$$

In the PT, the term $2\sqrt{\frac{D}{\pi t}}$ represents K_L and the OTR is governed by the same final equation as for the TFT (Equation 8.4). However, unlike the TFT, the PT predicts a square root relationship between K_L and D, which is consistent with that found experimentally.

Although the PT introduces time dependence into the equation and prediction of K_L from the PT is an improvement on that from the TFT, fault has been found with the PT regarding the assumption that gas contact times for each fluid element are identical. Identical contact times imply that turbulence is homogenous throughout. However, this is not the case; short contact times will occur in regions of high turbulence and longer contact times in regions of lesser turbulence. Consequently, the assumption of identical contact times limits the PT and suggests that a theory incorporating variable contact times would be more appropriate.

Non-uniform contact times were addressed by the SRT. The instantaneous molar flux per unit area (Equation 8.6) is combined with an age distribution function, written in terms of the fraction of liquid elements replaced at the interface during each time step, or the fractional rate of surface renewal, s (Equation 8.9). On integration, the time averaged molar flux per unit area is obtained (Equation 8.10).

$$J = \left(C_{sat} - C\right) \int_0^{\infty} \sqrt{\frac{D}{\pi t}}\, s e^{-st} dt \qquad [8.9]$$

$$J = \sqrt{Ds}\left(C_{sat} - C\right) \qquad [8.10]$$

As with the TFT and the PT, the molar flux per unit area is combined with the interfacial area per unit volume to give the molar flux per unit volume (Equation 8.11).

Published by Woodhead Publishing Limited, 2013

$$N = \sqrt{Ds}\, a\left(C_{sat} - C\right) \qquad [8.11]$$

In the SRT, the term $\sqrt{Ds}$ represents K_L and the OTR is governed by the same final equation as for the TFT (Equation 8.4). As for the PT, a square root dependence of K_L and D is predicted for the SRT, albeit by a different grouping of parameters.

The above analysis of the development of the TFT, PT and SRT models for prediction of the OTR in biological systems distinguishes important differences in the parameters and form of the equation for the prediction of K_L. And this has crucial implications with regard to our understanding of K_L in biological systems. Nevertheless all these models present the identical expression for OTR in terms of K_La and the driving force (Equation 8.4) and it is this equation which is used universally to predict and measure OTR in biological systems and which results in K_La being cited as the key parameter in the design and scale up of fermentation equipment for aerobic processes.

This expression for OTR predicts that the rate can be enhanced by increasing the K_La and/or the oxygen solubility. Increased K_La is achieved readily by amplified turbulence which both reduces transfer resistance and enhances transfer area. An increased concentration gradient is facilitated via improved solubility, affected through either an increased partial pressure of oxygen in the sparge gas or an increased total pressure. Solubility has also been increased by introducing hydrocarbon droplets which, due to the enhanced oxygen solubility in hydrocarbons relative to water, act as oxygen vectors to retain oxygen in the system. This has been effective in bioprocesses using carbohydrate substrates where the hydrocarbon concentration is low. However, in bioprocesses which use hydrocarbons as substrates, the hydrocarbon concentration may well be at a concentration

high enough to result in a K_La depression that eclipses the effect of increased oxygen solubility on the OTR. Temperature also affects the oxygen solubility with a decrease in temperature resulting in an improvement. However, it is usually not practicable to decrease temperature as this may adversely affect cell growth and product formation.

A wide range of system parameters affect K_La, some influencing the resistance, and hence K_L, some influencing the transfer area directly and yet others impacting on both. These include vessel and impeller design and geometry, fluid turbulence, fluid properties and rheology and each should be considered when adopting methods to improve the OTR should it be required. Cognisance should, however, be taken of interactive affects and constraints be applied. For instance, increasing OTR by enhancing interfacial area per unit volume is easily affected by increased agitation which, especially with good baffle design, will promote turbulence. Yet increased turbulence may damage shear sensitive microorganisms and while oxygen availability is increased, the method by which this has been achieved could diminish the microorganisms' ability for product formation.

8.2 Measurement of the oxygen transfer rate

A good many procedures for measurement of the OTR have been documented. Some of these have now been discredited, e.g. the so-called sulphite value. Here the rate of oxidation of sulphite to sulphate is determined by titration and related to the OTR. However, the rate has been observed to vary with the catalyst (copper or cobalt) used and anyway is inappropriate for large scale bioreactors.

Published by Woodhead Publishing Limited, 2013

The methodologies for OTR currently in use may be broadly categorised into the steady state (Section 8.2.1) and the dynamic (Section 8.2.2) procedures.

8.2.1 Quantification of OTR under steady state conditions

This methodology measures the OTR under steady state conditions where the dissolved oxygen concentration remains constant. Under conditions of constant dissolved oxygen concentration, the OUR of the microorganism equals the OTR.[4] OUR is calculated by means of an oxygen mass balance around the reactor, and since OUR = OTR, OTR is quantified as a result. An oxygen mass balance around the reactor is conceptually defined in Equation 8.12.

rate of oxygen entering – rate of oxygen exiting – rate of oxygen used = rate of accumulation of oxygen in the system [8.12]

Although this balance strictly refers to a mass rate, typically it is written in terms of a molar rate. The implied equality between mass and moles in this case is acceptable since no reaction is taking place and the convention of using molar flow rates will be applied. Mathematically, then, at steady state Equation 8.12 can be written in terms of molar flow rates (F), liquid volume (V) and oxygen mole fraction (y) (Equation 8.13).

$$F_{in}(y_{O_2})_{in} - F_{out}(y_{O_2})_{out} - V(OUR) = 0 \quad [8.13]$$

The molar flow rate of oxygen entering is known as it is a specified value. Not so the molar flow rate exiting; this is unknown because it is not known at this stage how much of the oxygen is being utilised. Nevertheless it can be calculated

Published by Woodhead Publishing Limited, 2013

by considering a nitrogen mass balance since the moles of nitrogen entering and exiting will remain constant (Equation 8.14).

$$F_{in}(y_{N_2})_{in} - F_{out}(y_{N_2})_{out} = 0 \quad [8.14]$$

Solving for the unknown exiting molar flow rate and noting that the mole fractions of oxygen, nitrogen and carbon dioxide equal unity, the exiting molar flow rate can be written as Equation 8.15.

$$F_{out} = \frac{F_{in}(y_{N_2})_{in}}{1-(y_{O_2})_{out}-(y_{CO_2})_{out}} \quad [8.15]$$

Finally, substitution of Equation 8.15 into Equation 8.13 and rearranging supplies the expression for OUR (Equation 8.16).

$$OUR = \frac{F_{in}}{V}\left[(y_{O_2})_{in} - \frac{(y_{O_2})_{out}(y_{N_2})_{in}}{1-(y_{O_2})_{out}-(y_{CO_2})_{out}}\right] \quad [8.16]$$

OUR can now be calculated and since OUR = OTR at steady state, OTR is known. Knowing OTR, $K_L a$ can be calculated from Equation 8.4, provided the dissolved concentration is measured[5] and the oxygen solubility is obtained. Data on solubility are scarce, but for an aqueous solution, oxygen solubility can be approximated by solubility in water at the same temperature, easily calculated via Henry's Law which relates the partial pressure in the gas phase with the oxygen concentration in the contacting liquid phase at equilibrium, i.e. the oxygen solubility in the liquid (Equation 8.17).[6] This value will be marginally higher than the solubility in the culture medium because the solutes in the medium tend to decrease the oxygen solubility below that in pure water.

One important question about the calculation of oxygen solubility remains. On which oxygen partial pressure should

it be based; that of the inlet air or that of the outlet air? In a well-mixed reactor, the fluid leaving the reactor is assumed to have the same concentration as that in the reactor, so under these conditions, the solubility should be based on the composition of the outlet gas. However, on the larger scale, mixing may not always be adequate and in this case, the log mean average of the inlet and outlet gas compositions is generally used.

$$x = pH \qquad [8.17]$$

For other than aqueous media, such as hydrocarbon–aqueous dispersions, calculation of the oxygen solubility is slightly more complicated. In this case, oxygen solubility can be approximated by means of averaging the solubility in the aqueous and hydrocarbon phases, according to the volume percentages of each of the different phases. The aqueous phase solubility is calculated using Equation 8.17 and the hydrocarbon phase solubility accessed from physical data tables.

This methodology, therefore, successfully quantifies both $K_L a$ and OTR. Moreover, it carries out the measurement with no disturbance to the culture and is the only methodology currently in use which is totally non-invasive. The method does, however, require on-line gas analysers which, being relatively expensive, are not necessarily standard equipment. Also, while it is an excellent method for calculating OTR in a culture, it cannot be used in a non-respiring (cell free) system. The advantage of calculating OTR in cell free systems is that the capacity to deliver oxygen in different bioreactors can be quickly and efficiently compared by measuring the $K_L a$ values in water in each of the bioreactors.

The most appropriate application of this method is during steady state in continuous culture where cell and substrate (and therefore oxygen) concentrations are constant.

Published by Woodhead Publishing Limited, 2013

Unfortunately this methodology has on occasion been erroneously used during transient conditions in batch culture during periods where the dissolved oxygen concentration varies with time, such as during balanced (exponential) growth, where this method is invalid. However, the method may still be used in batch and fed-batch cultures, but only if there is a significant time period where the dissolved oxygen concentration remains constant.

The prerequisite constant dissolved oxygen concentration should be verified by measurement of the dissolved oxygen with an oxygen probe. This probe measures the oxygen tension between the bulk solution and a cathode, at which a reaction reduces the oxygen concentration to zero. The difference in oxygen tension is then related to the oxygen concentration in the bulk fluid. The cathode is encased in an oxygen permeable membrane (usually silicone or Teflon). The membrane itself introduces a resistance to oxygen transfer and in some cases, is sufficient to generate a significant response lag in the probe reading. Teflon membranes incur a longer response lag than silicone but are more resistant so may be obligatory in corrosive situations, such as hydrocarbon-based bioprocesses. The response lag is irrelevant when using the steady state methodology but if significant, becomes important in the dynamic methods (Section 8.2.2.2).

8.2.2 Quantification of OTR under dynamic conditions

A frequently used methodology for determining OTR is via a dynamic method where $K_L a$ is measured first and OTR is then determined from this value and a calculated driving force according to Equation 8.4. The driving force is quantified from the difference between the oxygen solubility and bulk concentration, both described above (Section 8.2.1).

Published by Woodhead Publishing Limited, 2013

There are several measurement methodologies for K_La under dynamic conditions, but all are based on a common principle, i.e. they all depend on the response of the dissolved oxygen concentration to a step change in an input. The simplest of these methods assume that the response lag of the oxygen probe is negligible. This implies that the probe reading is not significantly different from the actual value of the dissolved oxygen concentration in the bulk liquid (Section 8.2.2.1). The more complex of these methodologies do not make this assumption and here the probe response lag is incorporated in the calculation of the K_La (Section 8.2.2.2).

8.2.2.1 Dynamic methodologies assuming a negligible probe response lag

The most widely used dynamic method to measure K_La is the 'gassing out procedure' which involves the gassing out of oxygen from the liquid in a cell-free system using a nitrogen sparge, followed by a step change in the sparge gas from nitrogen to air.[7] The response of the dissolved oxygen concentration $(\frac{dC}{dt})$ to the step change in the oxygen partial pressure in the inlet gas results solely from the OTR and can thus be modelled by the first order equation which defines the OTR (Equation 8.4), where the OTR equates to $(\frac{dC}{dt})$ (Equation 8.18).

$$\frac{dC}{dt} = K_La\left(C_{sat} - C\right) \qquad [8.18]$$

Integration of Equation 8.18 between the limits of $C = 0$ and $C = C$[8] linearises the data (Equation 8.19) to provide a negative gradient equal to the value of K_La. The graphical construction is straightforward, because the fractional approach to solubility $\frac{C}{C_{sat}}$ is obtained directly from the probe recordings. Knowing K_La, OTR can then be

Published by Woodhead Publishing Limited, 2013

obtained from Equation 8.4 for the appropriate driving force.

$$\ln\left[1-\frac{C}{C_{sat}}\right]=-K_L a t \qquad [8.19]$$

This methodology can similarly be used in systems containing respiring cells. Experimentally, the procedure is the same except that the system is not sparged with nitrogen initially.[9] Rather, the aeration to the culture is switched off and the dissolved oxygen concentration allowed to decrease naturally through respiration until it reaches a value of approximately 20% of the oxygen solubility (Figure 8.2). Lower values are avoided as these may lead to limiting oxygen concentrations which will adversely affect the growth rate. This is especially important with facultative microorganisms which would switch from aerobic to anaerobic metabolism and disadvantage the aerobic process performance.

Once the lowest oxygen concentration limit has been reached, the aeration is initiated and continued at the same rate as before it was interrupted. As a result, the dissolved oxygen concentration increases to approximately the same value as prior to the interruption of aeration.

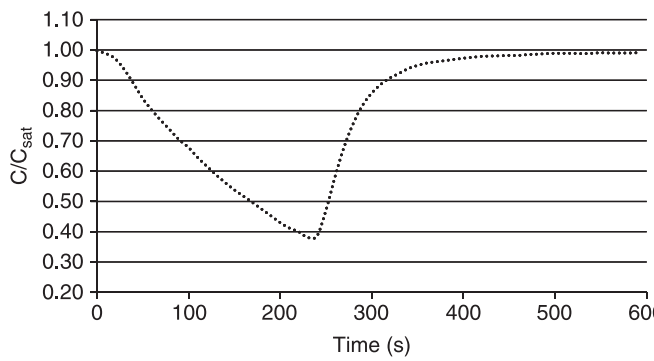

Figure 8.2 Oxygen concentration profile during the dynamic method in a system with respiring cells

Published by Woodhead Publishing Limited, 2013

The basis for the response of the dissolved oxygen concentration $\left(\frac{dC}{dt}\right)$ to the step change in the presence of cells is, however, very different from that in a cell-free system. In this case, the rate of change of dissolved oxygen concentration results from the difference between the OTR and the OUR according to Equation 8.20, where OTR is defined by Equation 8.4.

$$\frac{dC}{dt} = K_L a\left(C_{sat} - C\right) - OUR \qquad [8.20]$$

Rearrangement of Equation 8.20 generates Equation 8.21 which demonstrates that $K_L a$ can be obtained from the negative slope of $\frac{dC}{dt}$ versus C. OTR is then evaluated as before (Equation 8.4).

$$\frac{dC}{dt} = -K_L aC + (K_L aC_{sat} - OUR) \qquad [8.21]$$

This graphical evaluation, however, involves estimating gradients from tangents to the recorded dissolved oxygen response data in order to obtain values for $\frac{dC}{dt}$, a method which is inherently inaccurate. Consequently, an alternative procedure which involves curve fitting is generally preferred. Here, a best fit polynomial (R^2 greater than 0.999) is obtained from the recorded data using Excel. This is differentiated to yield the $\frac{dC}{dt}$ values for the $\frac{dC}{dt}$ versus C curve from the gradient of which $K_L a$ is evaluated.

This dynamic procedure also facilitates measurement of OUR. OUR can be calculated from the change in dissolved oxygen concentration data recorded during the initial period with no aeration. During this period, OTR is zero and the response of the dissolved oxygen concentration $\left(\frac{dC}{dt}\right)$ results

Published by Woodhead Publishing Limited, 2013

solely from the OUR and thus can be obtained directly from the recorded data as the negative gradient of the concentration time curve. Additionally, specific OUR values can be quantified by division of the OUR with the cell concentration at the time of measurement.

8.2.2.2 Dynamic methodologies incorporating a probe response lag

The dynamic methodologies described (Section 8.2.2.1) are accurate and reliable when the probe response lag can be considered negligible. An extensively used benchmark for the level at which the probe response lag can be neglected without compromising the measurement accuracy is defined in terms of a relationship between K_La and the response lag, i.e. the response lag is assumed negligible when it is very much less than the reciprocal of K_La.[10] Experimentally, neglect of the influence of the response lag in K_La measurement in aqueous systems has resulted in a low error (less than about 6%) when the response lag equals the reciprocal of the K_La. This has led to the widespread short cut where specific K_La values are used directly as the sole criterion when determining whether the response lag can be safely neglected. This approach may be sufficient in systems where the response lags are similar. However, in viscous systems, or systems which necessitate a membrane with superior resistance such as Teflon, the response lag is considerably longer than in non-viscous systems and the 'identification' of a specific K_La value as the sole criterion to determine whether the response lag can be neglected is not valid. Under these circumstances, the short cut should be avoided and the *relationship* between K_La and the response lag itself must be evaluated.

Moreover, even when comparing viscous and non-viscous systems with the same response lag, the threshold K_La can be

Published by Woodhead Publishing Limited, 2013

up to 3-fold lower in the viscous system than that in the corresponding non-viscous system.[11] The lower $K_L a$ threshold, compounded with the longer response lag in viscous systems, means that criteria established for aqueous systems cannot be applied when determining if the response lag will significantly affect the accuracy of the $K_L a$ value. This impacts on a broad range of bioprocesses, for instance bioprocesses containing viscous substrates such as hydrocarbons or cellulose and those containing high concentrations of filamentous fungi are all potentially affected. Suffice to say that caution should be exercised before neglecting the response lag, especially in viscous systems and it is strongly recommended that the default position should be to use a methodology which takes the response lag into account.

Two dynamic methodologies which incorporate the probe response lag have been established: the 'modified gassing out procedure' and the 'pressure step procedure'. The former is simpler to execute, both experimentally and mathematically, and is more widely used, but both give excellent results.

The 'modified gassing out procedure' is experimentally identical to the 'gassing out procedure' and is based on the same first order response. However, here the response lag is taken into account such that during aeration, the increase in oxygen concentration recorded by the probe (C_p) is acknowledged to lag the actual oxygen concentration (C). The recorded response in dissolved oxygen can thus be modelled by the first order equation which defines the OTR (Equation 8.4), where the OTR equates to $\left(\frac{dC_p}{dt}\right)$ (Equation 8.22).

$$\frac{dC_p}{dt} = K_L a\left(C_{sat} - C_p\right) \qquad [8.22]$$

The response lag itself is dynamically simulated with a characteristic probe constant (K_p), or inverse response lag time, according to a first order equation (Equation 8.23).

Published by Woodhead Publishing Limited, 2013

$$\frac{dC_p}{dt} = K_p\left(C - C_p\right) \qquad [8.23]$$

Incorporation of the response lag (Equation 8.23) into Equation 8.18 yields the second order equation which describes the response of the system to the step change whilst taking the response lag of the probe into account (Equation 8.24).[12] (In the presence of respiring cells, the OUR has to be incorporated into Equation 8.22.)

$$\frac{C_p}{C_{sat}} = 1 - \frac{1}{K_p - K_L a}\left[K_p e^{-K_L a \cdot t} - K_L a\, e^{-K_p \cdot t}\right] \qquad [8.24]$$

In order to evaluate $K_L a$ from Equation 8.24, the probe constant has to first be determined. This has to be done experimentally as the K_p will differ not only between probes and membranes, but also with different fluid properties and hydrodynamics and the system and impeller geometry. K_p can be measured by recording the dissolved oxygen response after transferring the probe from a zero oxygen solution to one of air saturation ($C = C_{sat}$). Linearisation of Equation 8.23 with $C = C_{sat}$ yields K_p from the negative gradient.

The experimentally determined K_p is substituted into Equation 8.24 which can then be used to predict $\frac{C_p}{C_{sat}}$ for a particular $K_L a$ value. $K_L a$ can be calculated iteratively by minimising the sum of the square root of the error between the $\frac{C_p}{C_{sat}}$ predicted by Equation 8.24 and the $\frac{C_p}{C_{sat}}$ data recorded by the probe using Equation Solver in Excel®.[13]

An alternative dynamic methodology for $K_L a$ measurement which incorporates the probe response lag has been developed more recently.[14] This methodology is termed the 'pressure step procedure' and is based on the change of dissolved oxygen in response to a step change in the total pressure

Published by Woodhead Publishing Limited, 2013

inside the reactor. This experimental procedure differs from that used in the 'gassing out procedure' in that the oxygen partial pressure in the inlet gas is changed via a change in the total gas pressure, rather than by a change in the mole fraction of the oxygen. The pressure step change can be facilitated by means of pressure regulators and valves on two air supply lines, one at a low pressure and one at a pressure 20 kPa higher. Initially the air enters the liquid through the sparger from the low pressure line. The pressure step change is initiated by switching the air sparge from the low pressure line to the high pressure line and simultaneously feeding air to the air space above the liquid level via an auxiliary high pressure line.

For each pressure step change, a series of dimensionless dissolved oxygen concentration–time profiles are calculated, using a range of estimated $K_L a$ values, according to mass balance equations which describe the response of the dissolved oxygen concentration to the step change. The calculated profiles are then adjusted to incorporate the probe response lag dynamics and can be solved numerically using Matlab®. Comparison of theses profiles with that obtained experimentally will identify which of the calculated profiles fit the experimentally recorded profile. The $K_L a$ value of the best fit calculated profile is that $K_L a$ value describing the oxygen transfer. This mathematical approach is considerably more difficult to execute than that of the 'modified gassing out procedure'. This is probably the main reason it has been comparatively little used as it gives as good results as the second order model in the 'gassing out procedure' (Equation 8.24).

8.3 Notes

1. Substances such as carboxymethyl cellulose or hydrocarbons.

Published by Woodhead Publishing Limited, 2013

2. In cases where there is build-up of substance at the interface (e.g. antifoam), this assumption does not necessarily hold.
3. In the case of clumping cells or mycelial pellets, the resistance in the stagnant liquid layer surrounding the clump or pellet may also become significant.
4. A constant dissolved oxygen concentration is a prerequisite of the validity of the equation OUR = OTR.
5. Dissolved oxygen measurement via an oxygen probe.
6. Henry's Law constants for oxygen in water as a function of temperature are readily available. Usually, Henry's Law constants relate to mole fraction in the liquid phase and partial pressure in the gas phase.
7. Developed in aqueous systems several decades ago by Bandyopadhyay, Humphrey and Taguchi (1967).
8. The more general limits of C_1 and C_2 can be used and the equation becomes marginally more complex. But there is little point in not using the simplest equation which merely requires that the nitrogen sparge continue until the probe records zero oxygen.
9. The method in the presence of respiring cells is nevertheless still referred to as the 'gassing out procedure'.
10. Attributed to K. van't Riet (1979)
11. Attributed to the author (2012).
12. The details of the mathematical derivation are left to the reader.
13. The K_La value obtained assuming $C = C_p$ is used as the initial guess for the iteration.
14. Developed in aqueous systems by Linek, Benes and Vacek (1989).

Published by Woodhead Publishing Limited, 2013

9

Bioprocess scale up

DOI: 10.1533/9781782421689.171

Abstract: Bioprocesses development is generally initiated on the laboratory scale and progressively scaled up to larger volumes at the pilot plant level, and finally, production scale. Transport phenomena are especially dependent on scale up, with phenomena such as oxygen transfer, mixing and shear stress altering with the process scale. Changes in these parameters invariably alter the microbial metabolism, thereby compromising kinetic parameters such as yields and productivities. The challenge of successful scale up is then to retain the optimum kinetics that were developed at the smaller scale.

To maintain the optimum physiological state of the microorganism on scale up, all physical and mechanical variables should ideally remain the same at the larger scale. Unfortunately, this is not possible and in practice, the operating ranges of the physical and mechanical variables that define the preferred physiological state are maintained on scale up.

Some scale up procedures tend to be largely unsystematic. At its simplest, scale up procedures rely on trial and error, using historical data of similar equipment from an existing plant, or alternatively, multiplication of elements of an existing process. The former is time consuming and neither guarantees optimum results. On the other hand, fundamental models of momentum, mass and heat transfer

Published by Woodhead Publishing Limited, 2013

have been developed to predict performance on scale up. However, these may be complicated and in some cases not necessarily reliable for complex turbulent flows.

There are scale up methodologies which are considerably less complex than the transfer models, but nevertheless provide a systematic approach. One such approach is based on evaluating the differences in the characteristic time constants for each phenomenon which has the potential to control the performance on scale up.[1] For example, time constants of the same order of magnitude for oxygen transfer and oxygen consumption suggest that oxygen transfer limitation is likely to be problematic. If, in addition, the time constant for liquid circulation is similarly of the same order, then oxygen gradients are likely to occur, and so on.

Another methodology of scale up, and arguably the most well documented, is that in which the specific physical or mechanical property which is most critical to process performance is identified (termed the scale up criterion) and maintained constant on scale up. The scale up criteria most commonly identified are oxygen transfer rate, mixing, shear stress and, to a lesser extent, flow regime.

The scale up criterion of choice depends on the specific circumstances and the Bioprocess Engineer will be required to use professional experience in judging the optimum criterion. For instance, a bioprocess with a high oxygen demand would likely be scaled up to maintain the oxygen transfer rate established as optimum on the small scale, while scale up of a bioprocess using shear sensitive filamentous fungi may need to maintain the shear stress at the threshold value determined on the small scale.

When using a scale up criterion, the scale up is carried out according to the principle of geometric similarity between the large and small scales. Geometric similarity implies identical aspect ratios of the vessel and internals on both scales, i.e. the ratios of vessel height to vessel

Published by Woodhead Publishing Limited, 2013

diameter, vessel height to impeller diameter, etc., remain constant on scale up. In this way the effect of different scales can be evaluated by comparing a characteristic length, say the impeller diameter (D).

While geometric similarity is a relatively simple and systematic approach, it is axiomatic that, if geometric similarity is to be maintained, parameters other than the scale up criterion will not remain constant on scale up. The potential exists for the changes in these parameters to adversely affect the microbial physiology on the large scale. Cognisance must be taken of the magnitude of the effect of the altered parameters before the scale up criterion can be implemented.

In Chapter 9, the scale up methodology based on the maintenance of selected scale up criteria according to geometrical similarity is developed. The scale up criteria will include: oxygen transfer rate, mixing, shear stress and flow regime. The increases in energy input to maintain the desired criterion on the larger scale is calculated in each case and further, the effect of maintaining the specific criterion constant on the other parameters is calculated and quantitatively and qualitatively assessed. By way of quantifying the effect of the distinct scale up criteria on the varying parameters on scale up, the example of scale up from a 10 L scale to a 10 m^3 scale will be examined.

Key words: geometric similarity, scale up criteria, power requirement, mixing, shear stress, flow regime.

9.1 Scale up with constant oxygen transfer rate

Frequently scale up of aerobic bioprocesses is executed on the basis of maintaining a constant OTR (Section 8.1) so

that the process does not become limited by oxygen transport to the cells. Typically the $K_L a$ rather than the OTR is used as the design parameter, solubility being a constant in the system under consideration.

Several empirical relationships relate $K_L a$ to agitation (in terms of power per unit volume, P/V) and aeration (in terms of superficial air velocity, V_s) similar to Equation 9.1.

$$K_L a = (P/V)^{\alpha}(V_s)^{\beta} \quad [9.1]$$

The values of the empirical constants α and β will differ depending on the fluid dynamics, fluid properties and scale under which the experiment was conducted so the absolute values are of little relevance here. Nevertheless, it has generally been demonstrated that the dependence of $K_L a$ on P/V is considerably more pronounced than that on V_s. In fact, a threshold V_s value of 0.6 to 0.8 vvm^2 exists, above which an increase in V_s will achieve a negligible increase in $K_L a$ and serve only to waste air and/or to generate foaming. This not only predisposes the wetting and contamination of air filters, but also has the potential to adversely affect the production kinetics. $K_L a$ is, therefore, often related empirically to P/V alone and, as a consequence, maintaining a constant OTR is equated to maintaining a constant P/V. P/V is then defined as the scale up criterion that needs to be maintained constant if the small scale OTR is to be maintained on the large scale.

9.1.1 Effect on power requirements

To maintain oxygen transfer characteristics, it is self-evident that the power input on the larger scale (designated 2) would be greater than that on the smaller scale (designated 1). To quantify the increase in power input required on

Published by Woodhead Publishing Limited, 2013

the larger scale, P/V on each scale is equated, leading to Equation 9.2.

$$P_2 = P_1 \frac{V_2}{V_1} \qquad [9.2]$$

The increased power is frequently defined in terms of the increase in impeller diameter. To calculate this, the relationship between the volume ratio and impeller diameter of geometrically similar vessels first needs to be determined.

The volume ratio of the two geometrically similar vessels in Figure 9.1 is given by Equation 9.3. And, since geometric similarity implies Equation 9.4, Equation 9.3 can be written as Equation 9.5.[3]

$$\frac{V_2}{V_1} = \frac{\pi T_2^2 H_2 / 4}{\pi T_1^2 H_1 / 4} = \frac{T_2^2 H_2}{T_1^2 H_1} \qquad [9.3]$$

$$H_1 = \frac{T_1 H_2}{T_2} \qquad [9.4]$$

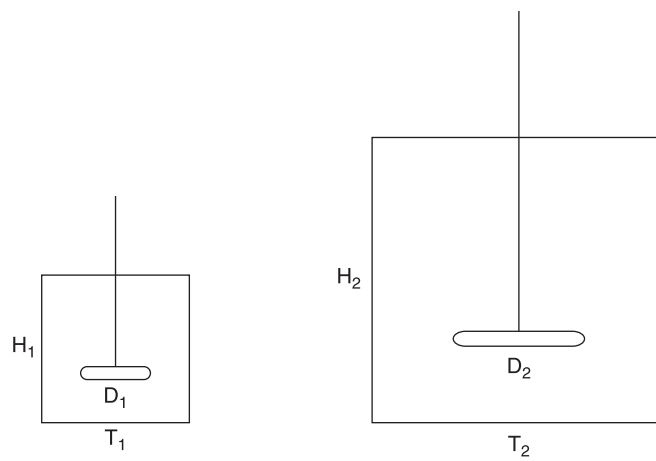

Figure 9.1 Geometrically similar vessels: $H_2/T_2 = H_1/T_1$; $H_2/D_2 = H_1/D_1$

Published by Woodhead Publishing Limited, 2013

$$\frac{V_2}{V_1} = \frac{T_2^2 H_2 T_2}{T_1^2 H_2 T_1} = \left(\frac{T_2}{T_1}\right)^3 = \left(\frac{D_2}{D_1}\right)^3 \quad [9.5]$$

The volume ratio in Equation 9.2 can then be substituted with the equivalent impeller diameter ratio in Equation 9.5 to yield the increase in power required on the large scale in terms of the impeller diameter ratio (Equation 9.6).

$$P_2 = P_1\left(\frac{D_2}{D_1}\right)^3 \quad [9.6]$$

So, for example, an increase in volume from 10 L to 10 m^3 represents a 10-fold increase in impeller diameter (Equation 9.5). A 10-fold increase in impeller diameter will, according to Equation 9.6, require a 1000-fold increase in energy input to maintain the oxygen transfer characteristics on the large scale.

When oxygen transfer characteristics remain constant on scale up, such an increase in energy input on scale up will obviously affect other parameters. The effect on the parameters most commonly of concern on scale up with constant oxygen transfer are quantified below for mixing (Section 9.1.2), shear stress (Section 9.1.3) and flow regime (Section 9.1.4).

9.1.2 Effect on mixing

Mixing performance is characterised by mixing times, where the mixing time is the time taken to reach a specified degree of homogeneity after a system change. Consequently, the effect of mixing on scale up can be quantified by examining the ratio of mixing times on the two scales.

Mixing time (t_m) is defined as the ratio of the liquid volume to the liquid volumetric flow (or pump) rate of the impeller

Published by Woodhead Publishing Limited, 2013

(V/Q). To define Q in terms of physical and/or mechanical parameters, use is made of the dimensionless pumping number ($Q/(ND^3)$). In common with all dimensionless numbers, the pumping number comprises variables which, when grouped together, form a new variable which has no dimensional units and which is insensitive to scale.

The pumping number has been correlated with another dimensionless number, the Reynolds number ($D^2N\rho/\mu$)[4] the value of which defines the flow regime (laminar, turbulent or intermediate), where D refers to the impeller diameter. The pumping number has been shown to be constant at Reynolds numbers associated with a fully turbulent flow regime. Since turbulent flow is invariably experienced in agitated bioreactors, it can be assumed that the pumping number is constant and hence, that Q is proportional to ND^3. Using this proportionality, the ratio of the mixing times on the small to large scales can be written as Equation 9.7.

$$\frac{t_{m1}}{t_{m2}} = \frac{\dfrac{V_1}{Q_1}}{\dfrac{V_2}{Q_2}} = \frac{\dfrac{V_1}{N_1D_1^3}}{\dfrac{V_2}{N_2D_2^3}} = \frac{V_1N_2D_2^3}{V_2N_1D_1^3} \qquad [9.7]$$

For geometric similarity, the volume ratio equals the corresponding ratio of the cube of the impeller diameters (Equation 9.5), and so Equation 9.7 becomes Equation 9.8. Thus, the mixing times, and hence mixing performance, can be quantified directly in terms of the inverse ratio of the rotational speeds at the two scales.

$$\frac{t_{m1}}{t_{m2}} = \frac{N_2}{N_1} \qquad [9.8]$$

The ratio of the rotational speeds is obtained from another dimensionless number, the power number ($P/N^3D^5\rho$) which, similar to the pumping number, is constant during turbulent

Published by Woodhead Publishing Limited, 2013

flow. A constant power number implies that P is proportional to N^3D^5 such that Equation 9.9 applies. Since under constant oxygen transfer conditions, the ratio of cube of the impeller diameters equals the ratio of the power input (Equation 9.6),[5] Equation 9.9 can be rearranged to give Equation 9.10.

$$\frac{P_2}{P_1} = \frac{N_2^3 D_2^5}{N_1^3 D_1^5} \quad [9.9]$$

$$\frac{N_2}{N_1} = \left(\frac{D_1}{D_2}\right)^{2/3} \quad [9.10]$$

This expression predicts that when oxygen transfer is used as the scale up criterion, the same mixing characteristics cannot be maintained. As the impeller diameter is increased, mixing efficiency will decrease according to $1/D^{2/3}$, or phrased another way, mixing time will increase by $D^{2/3}$. As an illustration, a 10-fold increase in impeller diameter would result in a 4.6-fold increase in mixing time.

During scale up operations, the rotational speed is often reduced, regardless of the scale up criterion. This is in part due to the overmixing typical at the small scale. So the lower rotational speed of the larger reactor does not necessarily compromise the mixing efficiency as adequate mixing may still be provided, despite the increase in mixing time. However, in viscous or non-Newtonian fluids, or where solid substrates need to be kept in suspension (e.g. slurry reactors), a decrease in mixing capacity may well affect performance.

9.1.3 Effect on shear stress

Since maximum shear is experienced at the highest velocities, and the highest velocities are associated with those at the tip of the impeller, the impeller tip speed (ND) is assumed

Published by Woodhead Publishing Limited, 2013

proportional to the shear stress exerted on the cells. So the ratio of shear stress at the different scales can be quantified by the corresponding ratio of ND. The ratio of ND can be determined from the proportionality of P to N^3D^5 according to Equation 9.9, which can be rearranged to Equation 9.11.

$$\frac{(ND)_2^3}{(ND)_1^3} = \frac{P_2 D_1^2}{P_1 D_2^2} \qquad [9.11]$$

Since under constant oxygen transfer conditions, the ratio of cube of the impeller diameters equals the ratio of the power input (Equation 9.6), Equation 9.11 can be rearranged to Equation 9.12.

$$\frac{(ND)_2}{(ND)_1} = \left[\frac{D_2^3 D_1^2}{D_1^3 D_2^2}\right]^{1/3} = \left[\frac{D_2}{D_1}\right]^{1/3} \qquad [9.12]$$

This means that when oxygen transfer is used as the scale up criterion, as the impeller diameter is increased, shear stress will increase according to $D^{1/3}$. As an illustration, a 10-fold increase in impeller diameter would result in a 2.2-fold increase in shear stress. For shear sensitive cells, this may well be problematic. However, for more robust cells, it may not be, and every individual case needs to be assessed according to the particular circumstances.

9.1.4 Effect on flow regime

The impact of change of flow regime can be assessed via the impact of the change of the Reynolds number. Since the Reynolds number is proportional to ND^2, the effect of a change in flow regime can be quantified in terms of the ratio of ND^2 on the two scales. Using this proportionality, the ratio of the flow regimes on the small to large scales can be written as Equation 9.13. Finally, substitution of the

relationship between the ratio of rotational speed and impeller diameters (Equation 9.10) yields Equation 9.14. Consequently, as D increases on scale up, turbulence increases despite a concomitant decrease in N. According to Equation 9.14, a 10-fold increase in D, for example, will result in a 21.5-fold increase in the Reynolds number.

$$\frac{\text{Reynolds number}_2}{\text{Reynolds number}_1} = \frac{N_2 D_2^2}{N_1 D_1^2} \quad [9.13]$$

$$\frac{\text{Reynolds number}_2}{\text{Reynolds number}_1} = \frac{D_1^{2/3} D_2^2}{D_2^{2/3} D_1^2} = \left(\frac{D_2}{D_1}\right)^{4/3} \quad [9.14]$$

9.2 Scale up with constant mixing

Adequate mixing is another key parameter in bioprocesses and as such is also commonly identified as the scale up criterion. Since mixing efficiency is proportional to the rotational speed during turbulent flow (Equation 9.8), a constant mixing time on scale up is analogous to a constant rotational speed ($N_1 = N_2$).

9.2.1 Effect on power requirements

The relationship between rotational speed and power input in turbulent flow is given by Equation 9.9 which, when $N_1 = N_2$, reduces to Equation 9.15. This predicts that to maintain the mixing characteristics on scale up, an extremely large increase in power input is required, namely D^5. This means that a 10-fold increase in impeller diameter would require a 10^5-fold increase in power input in order to maintain the same mixing times. This exceptionally large increase in power consumption suggests that a formal

Published by Woodhead Publishing Limited, 2013

application of maintaining constant mixing in geometrically similar systems may be unrealistic.

$$\frac{P_2}{P_1} = \left(\frac{D_2}{D_1}\right)^5 \qquad [9.15]$$

9.2.2 Effect on oxygen transfer

Oxygen transfer would be expected to increase if mixing time is used as the scale up criterion. This can easily be seen with the relative increase in power of D^5 with constant mixing compared with only D^3 with constant oxygen transfer.

The ratio of the power input under constant mixing conditions (Equation 9.15) can be written in terms of oxygen transfer characteristics or P/V (Equation 9.16). Geometric similarity implies a relationship between V and D^3 (Equation 9.5) which, when substituted into Equation 9.16, yields Equation 9.17. Thus an increase of oxygen transfer with D^2 on scale up is confirmed. So a hypothetical 10-fold increase in impeller diameter would result in a 10^2-fold increase in oxygen transfer should the mixing characteristics remain constant on scale up.

$$\frac{P_2/V_2}{P_1/V_1} = \left(\frac{D_2}{D_1}\right)^5 \frac{V_1}{V_2} \qquad [9.16]$$

$$\frac{P_2/V_2}{P_1/V_1} = \left(\frac{D_2}{D_1}\right)^5 \frac{D_1^3}{D_2^3} = \left(\frac{D_2}{D_1}\right)^2 \qquad [9.17]$$

9.2.3 Effect on shear stress

There will certainly be an increased shear when D is increased under conditions of constant N. Considering the ratio of

Published by Woodhead Publishing Limited, 2013

shear stress, or ND, at the different scales (Equation 9.11) and incorporating the relationship between the power ratio and the impeller diameter ratio under constant mixing conditions (Equation 9.15) results in Equation 9.18. Shear stress thus increases with D with constant mixing, indicating a 10-fold increase in shear stress coordinating with a 10-fold increase in D.

$$\frac{N_2 D_2}{N_1 D_1} = \left[\left(\frac{D_2}{D_1} \right)^5 \frac{D_1^2}{D_2^2} \right]^{1/3} = \frac{D_2}{D_1} \qquad [9.18]$$

9.2.4 Effect on flow regime

The change in flow regime is represented by the change in the Reynolds number according to Equation 9.13. With constant mixing, this reduces to Equation 9.19 which predicts a 10^2-fold increase in the Reynolds number for a hypothetical 10-fold increase in D.

$$\frac{\text{Reynolds number}_2}{\text{Reynolds number}_1} = \left(\frac{D_2}{D_1} \right)^2 \qquad [9.19]$$

9.3 Scale up with constant shear stress

For shear sensitive cells, scale up with constant shear stress may well be preferred. ND is then defined as the scale up criterion that needs to be maintained constant if the shear stress is to be maintained on the large scale.

Published by Woodhead Publishing Limited, 2013

9.3.1 Effect on power requirements

With ND constant, the power correlation of Equation 9.9 reduces to Equation 9.20 indicating that the power increases with the square of the impeller diameter when shear stress is used as the scale up criterion. So a 10-fold increase in impeller diameter, for example, will require a 10^2-fold increase in energy input.

$$\frac{P_2}{P_1} = \left(\frac{D_2}{D_1}\right)^2 \qquad [9.20]$$

9.3.2 Effect on oxygen transfer

The effect on oxygen transfer when shear stress is kept constant can be quantified through manipulation of Equation 9.20 from a power to a power per unit volume ratio, followed by substitution of the ratio between the volume and diameter for geometrically similar vessels (Equation 9.5). This gives the ratio of the oxygen transfer characteristics in terms of the ratios of the power per unit volume (Equation 9.21).

This expression predicts a decrease in oxygen transfer when shear stress is maintained constant on scale up. (This is to be expected since shear stress increases with constant oxygen transfer.) The oxygen transfer decreases with 1/D such that a 10-fold increase in D would result in an oxygen transfer on the large scale of only 0.1 of the oxygen transfer on the small scale. This could be a real problem for shear sensitive microorganisms with a high oxygen demand and calls for innovative approaches to enhance the oxygen transfer without increasing the shear. One such solution would simply to sparge oxygen-enriched air; another would be to introduce an immiscible liquid which has a high affinity

Published by Woodhead Publishing Limited, 2013

for oxygen (e.g. oil) as a dispersed phase to provide reservoirs of oxygen amongst the microorganisms.

$$\frac{P_2 / V_2}{P_1 / V_1} = \left(\frac{D_2}{D_1}\right)^2 \frac{V_1}{V_2} = \left(\frac{D_2}{D_1}\right)^2 \left(\frac{D_1}{D_2}\right)^3 = \frac{D_1}{D_2} \qquad [9.21]$$

9.3.3 Effect on mixing

The effect on mixing can be very simply calculated as ND is constant. Therefore, N is proportional to 1/D and Equation 9.22 follows. Thus, mixing is compromised to the same extent as is the oxygen transfer, i.e. reduced to 0.1 of its efficiency at the small scale for a 10-fold increase in impeller diameter. Effectively, this means that the mixing time would be increased 10-fold. Depending on the particular circumstances, this may have severe consequences. For instance, high concentrations of filamentous fungi are comparatively viscous and may suffer from inadequate mixing and oxygen transfer limitations yet are sensitive to shear stress through breakage of the hyphae. Scale up of these and similar bioprocesses is challenging and needs to be carried out with insight.

$$\frac{N_2}{N_1} = \frac{D_1}{D_2} \qquad [9.22]$$

9.3.4 Effect on flow regime

The effect of shear stress as the scale up criterion on flow regime can be quantified from Equation 9.13 with ND constant. This results in Equation 9.23 which predicts an increase in the Reynolds number proportional to the increase in impeller diameter, e.g. a 10-fold increase in impeller diameter on scale up would result in a similar 10-fold increase

Published by Woodhead Publishing Limited, 2013

in the Reynolds number. So a turbulent flow regime would remain during scale up with constant shear.

$$\frac{\text{Reynolds number}_2}{\text{Reynolds number}_1} = \frac{D_2}{D_1} \quad [9.23]$$

9.4 Scale up with constant flow regime

The flow regime can be maintained constant on scale up by maintaining a constant Reynolds number (although this scale up criterion has been used less frequently than other parameters).

9.4.1 Effect of scale up on power requirements

The power ratio (Equation 9.9) with ND^2 constant can be manipulated into Equation 9.24 which predicts a decrease in power on scale up with the inverse of the impeller diameter. For a hypothetical 10-fold increase in impeller diameter, then, only 0.1 of the small scale power input would be required.

$$\frac{P_2}{P_1} = \frac{N_2^3 D_2^6 D_1}{N_1^3 D_1^6 D_2} = \left(\frac{N_2 D_2^2}{N_1 D_1^2}\right)^3 \frac{D_1}{D_2} = \frac{D_1}{D_2} \quad [9.24]$$

9.4.2 Effect of scale up on oxygen transfer

This decrease in power requirement with flow regime as the scale up criterion would certainly have an adverse effect on the oxygen transfer. To calculate its effect, the power ratio with ND^2 constant (Equation 9.24) needs to be written in

Published by Woodhead Publishing Limited, 2013

terms of the power per unit volume ratio (Equation 9.25). So, as expected, the oxygen transfer is extremely low on the large scale, being only $1/D^4$ of that on the small scale. Quantifying the oxygen transfer on scale up in terms of a 10-fold increase in impeller diameter, shows that the oxygen transfer is only 10^{-4} of that on the small scale. This is a red flag to warn that scale up with constant flow regime should not be considered for an aerobic bioprocess.

$$\frac{P_2/V_2}{P_1/V_1} = \frac{D_1V_1}{D_2V_2} = \frac{D_1D_1^3}{D_2D_2^3} = \left(\frac{D_1}{D_2}\right)^4 \quad [9.25]$$

9.4.3 Effect of scale up on mixing

Under conditions of constant flow regime on scale up, ND^2 is constant and N is proportional to $1/D^2$, so Equation 9.26 applies. This predicts a decrease in mixing. Here the decrease is considerable with mixing on the large scale decreased 10^2-fold with a 10-fold increase in impeller diameter. This decrease is an order of magnitude larger than that experienced during scale up with either oxygen transfer or constant shear as the scale up criterion. Thus, the mixing on the large scale may not be sufficient for adequate substrate transfer, or for proper suspension of particles and unmixed pockets of solids and fluid may occur.

$$\frac{N_2}{N_1} = \left(\frac{D_1}{D_2}\right)^2 \quad [9.26]$$

9.4.4 Effect of scale up on sheer stress

The effect on shear stress is readily evaluated from multiplying Equation 9.26 by the impeller diameter ratio to yield

Published by Woodhead Publishing Limited, 2013

Equation 9.27. This shows a decrease in the shear stress on scale up; for instance a 10-fold increase in impeller diameter results in a 10-fold decrease in the shear stress.

$$\frac{N_2 D_2}{N_1 D_1} = \left(\frac{D_1}{D_2}\right)^2 \frac{D_2}{D_1} = \frac{D_1}{D_2} \qquad [9.27]$$

Considering shear stress alone, maintenance of flow regime on scale up appears advantageous. But it should be remembered that this advantage is achieved at the expense of serious compromises in the mixing and oxygen transfer characteristics. In general, scale up using the Reynolds number as the scale up criteron is not considered a viable proposition.

9.5 Notes

1. A time constant is defined as the time taken after a step change for the concentration to reach 0.63 ($1 - e^{-1}$) of its initial value. For example, a first order change in oxygen concentration has a time constant equal to the reciprocal $K_L a$. (The derivation is left to the reader.)
2. vvm = volume of air per volume of liquid per minute. A range of vvm is given because a lower vvm applies at a lower agitation rate.
3. In geometrically similar systems, volume is proportional to D^3 whereas area is proportional to D^2. Thus the surface/volume ratio decreases on scale up. This may affect bioprocesses where wall growth is significant, especially if cells adhering to surfaces have an altered metabolism to that of submerged cells.
4. Developed by Osborne Reynolds (1843–1912).
5. Remembering that under constant oxygen transfer conditions, P/V is constant.

Published by Woodhead Publishing Limited, 2013

10

Bioprocess asepsis and sterility

DOI: 10.1533/9781782421689.189

Abstract: Most bioprocesses require asepsis during the process. Exceptions to the rule are generally limited to bioremediation of wastes where the Bioprocess Engineer is grateful for any microorganism that can assist in utilising the substrate (pollution). In almost all other processes, sterility of the equipment and medium needs to be ensured prior to the inoculation of the desired microorganisms and ingress of foreign microorganisms prevented throughout the production. This requires sterilisation of the media and equipment prior to start-up and, in the case of continuous culture or fed-batch culture, sterilisation of media during operation. For aerobic processes, sterilisation of the air sparged into the reactor is also essential for maintenance of aseptic conditions.

Media and air sterilisation are based on entirely different principles. Equipment and media sterilisation utilises heat for sterilisation while air sterilisation takes place by filtration, usually by deep bed filtration but occasionally (and only on the small scale) by absolute filtration. Methodologies for media and equipment sterilisation by heat and air sterilisation by filtration are both developed, evaluated and discussed in Chapter 10.

Published by Woodhead Publishing Limited, 2013

Key words: heat sterilisation, thermal death rate, thermal degradation rate, batch media sterilisation, continuous media sterilisation, air sterilisation.

10.1 Heat sterilisation of media and equipment

Sterilisation of equipment and media by heat brings about cell lysis through denaturation of intracellular enzymes. This destroys the biocatalysts which mediate each and every biochemical reaction in the metabolic pathways and microbial death results. The biocatalysts are readily destroyed in this environment as they are in their hydrated form.[1] Importantly, however, during the application of heat, the loss of essential nutrients can result in medium degradation. Sugars can become caramelised or react with nitrogen sources, in the former reducing the amount of carbon available, in the latter reducing the availability of both carbon and nitrogen.[2] Essentially amino acids tend to oxidise with heat, and if not synthesised by the microorganism itself, the loss of amino acids in the medium will limit the metabolism. Additionally, heat-labile compounds in the media such as vitamins will be destroyed and render dependent enzymes inactive. It is therefore expedient that while ensuring a degree of sterilisation for aseptic conditions, the nutritional integrity of the medium must be safeguarded. Consequently, overdesign of the sterilisation unit is definitely not an option and should be rigorously avoided.

10.1.1 Kinetics of heat sterilisation

Design of steriliser units must simultaneously satisfy two opposing concerns during the application of heat: the

Published by Woodhead Publishing Limited, 2013

maximisation of the rate and extent of microbial death and the minimisation of the rate and extent of degradation of heat-labile compounds. As such, sterilisation by heat is governed not only by the rate equations for thermal death of the microorganisms, but also by the rate equations for thermal degradation of the heat-labile compounds in the medium.

The rate of thermal death has been empirically shown to follow first order kinetics at a constant sterilisation temperature according to Equation 10.1 where N is the number of viable microorganisms and k_d is the thermal death rate constant. Integration of Equation 10.1 yields Equation 10.2, the equation of a straight line graph with gradient equal to $-k_d$.

$$\frac{dN}{dt} = -k_d N \qquad [10.1]$$

$$\ln \frac{N}{N_0} = -k_d t \qquad [10.2]$$

k_d provides a quantitative indication of the resistance to thermal death: the lower the k_d, the more resistance is encountered and the more difficult it is to obtain sterility. The resistance depends on the entire process environment, including medium and pH, but mostly on the sterilisation temperature. Progressively higher sterilisation temperatures relate to correspondingly higher k_d values (Figure 10.1).

This is a deterministic model where the variations within the microbial culture (e.g. variations in cell wall permeability[3]) are not taken into account and the mean response is assumed to be the actual value with no statistical variation.

Different species, however, vary significantly in their response to thermal death with distinct k_d values resulting. Further, anomalous curves may be observed with sporulating microorganisms where there is an initial increase in the number of viable microorganisms before a decrease is observed. This is because the high temperature initially causes the spores to

Published by Woodhead Publishing Limited, 2013

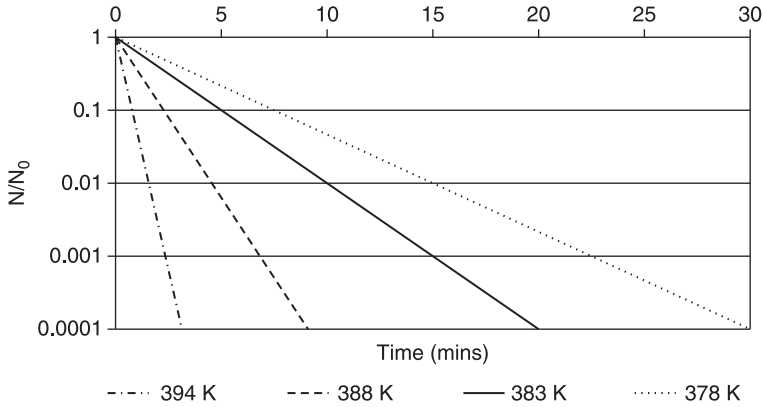

Figure 10.1 Influence of sterilisation temperature on efficiency of sterilisation

germinate resulting in an increase in vegetative microorganisms. These vegetative forms, however, quickly succumb to the high temperature and the number of viable microorganisms then decreases. This anomalous behaviour is typical of the sporulating *Bacillus stearothermophilus*. The sporulating nature of *B. stearothermophilus*, as well as its particularly low k_d value, has made it the preferred design microorganism; the rationale being that if the sterilisation specifications are met with respect to this organism, the procedure will be effective against all other possible contaminants.

The dependence of k_d on temperature has been empirically demonstrated to follow a trend which can be modelled effectively by an equation of the Arrhenius form (Equation 10.3)[4] where E is defined as the activation energy of thermal death,[5] T is the absolute temperature and R the universal gas constant. The kinetic constants E and k_{d_0} can be calculated by Equation 10.4 to yield a negative gradient of E/R and y-intercept of ln k_{d_0}.

$$k_d = k_{d_0} \bar{e}^{\frac{E}{RT}} \qquad [10.3]$$

Published by Woodhead Publishing Limited, 2013

$$\ln k_d = \ln k_{d_0} - \frac{E}{RT} \qquad [10.4]$$

The expression for k_d as a function of temperature (Equation 10.3) can now be inserted into the first order model for thermal death (Equation 10.1) to derive the design equation for heat sterilisation (Equation 10.5). Since sterilisation is seldom carried out at a single constant temperature, theoretically the temperature should be integrated over the entire sterilisation time (Equation 10.6). The acceptable level of contamination after sterilisation is by convention represented by $\ln\frac{N_0}{N}$. The steriliser is ultimately designed on the basis of $\left[\ln\frac{N_0}{N}\right]_{overall}$ which specifies the degree of sterility that has to be achieved after the entire sterilisation process has been completed. $\ln\frac{N_0}{N}$ is known as the 'Del Factor' and designated '∇'.

$$\frac{dN}{N} = -k_{d_0} e^{-\frac{E}{RT}} dt \qquad [10.5]$$

$$\ln\frac{N}{N_0} = -k_{d_0} \int_0^t e^{-\frac{E}{RT}} dt \qquad [10.6]$$

The kinetics of thermal degradation of heat-labile medium compounds follow a kinetic analysis identical to that of the thermal death of microorganisms. In the thermal degradation rate equations, however, N*, E*, k_d* and k_{d_0}* refer to the heat-labile compounds in the medium.

10.1.2 Batch sterilisation

During batch sterilisation, the medium is heated from room temperature to the desired sterilisation temperature and held at the sterilisation temperature for a specified time, after

Published by Woodhead Publishing Limited, 2013

which it is cooled to the operating temperature. This is universally carried out *in situ*, except for some laboratory scale bioreactors which are of sufficiently small scale to fit into an autoclave.

Sterilisation frequently takes place by injecting steam into a pressure jacket around the reactor. However, since the surface to volume decreases on scale up, the area available for heat transfer in jacketed vessels may not be sufficient to efficiently sterilise the entire volume in very large scale bioreactors. In this case, heat sterilisation can be effected by introducing heating coils into the medium, or by direct sparging into the reactor. With direct steam sparging, the initial medium would be made up to only 90% of its final liquid volume to account for the volume added by the steam condensate.

Most of the sterilisation takes place while the medium is being held at the sterilisation temperature where the k_d is highest. Nevertheless, some sterilisation also takes place during the heating and cooling periods, especially when the temperature approaches the sterilisation temperature. In fact, the contribution of sterilisation taking place during the heating and cooling periods may constitute as much as 25% to the total sterilisation and certainly cannot be neglected.

In batch sterilisation, the degree of sterility to be achieved after the entire sterilisation process has been completed comprises that contributed by the heating and cooling periods as well as that from the holding period. This can be expressed mathematically for each period (Equation 10.7). In this expression, the heating period takes place from time zero to t_h, the holding period from time t_h to t_c and the cooling period from time t_c to t. The kinetic constants can be evaluated as has been described in Section 10.1.1.

Published by Woodhead Publishing Limited, 2013

$$\left[\ln\frac{N_0}{N}\right]_{overall} = \left[\ln\frac{N_0}{N}\right]_{heating} + \left[\ln\frac{N_0}{N}\right]_{holding} + \left[\ln\frac{N_0}{N}\right]_{cooling}$$

$$= k_{d_0}\int_0^{t_h} e^{-\frac{E}{RT}}\,dt + k_{d_0}\int_{t_h}^{t_c} e^{-\frac{E}{RT}}\,dt + k_{d_0}\int_{t_c}^{t} e^{-\frac{E}{RT}}\,dt \quad [10.7]$$

Since the holding period takes place at a constant temperature, the k_d can be calculated at the constant sterilisation temperature (T) according to Equation 10.3 and the sterilisation taking place at this temperature calculated by multiplying the k_d by the time of the holding period (Equation 10.8).

$$\left[\ln\frac{N_0}{N}\right]_{holding} = k_{d_0} e^{-\frac{E}{RT}}(t_c - t_h) \quad [10.8]$$

A full analytical solution to Equation 10.7, however, requires substitution of time-dependent functions of temperature during the heating and cooling periods. The time-dependent temperature during heating can be obtained from a heat balance which takes into consideration the mass and specific heat of the medium, the heat transfer coefficient, transfer area and the temperature of the steam. Assuming these parameters are constant, the temperature can be obtained as Equation 10.9 where α and β are constants incorporating the mass and specific heat of the medium, the heat transfer coefficient and transfer area (α) and the steam temperature and the initial medium temperature (β).

$$T = T_{steam}\,(1 + \beta\, e^{-\alpha(t_c - t_h)}) \quad [10.9]$$

Similarly, the time-dependent temperature during cooling can be obtained from a heat balance which takes the same variables into consideration except that the temperature of the cooling water replaces that of the steam (Equation 10.10).

Published by Woodhead Publishing Limited, 2013

$$T = T_{\text{cooling water}} (1 + \beta' e^{-\alpha'(t - t_c)}) \quad [10.10]$$

Substitution of the time-dependent temperature profiles (Equations 10.9 and 10.10) into the expression for the degree of sterility over the entire sterilisation period (Equation 10.7) yields, after integration, the analytical solution in terms of k_{d_0}, E, R, α, β, T_{steam} and $T_{\text{cooling water}}$.[6] This approach requires operating data (temperatures of the steam and cooling water), equipment parameters (heat transfer coefficient and transfer area), thermodynamic data (specific heat of the medium) and kinetic constants. Moreover, it is relatively cumbersome to execute.

In view of the complexity of the mathematical solution, a simplified approach which makes use of graphical integration is often preferred. In this approach, the heating and the cooling periods are assumed to consist of a series of small time steps, each at a constant temperature equal to the temperature at the midpoint of the time step. The constant temperature assumption allows the sterility achieved in each time step to be calculated in an analogous manner to that for the holding period (Equation 10.8).

If constant time steps are used for each of the heating and cooling periods, the calculation is simplified further. For instance, if the heating period is divided into equal time steps of t_{heat} each with a corresponding temperature at its midpoint of say T_1, T_2, T_3, then the degree of sterilisation during the heating period can be evaluated from Equation 10.11. Similarly, the degree of sterilisation during the cooling period can be evaluated from Equation 10.12 where t_{cool} is the time of each time step in the cooling period with corresponding midpoint temperatures of say T_4, T_5, T_6. The sterilisation taking place in these heating and cooling periods, when combined with that achieved during the holding period at constant temperature (Equation 10.8), constitute the

Published by Woodhead Publishing Limited, 2013

combined degree of sterilisation for the entire sterilisation period, as presented in Equation 10.13.[7]

$$\left[\ln\frac{N_0}{N}\right]_{heating} = k_{d_0}\left[e^{-\frac{E}{RT_1}} + e^{-\frac{E}{RT_2}} + e^{-\frac{E}{RT_3}} + \cdots\right]t_{heat} \qquad [10.11]$$

$$\left[\ln\frac{N_0}{N}\right]_{cooling} = k_{d_0}\left[e^{-\frac{E}{RT_4}} + e^{-\frac{E}{RT_5}} + e^{-\frac{E}{RT_6}} + \cdots\right]t_{cool} \qquad [10.12]$$

$$\left[\ln\frac{N_0}{N}\right]_{overall} = k_{d_0}\left[e^{-\frac{E}{RT_1}} + e^{-\frac{E}{RT_2}} + e^{-\frac{E}{RT_3}} + \cdots\right]t_{heat} + k_{d_0}e^{\frac{-E}{RT}}(t_c - t_h) + k_{d_0}\left[e^{-\frac{E}{RT_4}} + e^{-\frac{E}{RT_5}} + e^{-\frac{E}{RT_6}} + \cdots\right]t_{cool} \qquad [10.13]$$

The accuracy of this method is acceptable, especially if small time steps are chosen. A shortcut which will reduce the calculation time even if very small time steps are used is to incorporate only those temperatures which are over 100°C (since k_d at temperatures below 100°C will be negligible). The only real disadvantage to this method is that the heating and cooling data needs to be available.[8] If these data are not available, they can be approximated by a curve fit based on historical data, or by a linear curve fit of say 1°C per minute, but this may compromise the overall accuracy somewhat.

This method, therefore, provides an uncomplicated methodology for calculating the required holding period at a specified temperature in order to meet the sterility specification. Alternately, using this method, the temperature required to meet the sterility specification can be calculated for a stated holding time. Since the holding time and the temperature are inversely proportional, equivalent degrees of sterility can be achieved either with a high sterilisation

temperature held for a short time (termed HTST sterilisation) or with a low sterilisation temperature held for a long time (termed LTLT sterilisation).

The choice between HTST sterilisation and LTLT sterilisation is based on the degree of degradation of the heat labile components in the medium. The degree of thermal degradation of compounds for equivalent sterilisation by the HTST and LTLT sterilisation methods can be assessed by comparing the dependence of the thermal death and degradation rate constants (k_d and k_d^* respectively) on temperature.

Both k_d and k_d^* follow Arrhenius-type behaviour (Equation 10.4) where activation energies can be assigned to each (E and E* respectively). However, E* is significantly lower than E which results in the E*/R gradient associated with thermal degradation being lower than the E/R gradient associated with thermal death (Figure 10.2). As a consequence, k_d is greater than k_d^* at high temperatures (low 1/T) and less than k_d^* at lower temperatures (high 1/T). This implies that at a high temperatures, less degradation will take place than

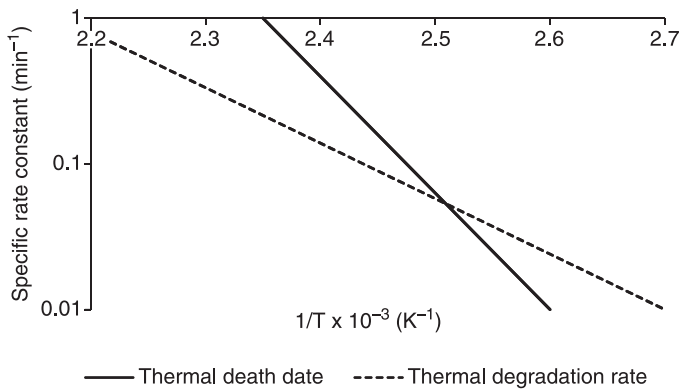

Figure 10.2 Dependence of thermal death and degradation rates on temperature

Published by Woodhead Publishing Limited, 2013

at a lower temperature for the same degree of sterilisation. Consequently, HTST sterilisation is the methodology that will best conserve the nutritional integrity of the nutrient medium.

10.1.3 Continuous sterilisation

Continuous sterilisers consist of a single pipe or multiple pipes in parallel through which the medium is pumped at the sterilisation temperature. Heating is accomplished either by direct steam injection or by indirect heat exchange.

In the case of continuous sterilisation by direct steam injection, the heating of the medium to the sterilisation temperature is almost instantaneous. Cooling of the hot medium after sterilisation takes place by flash vaporisation, similarly almost instantaneously.

Indirect heat exchange is typically carried out by two heat exchangers in series on each end of the steriliser. The medium at room temperature is heated initially via heat exchange with the hot medium exiting the steriliser, and subsequently via heat exchange with steam to the sterilisation temperature. This second heat exchanger also serves to cool the exiting hot sterile medium which, if necessary, undergoes further heat exchange with cooling water to the operating temperature.

Both the direct and indirect methods provide such fast heating and cooling that the heating and cooling periods can be neglected in terms of their effect on both thermal death and thermal degradation. Under continuous sterilisation conditions then, the time of heating and cooling is insignificant and the time at which the medium is held at the sterilisation temperature constitutes the total sterilisation time.

Published by Woodhead Publishing Limited, 2013

Continuous sterilisation then, is the epitome of the HTST method where the nutrient degradation is minimised for any specified degree of sterilisation. This is the basis of the process for milk sterilisation which extends the shelf-life considerably further than that of pasteurised milk.[9] Typically the milk is held at a temperature in the range of 130°C to 150°C for up to 30 seconds during which time the sterilisation takes place. At this temperature, the thermal degradation rate constant is much lower than the thermal death rate constant, comparatively little degradation takes place in this short time and the nutrient value of the milk is maintained.[10] A small degree of caramelisation does take place, however, resulting in a slightly altered taste from that of pasteurised milk.

During continuous sterilisation, as with batch sterilisation, the total sterilisation time required to reach the specified degree of sterilisation needs to be quantified. This is readily calculated from the ratio of the total pipe length to the velocity of the medium in the pipes. However, fluid flow in pipes experiences axial dispersion which means that the velocity of the medium in the pipes will differ depending on its radial position in the pipe. Maximal velocity will be experienced at the centre of the pipe but will decrease with position towards the pipe wall. This velocity gradient means that the medium near the centre of the pipe will have a shorter than average residence time in the pipe while the medium closer to the edges will have a longer than average residence time in the pipe. Consequently the design cannot simply be based on an average velocity because the elements near the centre will not be sufficiently sterilised while those at the edges will be over sterilised.

Clearly a design which does not enable the fluid elements at the centre to be subjected to the required sterilisation time is flawed as the specified sterilisation criterion will not be

Published by Woodhead Publishing Limited, 2013

met. However, the option of increasing the sterilisation time to account for the fluid elements moving at the maximum velocity is likewise flawed. Under these circumstances, all fluid elements moving with a velocity lower than average will be held at the sterilisation temperature for a time longer than is necessary to effect the specified degree of sterilisation. Thus all these fluid elements would have undergone a degree of thermal degradation above that which is necessary for efficient sterilisation.

In order to ensure efficient sterilisation of all the fluid elements, while at the same time minimising the effects of thermal degradation, it is imperative that the magnitude of the axial dispersion be quantified and taken into account in the calculations. This is particularly important at Reynolds numbers associated with laminar flow where axial dispersion results in a parabolic velocity profile with a maximum velocity twice that of the average. In turbulent flow, the effect of axial dispersion is less and the velocity profile is flattened. As plug flow is approached, the maximum velocity is only about 1.2-fold of the average velocity.

To account for the variations in sterilisation times, a dispersion model is used. The model is developed by executing a mass balance on a differential fluid volume, of length dx, in continuous steriliser with a uniform cross-sectional area. Microorganisms enter and leave the differential volume by convective flow and by diffusive (axial dispersion) flux. During the time spent in the differential volume, the number of viable microorganisms decreases by dN. The process is assumed to take place at steady state (i.e. no accumulation in the system) and the mass balance solved with the appropriate boundary conditions. The solution to the model is organised in terms of the dimensionless Péclet (Pe)[11] and Damköhler (Da)[12] numbers where $Pe = \bar{u}L/D_z$[13] and $Da = k_dL/\bar{u}$ (Equation 10.14), where δ is given by

Published by Woodhead Publishing Limited, 2013

Equation 10.15.[14] This equation predicts the fractional degree of sterilisation $\left(\frac{N}{N_0}\right)$ as a function of the extent of cell destruction (Da) and the extent of axial dispersion (Pe).

$$\frac{N}{N_0} = \frac{4\delta e^{Pe/2}}{(1+\delta)^2 e^{\delta Pe/2} - (1-\delta)^2 e^{-\delta Pe/2}} \quad [10.14]$$

$$\delta = \sqrt{1+\frac{4Da}{Pe}} \quad [10.15]$$

When axial dispersion is negligible, $D_z \rightarrow 0$, Pe $\rightarrow \infty$ and perfect plug flow is approached. Under these conditions, Equation 10.14 reduces to Equation 10.16 where $L/\bar{u}$ is the average residence time in the pipe. Thus this equation predicts the degree of sterilisation based purely on the average residence time and is analogous to that predicting the degree of sterilisation during the holding time in a batch sterilisation process (Equation 10.8). In reality, however, Pe falls mainly between 10 and 1000 and real flow behaviour has to be taken into account.

$$\frac{N}{N_0} = e^{-Da} = e^{-k_d L/\bar{u}} \quad [10.16]$$

The solution to the equation is traditionally depicted graphically on a semi log scale with $\frac{N}{N_0}$ on the y-axis, Da on the x-axis and Pe as the third parameter (Figure 10.3). This graphical representation shows that as plug flow is approached (Pe $\rightarrow \infty$), the length of piping, and hence the residence time, decreases for the same degree of sterility. Further, as the degree of sterility required increases, the effect of the deviation from plug flow on the increase in length of piping, or residence time, is enhanced. Since very high degrees of sterilisation are normally required (say 99%), this fact

Published by Woodhead Publishing Limited, 2013

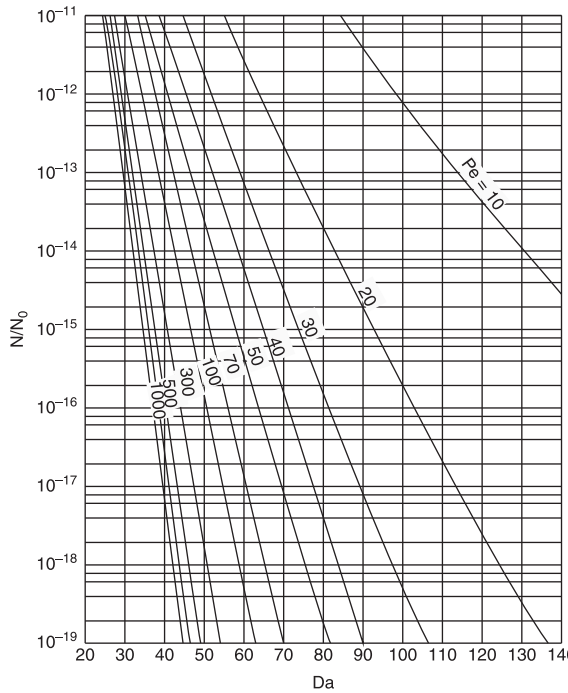

Figure 10.3 **Thermal destruction of contaminating microorganisms as a function of the extent of destruction and extent of axial dispersion (Reprinted from *Biochemical Engineering*, 2nd edition, Alba, Humphrey and Millis, University of Tokyo Press (1973))**

highlights the importance of the incorporation of the axial dispersion of flow on the design of the steriliser.

10.2 Filter sterilisation of air

Sterilisation of air is ubiquitously carried out by filtration. Deep bed filtration is by far the preferred mechanism of air sterilisation although absolute filtration may be carried out in laboratory scale operations.

Published by Woodhead Publishing Limited, 2013

Absolute filtration refers to filtration where the pores of the filter are smaller than the size of the microorganism which is to be filtered, typified by membrane filtration. This method is effective but does present with a relatively high pressure drop and, therefore, suffers from a low capacity. Further, membranes do tend to block when wet, a situation that could easily arise with unexpected foaming. Blocked membranes will result in a sharp increase in pressure drop and pressure build up inside the reactor, a situation which may become hazardous.

Deep bed filtration refers to filtration through the spaces between fibres. The fibres are about the same size as the microorganisms which are to be removed (diameters of about 5 to 30 microns) and are made from a number of materials, often glass fibre. These fibres are packed to form a highly porous bed where the porosity could be as high as 90%. The high voidage allows microorganisms to build up in the filter bed without increasing the pressure drop. So deep bed filtration has a much higher capacity than that of absolute filtration. The high voidage also renders this filter type less likely to present problems should inadvertent wetting occur.

The spaces between the fibres through which the air passes are much larger than the microorganisms to be filtered and may have pseudo diameters of as much as 100 to 200 microns. Although the spaces between the fibres are two orders of magnitude greater than the size of the microorganisms, the filter is designed so that it is deep enough for the probability of the microorganism being trapped to be very large, assuming that all microorganisms that come into contact with a fibre will adhere to that fibre.

Filter design is based on the so-called log penetration model. This model facilitates prediction of sterilisation in

Published by Woodhead Publishing Limited, 2013

terms of $\ln\frac{N_0}{N}$,[15] for a specified bed length, volume fraction of fibres, fibre diameter and efficiency of removal. The model is developed by considering a volume element of the bed of unit cross-sectional area and depth dz. The number of fibres of unit length in this volume element is given by Equation 10.17, where α is the volume fraction of fibres.

$$\frac{\text{total volume of fibres of unit length}}{\text{volume of one fibre of unit length}} = \frac{\alpha\, dz}{\pi d_f^2 / 4} \qquad [10.17]$$

The volume in the element that is totally cleared by the fibres in that element can now be defined as Equation 10.18 where b is the volume totally cleared by one fibre.

$$V_{cleared} = \frac{b\alpha\, dz}{\pi d_f^2 / 4} \qquad [10.18]$$

Thus the fractional change in number of microorganisms in this element (–dN) is expressed as Equation 10.19.

$$-dN = \frac{Nb\alpha\, dz}{\pi d_f^2 / 4} \qquad [10.19]$$

Since the efficiency of removal, η, is defined as b/d_f, Equation 10.19 can be written as Equation 10.20.

$$-\frac{dN}{dz} = \frac{4\eta\alpha N}{\pi d_f} \qquad [10.20]$$

Since η, α and d_f are constants, integration of Equation 10.20 yields Equation 10.21 which is known as the log penetration model (or law).

$$\ln\frac{N_0}{N} = \frac{4\eta\alpha L}{\pi d_f} \qquad [10.21]$$

The log penetration model facilitates the prediction of the length of bed necessary to achieve a specified sterility level, or conversely, the sterility achieved from a set length of bed.

While the mechanism of sterilisation by absolute filtration is based purely on size exclusion, that of sterilisation by deep bed filtration is regarded as a combination of inertial impaction, direct interception and Brownian diffusion. Inertial impaction occurs when the microorganism deviates from the streamline to impact on the fibre. The microorganism will deviate from the streamline since its density, and therefore its inertia,[16] is greater than that of an equivalent volume of air, making it more difficult to deflect around the fibre. This inertial impaction mechanism tends to dominate at higher air velocities and with larger microorganisms. With smaller microorganisms, the mechanism of direct interception predominates over that of inertial impaction. Here the density of the microorganism is negligible so theoretically the microorganism has no inertia and will follow the streamline as it deflects around the fibre. Thus, if the streamline is within half the diameter of the microorganism from the fibre, the fibre will intercept the microorganism. Very small microorganisms (less than 1 micron) will also exhibit Brownian motion especially at low air velocities, causing them to move randomly along the streamline and increasing the chance of contact with the streamline.

The changes in predominance of the mechanisms of removal in the deep bed filter result in differences in the efficiency of removal as the velocity of air flow and size of microorganisms vary. At low velocities, diffusion and interception mechanisms are predominant so efficiency of removal is decreased with increasing velocity. On the contrary, at high velocities, the inertial impaction mechanism is predominant, so efficiency of removal is increased with

Published by Woodhead Publishing Limited, 2013

increasing velocity. Consequently there exists a minimum removal efficiency at the velocity which correlates to a changeover of the controlling mechanism. This behavioural trend is independent of the size of the microorganism although the absolute values of the removal efficiency will alter with microbial size. A decrease in microbial size will increase removal efficiencies at low velocities and decrease removal efficiencies at high velocities such that the velocity corresponding to the minimum removal efficiency will shift to a lower value as the microbial size is increased.

Accordingly, there is an air flow velocity, specific for each microbial size, at which the deep bed filter operates at minimum efficiency. As it is not possible to control the size of the microbial contaminants, a range of velocities corresponding to minimum efficiencies spanning the range of possible microbial sizes should be defined so that the velocity for high efficiency can be chosen. Nevertheless, in practice, the choice of a high or a low velocity may depend largely on the process economics. For a particular air flow rate, a smaller filter will have a higher velocity compared with a larger filter. While the smaller filter requires a smaller capital investment, it will have a higher pressure drop and, therefore, a higher operating cost. The larger filter, on the contrary, will have a comparatively lower flow rate, thus incurring a lower operating cost, but will require a larger capital outlay.

10.3 Notes

1. Enzyme denaturation occurs more easily in the hydrated form than in the unhydrated form.
2. Reactions occur between carbonyl groups of reducing sugars and amino groups of amino acids.
3. For instance, cells in the exponential growth phase exhibit greater wall permeability than cells in the

Published by Woodhead Publishing Limited, 2013

stationary phase; this may result in different heat transfer characteristics.

4. The Arrhenius equation is used extensively in both chemical and biological kinetics to describe the effect of temperature on reaction rate.
5. Typically 50–100 kcal/mol.
6. The solution is discussed conceptually with key mathematical expressions. A detailed derivation is not provided.
7. Recall: T is the sterilisation temperature and $(t_c - t_h)$ the time of the holding period.
8. Usually determined experimentally.
9. The acronym UHT seen on milk containers refers to ultra high sterilisation.
10. Pasteurisation takes place at 70°C for about 15 seconds and functions to eliminate pathogens only. Sterilisation at this temperature would necessitate long holding times leading to a serious reduction in the nutrient value of the milk and altered taste.
11. Developed by Jean Claude Eugène Péclet (1793–1857).
12. Developed by Gerhard Damköhler (1908–1944) as a dimensionless reaction rate constant.
13. $\bar{u}$ is the average velocity, L the length of the steriliser and D_z the axial dispersion coefficient.
14. The solution is discussed conceptually with key mathematical expressions. A detailed derivation is not provided.
15. Analogous to the quantification of media sterilisation.
16. A tendency to continue to move in a straight line.

Published by Woodhead Publishing Limited, 2013

11

Downstream processing

DOI: 10.1533/9781782421689.209

Abstract: Downstream processing of biochemical products requires recovery from a complex mixture of molecules, impurities and contaminants by making use of dedicated unit operations. Each unit operation will bring about a physical change that will alter the product concentration and/or degree of purity. Usually, several unit operations in series are necessary to affect the product specifications.

The downstream concentration and purification programme is an integral part of the production process and contributes very significantly to the overall process costs. The actual contribution of the downstream purification programme to the complexity and cost of the entire process depends on the nature of the product and its concentration in the reactor at harvest. Dilute speciality products typically incur high purification costs which may range from 50% to 90% of the total production costs.

Products which are produced in low concentrations, such as vitamins (e.g. vitamin B_{12}, a few mg/L) require processing of large volumes per mass of product, thereby necessitating large process equipment for purification, with concomitantly high capital and operating costs. The low concentrations also mean that more recovery steps are needed, with attendant cumulative losses. Further, processing of speciality products may require costly processing in dedicated equipment, e.g. chromatography,

Published by Woodhead Publishing Limited, 2013

to achieve the level of purification required. Many of these speciality products are labile so the range of purification operations is limited and less costly options may not be suitable.

It is the responsibility of the Bioprocess Engineer to set up and configure an appropriate series of separation, recovery, concentration and purification unit operations to meet the product specifications. This requires, in the first instance, a thorough understanding of the mechanisms underpinning the function of each of the unit operations. In addition, it requires knowledge of the chemical and physical properties of the product so that an informed choice of unit operations that best exploit these physical properties can be made in order to affect concentration and/or purification. Finally, an appreciation of the final product application is necessary for the judicious choice between different unit operation options. For instance, a protein which is to be used as a biocatalyst will be required to retain its biological activity and unit operations which necessitate temperatures and pH values that would denature the enzyme and render the product useless. Overall, the Bioprocess Engineer needs to design a recovery programme that can meet product specifications in as few steps as possible. Not only does this reduce downstream processing capital and operating costs, but importantly, reduces product losses which accumulate with each step.

In Chapter 11, several unit operations common to bioproduct concentration and purification are described and their functionality with reference to labile bioproducts discussed.[1] Specific challenges related to maintaining the integrity of labile products (such as biologically active enzymes) will be highlighted. Conceptual designs of recovery programmes will be detailed for cell-associated products and for products excreted from the cell. Recovery programmes for products requiring different levels of purification will be discussed.

Published by Woodhead Publishing Limited, 2013

Key words: solid–solid separation, cell disintegration, precipitation, membrane separation, liquid extraction, chromatography, electrophoresis.

11.1 Overview of potential recovery operations

The unit operations which are used to recover bioproducts include those which facilitate disintegration of solids, separation and recovery of solids and liquids, recovery of soluble molecules and the so-called finishing operations which include processes such as drying and crystallization.

Each of these is described and evaluated with reference to the overview of the potential recovery steps as outlined in Figure 11.1.

The first consideration in a recovery programme is undoubtedly to optimise the product yield in the upstream process. A high product concentration entering the recovery programme reduces the number and size of the downstream processing operations and the associated recovery costs.

The first physical step in the recovery process is to separate the cells and the extracellular fluid (Section 11.2) so that the relevant stream can be processed for recovery of the product. The subsequent steps in the programme will differ depending on whether the solid or the liquid stream enters the process.

If the product is solubilised in the liquid stream, recovery of the liquid stream is carried out by unit operations designed to concentrate and purify a soluble molecule (Section 11.4). It is advisable to conduct those unit operations which afford some degree of concentration first so that the subsequent purification steps can be carried out with less material. This is especially important during the recovery of specialised biomolecules which require expensive equipment

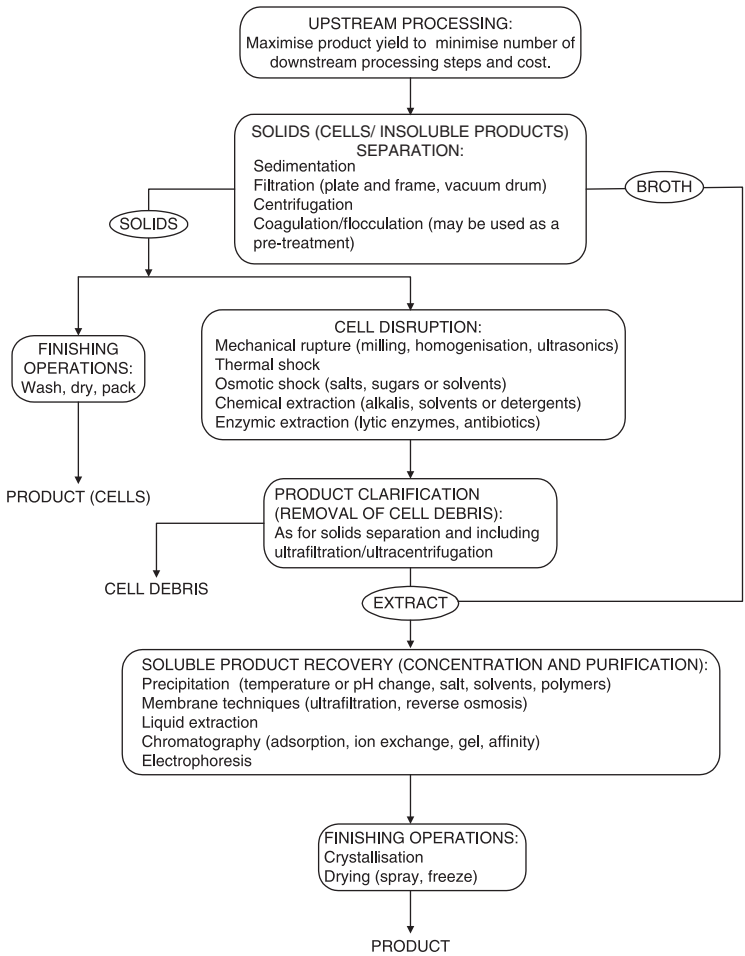

Figure 11.1 Recovery of microbial products: an overview

(e.g. certain types of chromatography) to meet the high purity specifications.

For a product that is associated with the solid stream, either within the cytoplasm or adhering to the cell surface, initial operations to extract the product have to be conducted before purification can take place. This requires disintegration of the cell and subsequent separation of the cell extract from

Published by Woodhead Publishing Limited, 2013

the cell debris (Section 11.3). The cell extract then enters one or more of the processes designed to concentrate and purify a soluble molecule (Section 11.4). Of course, if the product is the cells themselves (e.g. *S. cerevisiae* and *S. carlsbergensis* destined for the food and beverage industries), only finishing operations such as drying are required.

11.2 Separation of cells and extracellular fluid

Separation of the cells and extracellular fluid can be carried out by one of several standard solid–liquid separation operations, the most common being filtration and centrifugation with gravity sedimentation generally being used only in sewage treatment. The choice between filtration and centrifugation depends on the properties of the cells and of the fluid. Solid properties that influence this decision include particle diameter, density and mechanical strength while the fluid properties exerting the main influences are viscosity and density.

Filtration is widely used in the bioprocess industry, with both batch filtration and continuous filtration finding several applications. Continuous filtration is practised with large scale separation of cells, such as in the production of *Saccharomyces* spp., usually with the vacuum drum filter. This consists of a drum which rotates in a trough of cell suspension and which draws the cells onto the drum surface under constant presure conditions (vacuum). In this manner, a cake of cells is formed on the drum surface as it exits the trough. The filter cake is removed by a blade[2] or a string for further processing or discarding, whichever applies.

Batch filtration is also practised but for smaller scale operations, with the chamber press being the usual choice of

Published by Woodhead Publishing Limited, 2013

filter. This filter press consists of a series of chambers separated by filter plates, clamped together in a frame. The cell suspension is fed into the chambers under pressure and the cells are deposited as a filter cake on the filter medium as the filtrate moves through the filter press. Batch filtration can be conducted under constant pressure (in which case the filtration rate decreases with time), constant filtration rate (in which case the pressure increases with time) or variable pressure and variable rate.

The efficiency of filtration for an incompressible filter cake is dependent on the filter area (A), the specific cake resistance (r_c),[3] the pressure drop across the filter medium and filter cake (ΔP), and the viscosity of the fluid (μ). The rate of filtration $\left(\frac{dV}{dt}\right)$ can be predicted from the Carman-Kozeny equation[4] which relates this rate to the pressure drop across the filter medium and cake (Equation 11.1), where L is the thickness of cake equivalent to the medium resistance.

$$\frac{1}{A}\frac{dV}{dt} = \frac{\Delta P}{r_c \mu (1+L)} \qquad [11.1]$$

The time taken to deliver a certain volume of filtrate (V) under constant pressure or constant rate conditions is obtained by integration of Equation 11.1. Integration with constant ΔP yields Equation 11.2 (this applies to both batch and continuous operation) while integration with constant $\frac{dV}{dt}$ yields Equation 11.3. These expressions allow for the calculation of, for example, the time of filtration for a specified volume, for each mode of operation.

$$\frac{t}{V} = \frac{r_c \mu V}{2A^2 \Delta P} + \frac{r_c \mu L}{A \Delta P} \qquad [11.2]$$

$$\frac{V}{t} = \frac{A \Delta P}{r_c \mu (1+L)} \qquad [11.3]$$

Published by Woodhead Publishing Limited, 2013

When operating under conditions where pressure varies, the filter cake may compress as the pressure is increased. Compressibility is a major problem which leads to a decrease in voidage and a corresponding increase in the specific cake resistance, with a concomitant increase in pressure drop and reduced filtration rate. The dependence of specific cake resistance has been determined empirically to follow a power function (Equation 11.4) where r_0 and s[5] are empirical constants.

$$r_c = r_0(\Delta P)^s \qquad [11.4]$$

Despite the wide usage of filtration as a means to separate cells in the bioprocess industry, it would be wise to largely avoid this operation for separation of prokaryotes because solids with such small diameters tend to result in the formation of a compressible filter cake. Cells with low mechanical strength also tend to be compressible and are probably not suitable for separation by filtration for the same reason. In addition, filtration should also not be considered for separation of cells with slime layers, which reduces filtration rate essentially by blockage of the pores, unless harvesting can be carried out before the slime layer has formed.[6] An interesting example of this is the successful separation of the *Penicillium* mycelia by filtration during penicillin production; the mycelia are simply harvested prior to the onset of slime accumulation.

To some extent the effect of compressibility can be overcome with the use of a filter aid.[7] Filter aids prevent blockage of filter medium pores and improves porosity of cake but contaminates the solid product so cannot be used in processes where the product is associated with the cells.

For most prokaryotes, and cells which for other reasons would tend to form a compressible cake, centrifugation remains the separation operation of choice provided that the

density difference between the microorganism and the fluid is sufficient. This is not to say that centrifugation is only used for prokaryotes. In fact, it can be used for particles of 0.1–100 μm diameter and is particularly widely used for yeast, especially where a concentrated yeast cream is desired.

Centrifuges are operated continuously to separate cells from liquid by means of centrifugal force. In practice, centrifuges comprise a tubular bowl or a disc stack bowl in which the cells are pelletised towards the botom of the bowl and the fluid is removed from the top of the bowl. Centrifugation also has the advantage that it can be used if aseptic separation is required, which is not possible with separation by filtration.

The efficiency of centrifugation is dependent on the density difference between the solid (ρ_s) and the liquid (ρ_l), the dynamic viscosity (η), the diameter of the particle (ϕ_p), the angular velocity (ω) and the radius (r). The velocity of sedimentation in a centrifugal field (v) is described by Equation 11.5.

$$v = \frac{\phi_p^2(\rho_s - \rho_l)r\omega^2}{18\eta} \qquad [11.5]$$

On the other hand, separation by gravity rather than by centrifugal force (gravity sedimentation) is only used in specialised cases as the terminal settling velocities of microorganisms are too low to permit sufficient settling within a reasonable time. The most obvious case is in the biological treatment of domestic waste, where the microbes form microbial masses or flocs.[8] Here effluent clarification (i.e. purification of the product) takes place in gravity settlers where the higher terminal settling velocities of these microbial flocs enable efficient settling by gravity.

In the case of non-flocculating organisms, gravity sedimentation would only become an option if the terminal

Published by Woodhead Publishing Limited, 2013

falling velocity was increased, say by adding chemical coagulants[9] to form microbial flocs. Addition of flocculants[10] to form loose aggregates from the flocs would further increase the settling during gravity sedimentation. Coagulation and flocculation can likewise be combined with filtration and centrifugation to improve the potential for efficient separation. However, this approach potentially adds unwanted substances to the cells and would normally only be feasible if the product resided in the extracellular fluid.

11.3 Cell rupture and separation of cell extract

Intracellular products are recovered from the cell by a process of cell rupture and separation of the extract from the resulting cell fragments. Cell rupture is carried out by means of one of three types of procedures: mechanical rupture, non-mechanical rupture or a combination of mechanical and non-mechanical rupture.

Mechanical rupture by grinding or milling with abrasive ceramic beads is one of the most common and successful disintegration methods on the large scale.[11] A drum partially filled with beads and cell suspension rotates on a horizontal axis (typically at 6000 rpm) and the cells are ruptured by abrasion and attrition as they come into contact with the beads. Possibly the only drawback to this process is the frictional heating of the cell suspension which would adversely affect the properties of a heat-labile product such as enzymes. This is solved by the incorporation of a jacket around the drum through which cooling water is passed to keep the suspension below that which would harm the product.

High pressure homogenisation is another well used method of mechanical cell rupture, which in most cases can be scaled

Published by Woodhead Publishing Limited, 2013

up while retaining good efficiencies.[12] Here the cell suspension is forced through a narrow valve at high pressure (up to 10^5 kPa) where shear forces break up the cells. Control of the valve pressure enables regulation of the degree of cell rupture. Practical challenges associated with this methodology relate mainly to cooling of the valve head,[13] and valve seat replacement.

Other means of mechanical rupture are restricted to laboratory scale use. For example, ultrasound, a rapid and efficient method of cell rupture used extensively in laboratory scale applications, is unsuitable for large scale operation. During sonification, about 20 Hz is translated into oscillations of a titanium tip, thereby creating microbubbles. Implosion of the microbubbles causes shock waves, resulting in pressure changes which break the cells. The concomitant increase in temperature, however, is difficult to control, thus limiting the potential for scale up.

Non-mechanical rupture incorporates physical, chemical and biological methodologies. The most common physical method is based on inducing a phase change in the cell suspension. A frozen cell suspension is pushed through an orifice resulting in pressure and temperature changes which induce a change in the phase and correspondingly, in the crystal structure. Changes in crystal structure cause cell rupture. Generally this method is suitable for small scale applications only. Other physical methods include rupture of cell walls via osmotic shock using buffers, solvents or sugars or thermal shock during which cells are ruptured by ice crystals. Osmotic shock has particular applicability for the release of periplasmic enzymes.

Chemical and biological cell rupture, while effective, have limited applicability. Chemical extraction, mediated through lytic agents such as alkalis, solvents and detergents which dissociate or solubilise cell walls, may be too aggressive for

Published by Woodhead Publishing Limited, 2013

most products. Biological rupture by lytic enzymes which hydrolyse polysaccharides in the cell wall or by antibiotics which interfere with cell wall synthesis are effective but limited to specific products and are often expensive. The potential exists, however, to innovatively combine different cell disintegration methods, e.g. antibiotics and osmotic shock.

Once the cells are disrupted, the cell debris still has to be removed from the cell extract. Solid–liquid separation operations (Section 11.2) are employed, particularly those that are able to separate the fragmented cell debris with particle sizes of less than a micron. So in terms of conventional separating operations, centrifugation is preferred over filtration. However, ultrafiltration and ultracentrifugation with g forces up to 10^6 are often ideal options.

11.4 Concentration and purification of soluble products

Recovery of the soluble product, whether obtained directly from the extracellular fluid or from an extract of the cellular contents, can be achieved through a range of unit operations. Each of these operations exploits a specific characteristic of the product which facilitates its separation from the unwanted constituents. Most commonly, these characteristics are molecular size, solubility and ionic charge.

Product recovery typically requires a combination of unit operations. Since product losses occur with each operation, the downstream recovery programme should be designed to minimise the number of unit operations required to meet product specifications. This involves not only the correct choice of operations to optimise efficiency of product recovery in each operation, but also the most efficient

organisation of the individual operations in the recovery programme. For instance, unit operations which afford some measure of concentration should be preferably introduced as an early rather than late step in the programme. This reduces the processing volume and hence the size of equipment with concomitant reduction in both capital and operating costs.

The unit operations most frequently employed to recover soluble bioproducts include precipitation, membrane separation, liquid extraction and chromatography. Precipitation and liquid extraction exploit the difference in solubility between the product and unwanted constituents, while membrane separation exploits the difference in molecular size. The specific characteristics exploited in the chromatographic techniques depend on the particular chromatography involved. Ion exchange chromatography, for instance, exploits the difference in ionic charge, gel chromatography exploits the difference in molecular size and affinity chromatography exploits the difference in an affinity for a particular molecule (e.g. antigen or co-substrate). An additional technique, electrophoresis, exclusive to bioproduct recovery, is used to separate proteins on the basis of their different electrical charge.

Generally most recovery processes will have some degree of both concentration and purification even if purification specifications are not necessarily high; these recovery programmes may include one or more of the following: precipitation, membrane separation and liquid extraction. A higher purity specification may need more selective fractionation techniques such as affinity chromatography. Ultimately, the degree of purity specified needs to be matched to its marketable use to optimise the cost of product recovery. As an example, the complexity and cost of recovery of the enzyme glucose oxidase will be dictated by its end use: a diagnostic tool in the pharmaceutical industry for analysis of

Published by Woodhead Publishing Limited, 2013

blood glucose, or an enzyme added to food to delay rancidity by eliminating oxygen in packaging.

11.4.1 Precipitation

Precipitation is mainly used for the concentration and separation of a protein mix from other products or for separation of different proteins, in which case it is called fractional precipitation. However, in the context of biological processing, precipitation is not used in the conventional sense as in precipitation of crystal structures. Rather, it refers to precipitation of an amorphous mass which has a reduced solubility relative to the other components in solution.

The solubility of a protein is governed by environmental conditions (pH, temperature, salt concentration, etc.) and the properties of the protein (shape, charge, hydrophobicity, etc.). This means that the environmental parameters can be adjusted to decrease the solubility of the protein and effect its precipitation. Fractional precipitation, the separation of individual proteins from a mix of proteins, is made possible by the fact that different proteins have different properties and, therefore, different solubilities in a specific environment.

Precipitation can be induced in one of several ways. If biological activity of the protein is not a factor, precipitation can be induced through protein denaturation via an increase in temperature or a change in pH. Temperatures above 60°C denature most proteins so a rise in temperature to above this value will lead to protein precipitation through denaturation. This is a useful method for removing unwanted proteins.

A change in pH changes the number of ionised groups associated with the surface of the protein, thus altering the electrostatic forces. At its isoelectric pH, the protein has its lowest net charge and the repulsive forces are absent. This leads to hydrophobic interaction, aggregation and

precipitation. Different proteins have different acid and base groups and, therefore, different isoelectric pH values. This concept can be exploited for fractionation of proteins within a protein mixture.

If biological activity is to be maintained, precipitation can be carried out by the addition of a salt, or less often by addition of non-ionic polymers, polyelectrolytes, water miscible solvents or metal ions. Salt precipitation, traditionally referred to as the 'salting out' technique, is most commonly carried out by the addition of ammonium sulphate because of the wide solubility range and low cost of this salt, although potassium and sodium phosphate are also used to a lesser extent. Salts with higher ionic strengths are favoured because solubility decreases logarithmically with increased ionic strength (empirically verified). This relationship, known as the 'salting out' equation, is defined in terms of a 'salting out' constant, K_s, which is a function of the pH, temperature, salt moiety and type of protein, and an empirical constant, B (Equation 11.6).

$$\log \text{solubility} = B - K_s [\text{ionic strength}] \qquad [11.6]$$

Caution should be exercised with this empirical relationship, however, as it does not apply to all salts. For instance, sodium chloride has been shown to increase solubility with increasing ionic strength at low salt concentrations.[14] The mechanism underpinning this phenomenon is not very well understood but may be related to the removal of the water of hydration from the protein surface by the ions. The hydrophobic groups of the protein are thus exposed and interact with hydrophobic groups on other molecules, leading to aggregation.

Precipitation by the addition of non-ionic high molecular weight polymers (e.g. polyethylene glycol (PEG) or dextran) is particularly useful for labile products. The decrease in

Published by Woodhead Publishing Limited, 2013

solubility with increasing polymer concentration follows an equation analogous to the 'salting out' equation (Equation 11.7). The mechanism in this case is said to be related to the polymers causing the proteins to approach one another and aggregate.

$$\log \text{solubility} = B' - K'_s\,[\text{polymer concentration}] \quad [11.7]$$

Ionic polymers (polyelectrolytes) will also cause protein precipitation if the polyelectrolyte and the protein have opposite charges. The electrostatic interaction between opposite charges neutralises the charge and so allows aggregation and precipitation to occur.

The decrease in solubility with increasing concentration of water miscible organic solvents (e.g. ethanol, acetone) likewise follows an empirical relationship analogous to the 'salting out' equation, where D_m is the dielectric constant of the mixture (Equation 11.8). Organic solvents decrease the dielectric constant, i.e. they increase the electrostatic force of attraction, thereby decreasing the solubility by allowing proteins to react more readily with one another than with water. The tendency of the solvent to denature the protein is, however, a perennial challenge with this method. Usually this is addressed by decreasing the temperature to less than –5°C before adding the solvent.

$$\log \text{solubility} = B'' - K''_s / D_m^2 \quad [11.8]$$

Finally, metal ions can be added as complexing agents, thereby causing the formation of insoluble complexes, e.g. calcium salts of streptomycin and penicillin. This method has a high degree of specificity but also suffers from the potential to denature the product.

Precipitation is often used as an early step as it concentrates as well as affording up to about twenty times purification.

However, it is usually relatively non-specific for one step and the precipitate may contain several proteins in the mixture. Precise fractionation is not always possible even in several steps, especially when proteins have similar solubilities. Moreover, some contamination of the mixture is inevitable. The salt, PEG or other additives have to be removed in a subsequent step (frequently ultrafiltration detailed in Section 11.4.2). Some scale up problems may be experienced in large volumes in which variations in temperature and mixing may precipitate different proteins in different locations in the tank.

11.4.2 Membrane separation

Membrane techniques, specifically ultrafiltration, are widely used for separation of high molecular mass proteins from smaller unwanted constituents on the basis of molecular size. Separation is facilitated by the permeation of smaller molecules through the membrane under applied pressure (500 to 700 kPa) while the larger molecules are retained by the membrane. This method of separation has broad applicability as it can be used to separate large molecules over a wide range of molecular sizes from 2000 to 500 000 Daltons. It is especially appropriate for labile bioproducts, such as enzymes and vaccines, whose recovery requires moderate conditions. A major use of ultrafiltration is the removal of salts added during a protein precipitation operation. Ultrafiltration has the added advantage of providing a measure of concentration as well as purification of the retentate.

In addition to the ultrafiltration membranes used for the retention of large molecules, membranes with considerably smaller molecular weight cut offs are used to retain all molecules other than water molecules, including molecules

Published by Woodhead Publishing Limited, 2013

as small as monovalent salts. Under these conditions, high pressure (3000 kPa to 4000 kPa) is applied to facilitate the permeation of water molecules through the membrane against the osmotic pressure; this process is referred to as reverse osmosis. In the context of product recovery, reverse osmosis is solely a concentration operation, unlike ultrafiltration which facilitates both concentration and purification. Reverse osmosis is used almost exclusively for water purification purposes.

The ultrafiltration and reverse osmosis membranes are very different from the conventional filters used for solid–liquid separation operations. The filters for solids separation comprise symmetric or isotropic pores[15] which are able to separate particles of 10 microns or larger with conventional filtration operations and particles between the range of 1000 angströms to 10 microns with microfiltration operations. The ultrafiltration and reverse osmosis membranes, on the contrary, have asymmetric or anisotropic pores which function as a selective molecular sieve to separate molecules of about 30 to 1000 angströms (ultrafiltration) or about 2 to 50 angströms (reverse osmosis). The separation in these membranes is quantified in terms of a molecular weight cut off, defined as the molecular weight of the solute that is 90% retained by the membrane. Since the membranes have a distribution of pore sizes, the molecular weight cut off is not absolutely sharp. This limits use of ultrafiltration membranes for protein fractionation.

Ease of separation is dependent on the sharpness of the molecular weight cut off. This is measured by a rejection coefficient where the rejection coefficient is the fraction of solute present in the upstream that is rejected by the membrane. Theoretically the coefficient can vary between zero and unity, but in practice, it should be around 0.95 for an efficient separation.

The development of the technology to produce these membranes spans 150 years, culminating with the breakthrough of cellulose acetate membranes comprising an active layer or skin 0.2 to 0.5 microns thick acting as the molecular sieve. The active layer is attached to a porous substructure 125 to 250 microns thick which serves as a mechanical support only. However, the range of operation of cellulose acetate is constrained by temperature (softening at temperatures over 40°C) and pH (hydrolyses at high pH) and this membrane was soon replaced by non-cellulosic membranes, such as polysulphones which can tolerate temperatures up to 75°C and pH values between 1 and 13. More recently, ceramic membranes have been developed and preferred under certain situations for their high resistance and durability.

Ultrafiltration and reverse osmosis membranes operate under a transmembrane pressure drop, where the flux initially increases linearly with increase in pressure drop. As the pressure is increased, the flux of solute to the membrane surface eventually exceeds the flux of solute through the membrane. The rejected solute is then returned to the bulk solution by back diffusion and a build-up of solute between the bulk solution and the membrane surface results. This is called concentration polarisation and is the major drawback of ultrafiltration and reverse osmosis membranes. Concentration polarisation increases the resistance to transfer and the increase in flux with increased transmembrane pressure drop is slowed. Under extreme conditions, concentration polarisation may lead to a slime or gel layer on the membrane surface. At this point, the resistance is so great that an increase in transmembrane pressure drop no longer has any effect on the flux. In this, the so-called gel regime, the transport through the gel layer limits the maximum attainable flux. This is particularly serious at high

Published by Woodhead Publishing Limited, 2013

solute concentrations where the gel regime is reached sooner and at a lower flux. Increasing the transmembrane pressure drop in the gel regime may lead to membrane deformation. In practice, these units are operated at transmembrane pressure drops near the end of the range where flux and pressure drop enjoy a linear relationship. This is often referred to as the critical flux.

Efforts to reduce or eliminate solute build up at the membrane surface have focused on increasing the turbulence at the surface. This is carried out by mechanical agitation or, more frequently, by cross flow filtration. In cross flow filtration, tangential flow is used so that the flow moves parallel to the surface of the membrane while passing through the pores. Tangential flow is mediated through one of several membrane configurations. The hollow fibre cartridge, ubiquitous in water purification by reverse osmosis but with many other applications as well, comprises a number of hollow fibre membranes through which the solution flows along the membrane surface. This configuration has the advantage of high surface to volume ratio but is susceptible to plugging. The plate and frame arrangement has a lower surface to volume ratio but is less susceptible to plugging than the hollow fibre device. Spiral cartridges also have a type of plate and frame arrangement but are wound in a spiral which increases the surface to volume ratio. In general, the end purpose will dictate the best specific arrangement of the membranes.

11.4.3 Liquid extraction

Solvent extraction is the most well established liquid extraction operation; this relies on the preferential solubility of the product in an added organic phase, immiscible with the aqueous phase. The efficiency of solvent extraction,

measured in terms of a distribution coefficient which relates the concentrations of the solute in the different phases, depends largely on the suitability of the solvent. A high distribution coefficient indicates preferential solubility in the solvent and hence good separation.

Solvent extraction with amylacetate as the solvent has been used successfully to recover penicillin. Efficient recovery is made possible because penicillin exists as a salt at high pH and an acid at low pH. The salt is preferentially soluble in the aqueous phase and the acid preferentially soluble in the organic (amylacetate) phase which facilitates transfer of penicillin between the aqueous and organic phases simply by altering the pH. During the penicillin recovery process, acid is initially added to the entering crude aqueous stream to promote extraction into amylacetate on contact. Since prolonged contact with amylacetate is detrimental to the penicillin product, alkali is then added to the amylacetate extract and the penicillin salt is extracted into water. Penicillin degradation is minimised during this process through the use of centrifugal extractors which minimise the contact time between the penicillin and the amylacetate. The entire solvent extraction process from start to re-entry of the penicillin into the final aqueous phase can be less than two minutes.

Solvent extraction is, however, unsuitable for many labile bioproducts, especially enzymes destined for use as biocatalysts. In this case, the bioproduct is protected from solvent damage by substituting the immiscible solvent phase with a second immiscible aqueous phase. The two aqueous phases are immiscible due to small amounts of polymers added to one or both of the phases but are still referred to as aqueous because they comprise mostly water (75 to 95%). Two common polymer additives are dextran and PEG, each added to a separate phase. Other applications use a polymer

Published by Woodhead Publishing Limited, 2013

in one phase with added salt in the other, such as PEG in one phase and potassium phosphate in the other.

This form of liquid extraction is known as aqueous two phase extraction and in all respects other than the nature of the phases, is governed by the same principles as solvent extraction. The distribution of the solvent is described by a partition coefficient. The partition coefficient is dependent on several variables, namely the nature of the solute, the nature of the phases, pH, ionic strength, polymer concentration and number of polymers. For instance, the partition coefficient for the separation of hydrophobic and ionic proteins could be enhanced by using a polymer in one phase and a salt in the other so that the former would preferentially solubilise in the aqueous phase containing the polymer while the latter would preferentially solubilise in the aqueous phase containing the salt. The large number of variables means that although extensive experimentation may be required to optimise the process, aqueous extraction is likely to be applicable to a wide range of solutes. Unfortunately, the need to recover often expensive polymers does increase the complexity and cost of this recovery operation.

11.4.4 Chromatography

Chromatography is carried out in a column containing a solid adsorbent as a stationary phase and a solvent containing the solute(s) which moves through the column as a mobile phase. The solutes are distributed between the mobile and stationary phases according to their specific equilibrium characteristics. These are described by adsorption isotherms which relate the solute concentration in the mobile phase to the solute concentration on the adsorbent's surface.

Published by Woodhead Publishing Limited, 2013

Separation using chromatographic techniques is based on a similar mechanism, irrespective of the type of chromatography, in that separation or resolution of solutes in a mix results from different rates of migration of each solute in the column, each with its own adsorption isotherm. The solutes are resolved into distinct bands as they migrate through the column such that separation of different solutes occurs along the column length. That is, the solvent will carry the least adsorbed solute to the far end of the column while the most adsorptive will be retained at the start of the column.

Chromatographic separation takes place in several steps. Initially, the adsorbent in the column is loaded with solutes from the mobile phase. When the first solute appears in the eluent, loading is stopped and the adsorbed solute(s) eluted with appropriate eluent. This could be a solvent or a buffer at a different pH, for instance. Several different eluting steps will be necessary if solutes are to be eluted separately. The column is then regenerated before the next loading can take place.

Several types of chromatographic separation are available. These depend on the type of adsorption between the solute and the stationary phases. In the simplest of these, adsorption chromatography, adsorption of the solute takes place by weak Van der Waals forces. The non-specificity of the Van der Waals bonds limits the applicability of this method mainly to bioremediation type processes where removal of all constituents from the stream is the end goal (e.g. use of activated carbon in water treatment).

The other chromatographic techniques (ion exchange, gel and affinity) are used for purification of products, principally when a high degree of purity is required. The most common of these chromatographic separations is ion exchange chromatography where charged solutes are adsorbed onto

Published by Woodhead Publishing Limited, 2013

anionic or cationic resins by electrostatic forces, depending on the charge of the solute. Anionic resins have negative ions attached while cationic resins have positive ions attached. A large number of different resins and ions are available and ion exchange has broad applicability for both low and high molecular weight products (including but not limited to, amino acids, antibiotics (e.g. streptomycin) and vitamins), is widely used for fractionation of proteins and scales up successfully. Care should be taken not to introduce weak resins or strong eluting conditions, both of which can result in product loss.

Affinity chromatography is a highly specialised technique which is used when superior purity is required for high cost products. A hundred times purification can be achieved in just one step and it is widely used for enzyme recovery. In this chromatographic technique, the column is packed with ligands covalently bound onto a solid support such as polyacrylamide, agarose or cellulose, where the ligands have a very specific affinity for the solute so that, by bonding with the ligand, the solute will be retained in the column. For instance, an enzyme could be retained by bonding with its co-enzyme or its inhibitor, or an antibody retained by bonding with its antigen. The solute is loaded under conditions of pH, temperature, ionic strength, etc., that will favour the linkage. The solute is subsequently eluted by introducing another molecule for which the solute has a higher affinity than it has for the ligand, for example enzyme substrate.

Gel chromatography, also called gel filtration, separates solutes on the basis of size exclusion. Porous gel beads with controlled pore sizes, made from polysaccharides such as dextran or polyacrylamides, allow smaller molecules to penetrate into the bead pores. The largest solutes penetrate the pores least and so are carried to the far end of the column. The

smallest solutes which penetrate the pores most deeply are retained the longest. This results in a gradient of sizes through the column. Each gel is distinguished by its exclusion limit and pore size distribution. A wider pore size distribution fractionates a broader range of sizes while a narrower pore size distribution increases the resolution of molecules of similar sizes.

11.4.5 Electrophoresis

Finally, electrophoresis can be used to separate molecules of different charges but is used exclusively to separate different proteins on a small scale. Essentially, an electrical charge is applied to the ends of a column containing charged macromolecules (e.g. proteins) in a fluid or gel (e.g. agar or polyacrylamide). Since proteins have net charges,[16] they will move within the gel to the end of opposite charge at a rate proportional to the magnitude of their charge. In this way, the proteins will accumulate at different positions in the gel. This method offers a very high resolution of protein fractionation and is a leading method for resolving mixtures of charged macromolecules on the small scale. Unfortunately, the high current required to produce migration, and the high electrical resistance of the buffer, lead to ohmic heating of the buffer. This causes convection currents which decrease separation efficiency, as well as resulting in protein denaturation. To date, ohmic heating has prevented the effective scale up of this technology.

11.5 Notes

1. The rationale here is that should the unit operation be suitable for recovery of a labile bioproduct, it would generally be suitable for all bioproducts.

Published by Woodhead Publishing Limited, 2013

2. The blade is somewhat quaintly called the doctor's knife.
3. The average specific cake resistance is a measure of the resistance of the cake to flow and is dependent on the shape and size of the solid and the porosity of the filter cake.
4. The complete derivation can be found in standard texts on particle technology.
5. The value of 's', the coefficient of compressibility, lies between 0 and 1.
6. Typically, slime layers form when growth is limited by an essential nutrient while carbon remains in excess. Under these conditions, slime will only form towards the end of the batch process.
7. Different materials are available. Traditionally diatomaceous earth has been used.
8. These flocs are known as activated sludge.
9. Chemical coagulants such as $CaCl_2$ and $Al_3(SO_4)_2$ neutralise charges on cell walls causing small flocs to form from dispersed cells.
10. Flocculants are polymers which form bridges between the flocs.
11. This is also used successfully on the small scale when glass beads are preferred.
12. One common implementation of this technology is the French Press (which unfortunately in this case is limited to laboratory scale use).
13. High energy inputs cause heating of the valve head.
14. This is referred to as the 'salting in' effect.
15. Pores which are the same size throughout.
16. At pH values other than their isoelectric point.

Published by Woodhead Publishing Limited, 2013

Index

absolute filtration, 204
acceleration phase, 106
activation energy of thermal death, 192
adaptive enzyme, 45, 48, 106
adenosine phosphates, 34
ADP, 34, 54, 55, 57, 58, 61, 62, 64, 65, 66, 68, 70
adsorption, 87
adsorption isotherms, 229
aerobic respiration, 57, 58, 59, 74, 98, 141, 142
aerotolerant anaerobes, 59
affinity chromatography, 231
air sterilisation, 189, 190, 203
aldoses, 26
alkaline solution, 99
alkanes, 71
allolactose, 47
allosteric enzyme, 83
amino acids, 3, 21, 22, 31, 32, 33, 38, 42, 99, 100, 101, 113, 190, 231
AMP, 34, 48, 54
amylases, 4, 30, 75
amylopectin, 28, 29
amylose, 28
anabolic pathways, 71–3
anabolism, 53
anaerobic fermentation, 58, 59, 62, 66, 142
anaerobic respiration, 22, 58, 59
anaplerotic reactions, 67
anticodon, 41
aqueous two phase extraction, 229
archaebacteria, 9
archea, 8, 9, 10, 15, 20
Arrhenius form, 192
ATP, 31, 34, 54, 55, 57, 58, 61, 62, 64, 65, 66, 67, 68, 70, 72
axial dispersion, 200, 201, 202, 203

β-oxidation, 31, 62, 72
  fats, 68–71
balanced growth, 109
batch culture, 11, 97, 98, 101, 102, 103, 104, 112, 123, 124, 140, 161
batch enzyme reactor, 86
batch filtration, 213–14
batch process
  bubble density distribution, 103
  dependence of growth rate on substrate concentration, 112–15
  design equations, 101–16

Published by Woodhead Publishing Limited, 2013

flask cultures in shaker incubator on the lab bench, 104
instrumented laboratory stirred tank reactor, 105
microbial growth rate, 102–11
batch growth curves, 110
characteristic microbial growth phases, 107
effect of substrate concentration on specific growth rate, 113
exponential growth of single bacterial cell, 107
rate of substrate utilisation and product formation, 115–16
batch sterilisation, 193–9, 200, 202
binomial nomenclature, 10
biocatalysts, 75–96
enzyme kinetics with inhibition, 78–84
enzyme kinetics with no inhibition, 76–8
enzyme reactors with immobilised enzymes, 86–95
enzyme reactors with soluble enzymes, 84–6
biodiesel, 20
bioprocess
asepsis and sterility, 189–207
air filter sterilisation, 203–7
media and equipment heat sterilisation, 190–203
bioprocess engineering, 1–6
bioprocess scale up, 171–87
constant flow regime, 185–7
mixing, 186
oxygen transfer, 185–6
power requirements, 185
shear stress, 186
constant mixing, 180–2
flow regime, 182
oxygen transfer, 181
power requirements, 180–1
shear stress, 181–2
constant oxygen transfer rate, 173–80
flow regime, 179–80
geometrically similar vessels, 175
mixing, 176–8
power requirements, 174–6
shear stress, 178–9
constant shear stress, 182–6
flow regime, 184–5
mixing, 184
oxygen transfer, 183–4
power requirements, 183
biotechnology, 1
biotransformation, 75
BIOX process, 4
bubble density distribution, 102
buffering capacity, 22, 100

CAP, 48
carbohydrates, 18, 21, 26–30, 31, 59, 62, 71, 130, 148
cellulose, 29
D-glucose conversion from straight chain to pyranose form, 28
families of D-aldoses and ketoses, 27
starch, 29
sucrose, 28
carbon, 99

Published by Woodhead Publishing Limited, 2013

carbon metabolism, 53–74
  anabolic pathways, 71–3
    fatty acid synthesis, 71–3
    gluconeogenesis, 73
  catabolic pathways, 59–71
    β-oxidation of fats, 68–71
    glycolysis, 59–62
    schematic of β-oxidation of fats, 69
    schematic of glycolysis, 60
    schematic of tricarboxylic acid cycle, 63
    tricarboxylic acid cycle, 62–8
  energy generation, storage and transfer, 54–9
    active groups NAD, FAD and CoQ reduction, 56
    electron transport chain or oxidative phosphorylation, 56
    energy release and sequestration, 54
    oxidative and substrate level phosphorylation, 55–9
    role of adenosine triphosphate, 54–5
Carman-Kozeny equation, 214
catabolic pathways, 59–71
catabolism, 18, 53, 59, 62
catabolite activator protein, 48
cell concentration data, 109, 110
cell counts, 110
cell death rate, 132
cell disintegration, 211, 219
cell dry weight, 109, 110, 111
cell rupture, 217–19
cellulases, 29, 30
cellulose, 21, 28, 29, 59, 166, 226, 231
centrifugation, 109, 213, 216, 217, 219
chemo-autotrophs, 19, 20
chemo-heterotrophs, 53, 59, 98
chromatography, 209, 211, 212, 220, 229–32
CLEA, 87
co-repressor, 47
CoA, 35
coagulation, 217
codon, 41
coenzyme A, 35
competitive inhibition, 79, 80, 82
complex media, 130
compressibility, 215
concentration polarisation, 226
constitutive enzyme, 45, 48
continuous culture, 12, 50, 97, 116, 117, 119, 120, 122, 123, 129, 130, 134, 137, 138, 140, 142, 143, 160, 189
continuous filtration, 213
continuous operation, 12, 88, 116, 117, 214
continuous plug flow reactor, 88
continuous process
  basic model equations development, 117–27
  cell and substrate concentrations with multiple feed concentration, 126
  cell and substrate concentrations with single feed concentration, 125
  customised continuous culture configurations, 138–40
  design equations, 116–40

Published by Woodhead Publishing Limited, 2013

empirical deviations from predictions of basic model equations, 127–32
laboratory scale bubble column reactor, 118
modified model equations incorporating endogenous metabolism, 132–58
modified model equations incorporating energy of maintenance, 135–8
simple continuous culture system incorporating a CSTR, 119
wild type selection during culture of genetically modified organisms, 129
continuous sterilisation, 199–203
continuous stirred tank reactor, 88, 116
CPFR, 88, 91, 92
critical dilution rate, 125, 126, 127, 128, 130
cross-linked enzyme aggregates, 87
CSTR, 88, 89, 91, 92, 116, 117, 119, 120
cyclic fed-batch, 144
cyclic fed-batch operation, 144
cysteine, 31–2

D-stereoisomers, 26
Damköhler number, 201
deacceleration phase, 112
death phase, 107, 111
deep bed filtration, 189, 203, 204, 206
degree of sterilisation, 190, 196, 197, 199, 200, 201, 202
degree of sterility, 193, 194, 196, 202
Del Factor, 193
deoxyribonucleic acid, 36
desorption, 87
diauxie effect, 48
dilution rate, 119, 120, 122, 123, 124, 125, 126, 127, 129, 130, 132, 133, 134, 135, 142
disaccharides, 28
dispersion model, 201
DNA, 16, 36, 37, 38, 40, 41, 42, 43, 44, 45, 46, 49, 109, 110
doubling time, 107, 108
downstream processing, 209–32
cell rupture and cell extract separation, 217–19
cells and extracellular fluid separation, 213–17
microbial products recovery, 212
potential recovery operations, 211–13
soluble products concentration and purification, 219–32

'e-fold' generations, 108
Eadie–Hofstee relationship, 78, 114, 123
effectiveness factor, 95
electron transport chain, 56, 57
electrophoresis, 211, 220, 232
endogenous metabolism, 98, 132–5, 137, 139, 142
endogenous respiration, 132
endogenous respiration constant, 132

Published by Woodhead Publishing Limited, 2013

energy generation, 10, 17, 34, 53, 54–9, 59–71
energy of maintenance, 98, 135–8, 142
entrapment, 87
environmental conditions, 221
enzyme activity, 44
enzyme decay constant, 85
enzyme factories, 13
enzyme immobilisation, 87, 88
enzyme induction, 46
enzyme-inhibitor complex, 79, 83
enzyme kinetics, 76, 78
  with inhibition, 78–84
    competitive inhibition kinetics, 79–81
    mixed inhibition kinetics, 82–4
    uncompetitive inhibition kinetics, 81–2
  with no inhibition, 76–8
enzyme reactors, 76, 84, 86, 91, 92
  with immobilised enzymes, 86–95
    continuous enzyme processes with kinetically controlled reaction, 88–92
    continuous enzyme processes with transport controlled reaction, 92–5
    CPFR schematic, 90
    CSTR schematic, 89
    immobilisation techniques, 86–8
    laboratory membrane reactor housing ceramic support for enzyme immobilisation, 88
  with soluble enzymes, 84–6
enzyme respression, 47
enzyme retention, 86
enzyme–substrate complex, 83
enzyme–substrate–inhibitor complex, 81, 83
enzyme synthesis, 44
enzymes
  as biocatalysts, 75–96
  enzyme kinetics with inhibition, 78–84
  enzyme kinetics with no inhibition, 76–8
  enzyme reactors with immobilised enzymes, 86–95
  enzyme reactors with soluble enzymes, 84–6
Equation Solver in Excel, 167
eubacteria, 9
eukaryotes, 8, 12–15, 16, 17–18
  cellular structure and metabolic reactions sites, 17–18
  intracellular structures, 16
  microscopic morphology, 12–15
exponential growth phase, 106, 107, 109, 110, 111, 112, 113

facultative anaerobes, 59
FAD, 34
fatty acid synthesis, 71–3
fatty acids, 20, 30, 31, 63, 68, 70, 71, 72
fed-batch bioprocess design equations, 140–4
fed-batch culture, 97, 140, 141, 142, 161, 189
fed-batch process, 67
Fick's Second Law, 154

filter sterilisation, 203–7
filtration, 109, 189, 203, 204, 213, 214, 215, 216, 217, 219, 225, 227
final electron acceptor, 64, 147
flavin adenine dinucleotide, 34
flocculation, 217
flow regime, 172, 173, 176, 177, 179–80, 182, 184–5, 185–7
fractional precipitation, 221
fungi, 12–15

gassing out procedure, 162, 166, 168
gel chromatography, 231
gel filtration, 231
gel regime, 226
gene, 8, 44, 45, 46, 47, 48
generation time, 108, 109
genetic engineering, 49, 50, 76
genetic modification, 49–50
genetic regulation, 44–8
geometric similarity, 172, 173, 175, 177, 181
geometrical similarity, 173
gluconeogenesis, 31, 67, 73
glucose isomerase, 75
glycogen, 29, 73
glycolysis, 31, 59–62, 63, 65, 66, 72
glyoxylate shunt, 67
GMO, 39, 50, 86, 101, 129, 130
Gram negative, 17
Gram positive, 17
gravity sedimentation, 216–17

heat sterilisation
  batch sterilisation, 193–9
  continuous sterilisation, 199–203
  dependence of thermal death and degradation rates on temperature, 198
  influence of sterilisation temperature on sterilisation efficiency, 192
  kinetics, 190–3
  media and equipment, 190–203
  thermal destruction of contaminating microorganisms, 203
hemicellulose, 29
Henry's Law, 159
hierachical system, 8
high pressure homogenisation, 217–18
HTST sterilisation, 198, 200
hydrocarbons, 21

impeller tip speed, 178–9
in situ product removal, 139
inducer, 46, 48, 101, 123, 141
inertial impaction, 206
insulin, 4–5
interfacial area per unit liquid volume, 94
interfacial area per unit volume, 151, 152, 154, 155, 157
ionic polymers, 223
iron, 99

ketones, 26, 28
ketoses, 26

lac operon, 46, 47
lacI, 47
lactose, 28

Published by Woodhead Publishing Limited, 2013

lag phase, 48, 106, 112
Latin binomial system, 10
Le Chatelier's Principle, 82
limiting substrate, 112, 113, 130
Lineweaver–Burk relationship, 78, 80, 82, 84, 114, 123
lipids, 30–1, 33, 130
liquid extraction, 220, 227–9
log penetration model, 204, 205, 206
low dilution rate, 130, 131, 134, 135, 137, 138, 139
LTLT sterilisation, 199

maintenance coefficient, 136
maltose, 28
mass transfer limitation, 87, 93, 95
Matlab, 168
mechanical rupture, 217
media sterilisation, 189, 190
membrane separation, 211, 220, 224–7
metabolic macromolecules, 25–38
  carbohydrates, 26–30
  lipids, 30–1
  nucleosides, nucleotides and nucleic acids, 33–8
  proteins, 31–3
metabolic pathways, 8, 25, 26, 30, 31, 33, 53, 190
metabolism, 25, 48, 53, 54, 57, 62, 63, 66, 99, 132, 133, 134, 135, 137, 139, 142, 147, 163, 171, 190
methanogens, 20
Methanopyrus, 10
Michaelis–Menten constant, 77, 81, 84
Michaelis–Menten equation, 77, 78, 80, 81, 84, 85, 94, 95
Michaelis–Menten kinetics, 93
microbial kinetics
  batch, continuous and fed-batch processes, 97–146
  batch process design equations, 101–16
  continuous process design equations, 116–40
  fed-batch bioprocess design equations, 140–4
  nutrient medium, 98–101
microbiology, 7–23
  cellular structure and metabolic reactions sites, 15–18
  classification according to carbon and energy requirements, 18–20
  filamentous fungal colonies, 14
  intracellular structures of prokaryotes and eukaryotes, 16
  microorganisms, 8–15
  nutrient requirements, 21–2
  schematic of classification according to carbon and energy requirements, 19
  the Phylogenetic Tree of Life, 9
microorganisms, 8–15
  microscopic morphology, 11–15
    eukaryotes, 12–15
    filamentous fungal colonies, 14
    prokaryotes, 11–12
  taxonomy, 8–11
mitochondria, 17, 68, 72
mixed inhibition, 79, 82–4
mixing, 66, 102, 117, 128, 142,

Published by Woodhead Publishing Limited, 2013

160, 171, 172, 173, 176, 177, 178, 180, 181, 182, 184, 186, 187, 224
mixing time, 176
modified gassing out procedure, 166
molar flow rate of oxygen entering, 158
molar flow rate of oxygen exiting, 158–9
molar flux, 151
molecular biology, 8, 39–51
  enzyme synthesis regulation, 45
  genetic modification, 49–50
  genetic regulation, 44–8
  protein synthesis, 43
  replication, 40–1
  transcription, 41
  translation, 41–4
molecular cloning, 49
molecular diffusion, 151
Monod growth kinetics, 11, 13, 108–9, 111, 121
Monod Model, 112, 113, 114, 120, 123, 129, 133, 136, 143, 147
monohydroxyaldehydes, 26
monohydroxyketones, 26
monosaccharides, 26
morphology, 7, 11, 12, 13, 14, 111
mRNA, 41, 42, 43, 44, 45, 47, 48

NAD^+, 34
negative modulation, 83
nicotinamide dinucleotide, 34
nitrogen, 22, 99–100
non-competitive inhibition, 79, 84
nucleic acids, 33, 36–8, 99
nucleosides, 33–6
nucleotides, 33–6, 37, 38, 40, 42, 44, 53, 54, 99
  adenosine mono-, di- and triphosphate, 35
  nicotinamide adenine dinucleotide, flavin adenine dinucleotide and coenzyme A, 36
  parent purine and pyrimidine compounds, 34
  RNA and DNA, 37
nutrient medium, 21, 22, 97, 98–101, 104, 117, 120, 141, 199

obligate aerobes, 58
operator, 45, 46, 47
operon, 45, 46, 47, 48
OTR, 148, 149, 150, 151, 152, 155, 156, 157, 158, 159, 160, 161, 162, 164, 166, 173, 174
OUR, 148, 158, 159, 164, 165, 167
overall volumetric mass transfer coefficient, 94
overall volumetric oxygen transfer coefficient, 147–69
oxidative phosphorylation, 56, 57, 58, 59, 62, 65, 147
oxygen, 99
oxygen limiting, 58
oxygen mass balance, 158
oxygen probe, 161, 162
oxygen solubility, 147, 148, 150, 151, 156, 157, 159, 160, 161, 163

Published by Woodhead Publishing Limited, 2013

oxygen transfer, 7, 21, 58, 102, 117, 148, 149, 150, 161, 168, 171, 172, 174, 176, 178, 179, 181, 183–4, 185, 186, 187
oxygen transfer coefficient, 152
oxygen transfer limitation, 13, 172, 184
oxygen transfer rate, 147–69, 172, 173
  design equations, 149–57
    bubble diameter and size distribution in bubble column reactor, 153
    edge detection on original image and contrast mapping of detected bubbles, 154
    possible resistances to oxygen transfer according to Two Film Theory model, 150
  measurement, 157–68
  quantification under dynamic conditions, 161–8
    dynamic methodologies assuming a negligible probe response lag, 162–5
    dynamic methodologies incorporating a probe response lag, 165–8
    oxygen concentration profile during the dynamic method in a system with respiring cells, 163
  quantification under steady state conditions, 158–61
oxygen utilisation rate, 147, 148
palmitic acid, 70
Péclet number, 201
Penetration Theory, 149
penicillin amidase, 76
peptidoglycan, 15
pharming, 49
phospholipids, 30
phosphorous, 100
photo-autotrophs, 20
Phylogenetic Tree of Life, 9
plasmids, 16, 49
polyhydroxyaldehydes, 28
polyhydroxyalkonates, 71
polymerase chain reaction, 49
polypeptide, 31, 32, 41, 42, 43, 44, 45
polypeptide chains, 32
polysaccharides, 28
positive modulation, 83
potassium, 22
precipitation, 87, 88, 220, 221–4
precise fractionation, 224
pressure step procedure, 166, 167, 168
probe constant, 166, 167
prokaryotes, 8, 11–12, 15–17, 45, 111, 215, 216
  cellular structure and metabolic reactions sites, 15–17
  intracellular structures, 16
  microscopic morphology, 11–12
promoter, 45, 46, 47, 48
proteins, 4, 15, 31–3, 38, 47, 99, 220, 221, 222, 223, 224, 229, 231, 232
pseudo steady state, 143, 144
PT, 149
purification programme, 33, 209

Published by Woodhead Publishing Limited, 2013

rate of thermal death, 191
reaction velocity, 76, 77, 80, 81, 84, 94, 95
recombinant DNA, 4, 5, 49
regulatory gene, 46
replication, 11, 40–1, 107, 111
repressor, 46, 47, 123
repressor molecule, 46
respiratory chain oxidation, 57
respiratory quotient, 142
response lag, 161, 162, 165, 166, 167, 168
reverse osmosis, 225, 226, 227
Reynolds number, 177, 179, 180, 182, 184, 185, 187, 201
ribonucleic acid, 36, 37, 41, 45, 46, 47, 48, 109, 131
ribosomes, 16, 17, 42, 46
RQ, 142
rRNA, 42

salt precipitation, 222
salting out, 222, 223
'salting out' constant, 222
'salting out' equation, 222
'salting out' technique, 222
saturation constant, 112
Sauter mean diameters, 152
scale up criterion, 172, 173, 174, 178, 179, 180, 181, 182, 183, 184, 185
secondary metabolites, 116, 138, 140
sedimentation, 213, 216, 217
selective pressure of continuous culture, 130
shear stress, 171, 172, 173, 176, 178, 179, 181, 182, 183, 184, 186, 187
slime layers, 16, 128, 215
solvent extraction, 227–8, 229
specific growth rate, 108, 109, 111, 112, 113, 114, 115, 120, 122, 123, 126, 127, 129, 147
spores, 11, 12, 13, 14
sporulation, 12
SRT, 149
starch, 4, 28, 29, 30, 59, 75
stationary phase, 107, 110, 111, 229, 230
steady state, 89, 90, 120, 121, 123, 124, 125, 126, 127, 133, 136, 137, 138, 140, 143, 144, 152, 153, 154, 158, 159, 160, 161, 201
stirred tank reactor, 102, 105
structural genes, 45, 46, 47, 48
substrate inhibition, 114
substrate level phosphorylation, 55–9, 61, 64, 65, 67
substrate limitation, 130, 131, 141
sucrose, 28
Sulfolobus, 10
Surface Renewal Theory, 149

thermal death, 191, 192, 193, 198, 199, 200
thermal death rate constant, 191
thermal degradation, 191, 193, 198, 199, 200, 201
Thiele modulus, 95
transcription, 40, 41, 44, 45, 46, 47, 48
translation, 40, 41, 42, 43, 45

Published by Woodhead Publishing Limited, 2013

tricarboxylic acid cycle, 31, 35, 62–8, 64, 66, 67, 68, 70, 72
triglycerides, 20
triplet code, 41, 42
tRNA, 41, 42, 43
Two Film Theory, 149

ultrafiltration, 86, 219, 224, 225, 226
ultrasound, 218
uncompetitive inhibition, 79, 81–2, 84

wall growth, 128

xylose isomerase, 4

yield coefficient, 115
yield constant, 124

Published by Woodhead Publishing Limited, 2013